

THEME III

SEISMIC BEHAVIOUR OF STRUCTURAL CONCRETE TWO-DIMENSIONAL
ELEMENTS (SHEAR WALLS AND OTHERS)

COMPORTEMENT SISMIQUE DES ELEMENTS STRUCTURAUX PLANS
(MURS DE CONTREVENTEMENT ET AUTRES)

Reporter
Rapporteur

George SERBANESCU
Institutul de Cercetari
in Constructii si Economia Constructiilor
Bucharest, Roumania

NON-LINEAR ANALYSIS OF REINFORCED CONCRETE SHEAR WALLS

Luigi CEDOLIN

Politecnico di Milano
Italy

Antonio MIGLIACCI

Politecnico di Milano
Italy

Sergio LEVATI

M.S.C. Engineering
Milano, Italy

INTRODUCTION

The structural response to earthquake excitations of different time-histories and severities has been the object of a great deal of research in recent years, and the finite element method has proved to be successful in the analysis of complex structures under the assumption of a linear elastic behaviour of the material. In the case of reinforced concrete structures, however, this assumption is valid only for the analysis of the service-ability condition under design earthquake forces.

Under extreme conditions, however, concrete will be extensively cracked or subjected to inelastic deformations, and slippage between steel and concrete will occur. These strong nonlinearities preclude the use of mode superposition analysis and response spectra, so that the nonlinear time-history analysis is the only correct technique.

Reinforced concrete shear walls are often used in order to provide resistance to lateral forces. A nonlinear time-history analysis of such walls through a finite element grid of plane stress elements would give rise to tremendous computational as well as economic problems, and its credibility would be endangered by the lack of information on concrete

Note – Paper presented at the AICAP-CEB Symposium,
Structural Concrete Under Seismic Actions,
May 25-28, 1979, Rome.

¹Dept. of Structural Engineering, Politecnico di Milano, Italy

²M.S.C. Engineering, Milano, Italy

behaviour under cyclic biaxial loading and on steel-concrete slippage under load reversals. Moreover, the results would provide a detail not necessary for engineering purposes, and too strictly related to the selected time-history of the excitation.

A nonlinear static analysis under cyclic loads may be more helpful for the design of shear walls against ultimate earthquake loads. This analysis may be done with methods presented by Pinto and Menegotto (1) and more recently by Schnobrich and Takayanagi (2) for the case in which the shear wall may be represented by a plane frame. For a shear panel, Cervenka and Gerstle (3) and Darwin and Pecknold (4) have used a plane stress finite element representation. In this latter work, the uniaxial experimental data of Karsand and Jirsa (5) have been used for the biaxial case through the introduction of the concept of an equivalent uniaxial stress. The frame analysis method, however, cannot be applied to shear walls of high-rise buildings, if these are not slender or present an irregular distribution of openings. For larger sized walls, on the other hand, a two-dimensional nonlinear finite element model under cyclic loads is computationally too expensive. The only realistic possibility is an ultimate load analysis under a monotonically increasing distribution of earthquake forces. This analysis may provide helpful indications on the zones which will be affected by cracking and yielding.

The scope of this presentation is to illustrate the use of a finite element model in predicting the behavioral sequence of a shear wall up to failure and to discuss its design implications.

NONLINEAR FINITE ELEMENT MODEL

Comprehensive reviews of the application of finite element models to the analysis of reinforced concrete members have been published by Scordelis (6) and more recently by Schnobrich (7). For the case of planar members a finite element model capable of predicting the behaviour up to failure has been developed by Cedolin and Dei Poli (8) and is briefly presented here.

Concrete

Constant stress triangular elements have been selected, because they allow a very simple representation of cracks, and a very fast calculation of the stiffness matrix. The constitutive relation proposed by Liu, Nilson and Slate (9) has been adopted, which considers concrete as an orthotropic material in the directions of existing principal stresses. The relation between principal stresses and strains is given by

$$\sigma = \frac{A + B E \epsilon}{(1 - \nu \alpha) (1 + C \epsilon + D \epsilon^2)}$$

in which σ , ϵ = stress and strain in one principal direction; α = ratio between the stress in the perpendicular direction to the stress in the direction considered; E , ν = initial tangent modulus and Poisson's ratio in uniaxial loading. The values of the parameters A , B , C and D have been derived from the test results in biaxial loading by Kupfer, Hilsdorf and Rusch (10).

Crack propagation through the region occupied by one element has been modeled by modifying its material matrix so that it becomes unable to transmit stresses in the direction normal to the crack. Although this representation of cracking gives rise to cracked regions rather than discrete cracks, it is still the only feasible alternative in finite element analysis, and it may be improved by introducing fracture-mechanics concepts (11).

With the previously mentioned crack representation, the only way to introduce aggregate interlocking is to attribute a conventional value to the shear modulus G in the material

matrix. In the present study, following Ref. (12), G has been assumed constant, although in Ref. (8) it is shown that a more realistic representation of aggregate interlocking could be obtained on the basis of experimental investigations on shear transfer across cracks (13).

Reinforcing steel

One-dimensional bars and beam elements have been used in order to represent the reinforcement. An elastic-perfectly plastic behaviour has been assumed for the material.

Steel-Concrete Interaction

Linkage elements may be used in order to model steel-concrete interaction. In a direction parallel to the reinforcement, the stiffness of the linkage element has been modeled after the experimental investigation of Nilson (14) on the bond-slip relation.

Solution Procedure

The load is applied incrementally, and during each load increment an iterative procedure reapplies to the structure the unbalanced nodal loads arising from material nonlinear behaviour and cracking. The failure to converge of this procedure for a certain load increment indicates that the structure has reached its ultimate load.

SOME NUMERICAL RESULTS

The method of analysis previously illustrated has been applied to actual cases of shear walls belonging to multistory buildings of the new San Polo complex in Brescia, Italy. These buildings will be constructed with the use of either "tunnel" formwork or large formworks for vertical walls, and in both cases the resistance to lateral loads is provided by shear walls correctly placed in plan, with openings randomly distributed. Although the zone does not present a recognized seismic risk, the design of these structures has been done on the basis of adequate earthquake forces, the effect of which is not far from the one caused by the design wind loads.

The lateral earthquake loads applied to the building have been calculated on the basis on the Italian Code Provisions, expressed by

$$F_h = C \times R \times g \times M$$

where C is a numerical coefficient which depends on the seismic zone, R is a factor which depends on the type of structural system, g is the gravity acceleration and M is the mass concentrated at the level considered. These loads are redistributed to the various walls in proportion to their relative stiffness and position in plan, assuming linear elastic concrete behaviour of the material and floor slabs which are infinitely rigid in their own plane.

The shear wall selected for the analysis is shown in Fig. 1(a), with the lateral forces F_{hi} acting on it, corresponding to a $C \times R$ value of 0.07. Since the upper part of this wall shows openings regularly distributed and is thus less affected by shear deformations, it can be idealized with a frame (15). The lower part (Fig. 1(b)) which shows openings randomly distributed, has been studied with the finite element procedure previously illustrated. The actions transferred from the columns of the idealized frame in the upper part, to the lower two-dimensional model, have been applied with a stress distribution calculated on the basis of a cracked cross section.

The finite element grid used is shown in Fig. 2. Each rectangular concrete element is subdivided in to two triangular constant-stress elements. The reinforcement, distributed verti

cally and horizontally with the ratio $p = 1.0\%$, has been concentrated into bar elements running along the sides of the finite element subdivision.

Fig. 2 shows the direction of crack propagation for the various load increments resulting from the analysis. The cracks which are initially horizontal are caused by the flexural action, and subsequently slant showing the effect of shear. On the same figure is shown the position of yielded bars under the effect of lateral forces corresponding to $C \times R = 0.07$, at which the wall fails.

Fig. 3 shows the distribution of normal stresses in the vertical direction, in concrete and steel. The effects of the irregular distribution of the openings and of concrete cracking are evident, especially if compared to the distribution obtained with a linear analysis.

Fig. 4 shows the lateral deflection at the top of the bottom part of the shear wall for increasing values of earthquake forces. One can notice the sharp bend in the curve when cracking starts. For the sake of comparison, on the same drawing are represented the deflections calculated with frame analysis, and the deflection due to design wind load, calculated with finite element analysis.

The data relative to the computer run for the nonlinear finite element analysis are: (a) Number of elements = 3161; (b) number of degrees of freedom = 2392; (c) number of load increments = 5; number of iterations for load increment = 8; CPU time (UNIVAC 1108) = 68 min.

CONCLUSIONS

The application of the nonlinear finite element analysis to the study of a monolithic shear wall shows the location of cracked and yielded zones at failure. Moreover, it shows the unreliability of elastic frame analysis (which is usually used for design purposes) in predicting stress distributions and deflections at load levels at which cracking becomes important. The increase of the real lateral deflection with respect to a linear analysis, besides being dangerous for stability reasons, makes incorrect the redistribution of earthquake forces on the

single wall. The more the wall softens due to cracking, the more the forces will be carried by stiffer elements. The real failure load of the building could be obtained by a redistribution of the earthquake forces made on the basis of the nonlinear load-deflection diagram of each wall.

ACKNOWLEDGEMENTS

This work has been carried out with the support of the Consiglio Nazionale delle Ricerche, Rome, Italy. The helpful suggestions of Dr. R. Villa are gratefully acknowledged.

REFERENCES

- (1) Pinto, P.E., and Menegotto, M., "Method of Analysis for Cyclically Loaded Reinforced Concrete Frames", IABSE Report, Vol. 13, 1973, pp. 15-22
- (2) Takayanagi, T. and Schnobrich, W.C., "Computed Behaviour of Reinforced Concrete Coupled Shear Walls", Civil Engineering Studies, SRS 434, University of Illinois at Urbana, 1976
- (3) Cervenka, V. and Gerstle, K.H., "Inelastic Analysis of Reinforced Concrete Panels", IASBE Report, Vol. 31 - II, 1971
- (4) Darwin, D., and Pecknold, D.A.W., "Inelastic Model for Cyclic Biaxial Loading of Reinforced Concrete", Civil Engineering Studies SRS 409, University of Illinois at Urbana, July 1974
- (5) Karsan, J.D., and Jirsa, J.O., "Behaviour of Concrete Under Compressive Loadings", J. of Str. Div. ASCE, Vol. 95, ST12, Dec. 1969, pp. 2543-2563

- (6) Scordelis, A.C., "Finite Element Analysis of Reinforced Concrete Structures", Proceedings of the Specialty Conference on the Finite Element Method in Civil Engineering, Montreal, Quebec, Canada, 1972
- (7) Schnobrich, W.C., "Behaviour of Reinforced Concrete Structures Predicted by the Finite Element Method", Computer and Structures, Vol. 7, pp. 365-376, 1977
- (8) Cedolin, L. and Dei Poli, S., "Finite Element Studies of Shear-Critical R/C Beams", J. of the Eng. Mech. Div., No. EM3, June 1977, pp. 395-410
- (9) Liu, T.C.Y., Nilson, A.H., and Slate, F.O., "Biaxial Stress-Strain Relations for Concrete", Journal of the Structural Division, ASCE, Vol. 98, No. ST5, May 1972, pp. 1025-1034
- (10) Kupfer, H., Hilsdorf, H., and Rusch, H., "Behaviour of Concrete Under Biaxial Stress, Proceedings, ACI, Vol. 66, No. 8, Aug. 1969, pp. 656-666
- (11) Bazant, Z.P., and Cedolin, L., "Blunt Crack Propagation in Finite Element Analysis", to appear in ASCE, Eng. Mech. Div. Journal, April 1979
- (12) Hand, F.R., Pecknold, D.A., and Schnobrich, W.C., "A Layered Finite Element Nonlinear Analysis of Reinforced Concrete Plates and Shells", ASCE Journal, No. ST7, Vol. 99, July 1973, pp. 1491-1505
- (13) Paulay, T., and Loeber, P. J., "Shear Transfer by Aggregate Interlock", ACI Special Publication SP-42, Vol. 1, 1973
- (14) Nilson, A.H., "Internal Measurement of Bond Slip", ACI Journal, Vol. 64, No. 3, Mar. 1967, pp. 152-163
- (15) Mehlhorn, G. and Schwing, H., "Behaviour of Panel Shear Walls", Int. Council for Building Research Studies and Documentation, Darmstadt, Oct. 1974

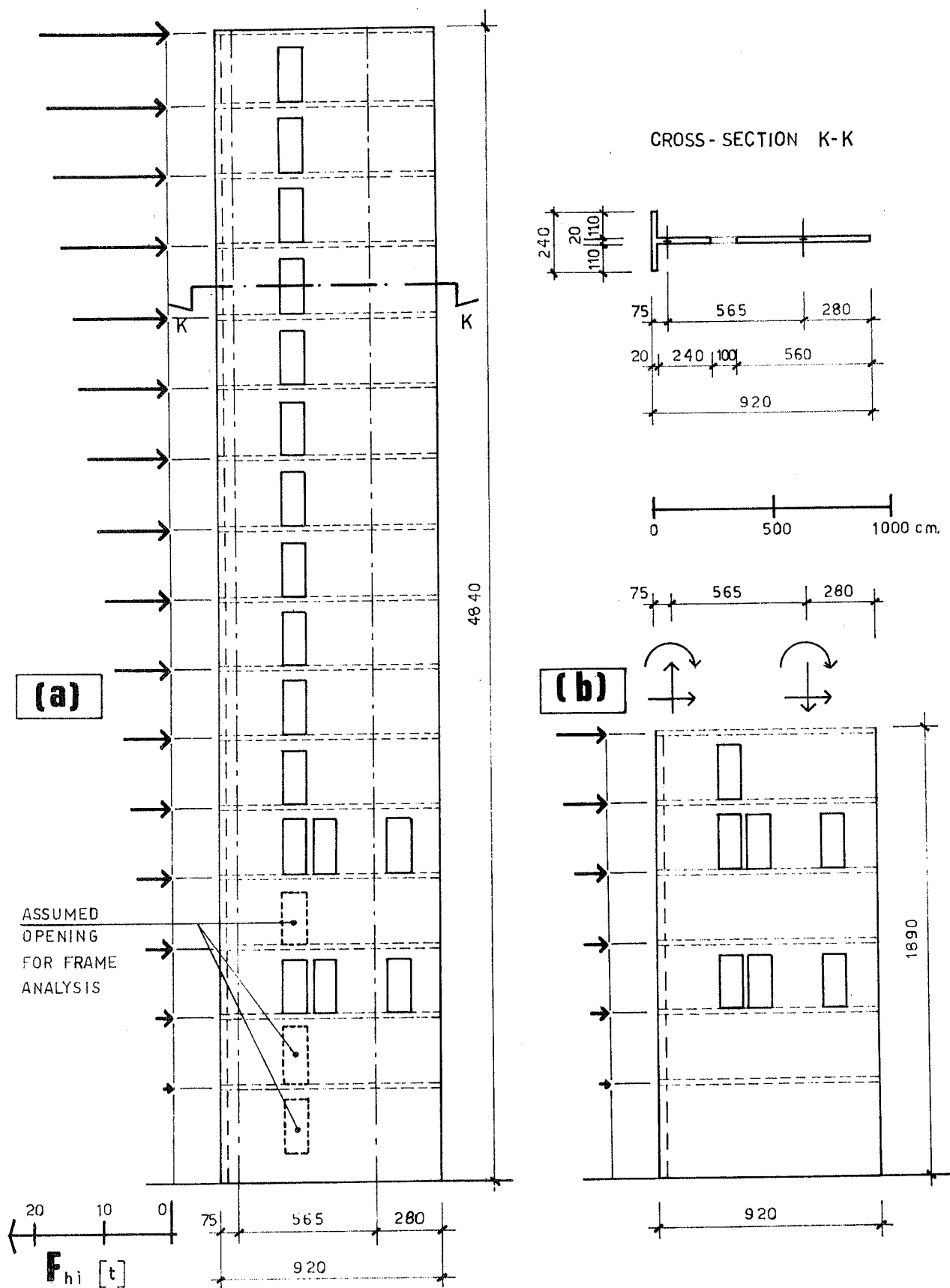


Fig. 1

— (a) Actual shear wall and idealized frame;
 (b) bottom part, analyzed with finite elements.

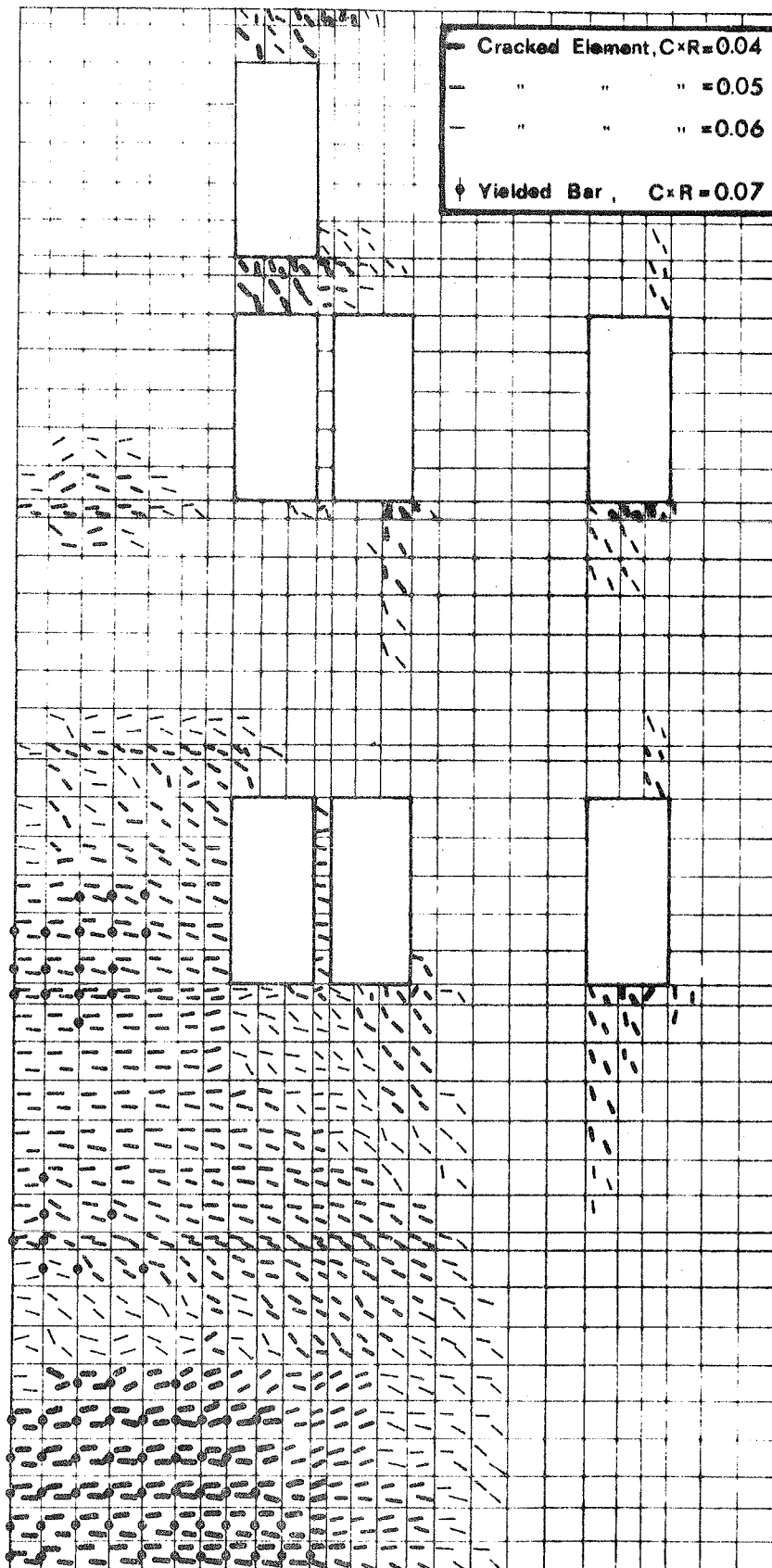


Fig. 2

- Crack distribution
 for lateral forces
 corresponding to
 $C \times R = 0.06$

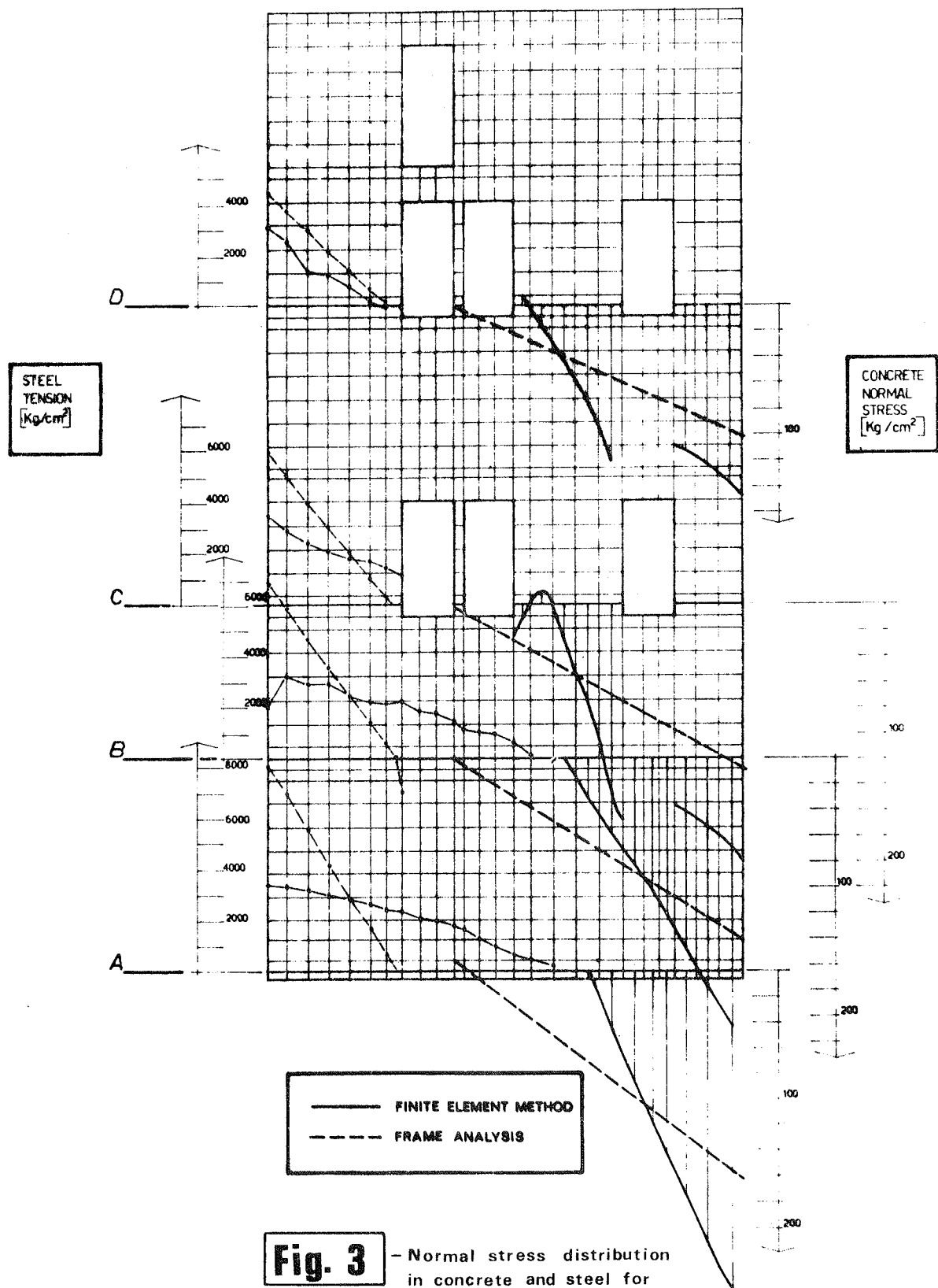


Fig. 3 - Normal stress distribution in concrete and steel for lateral forces corresponding to $C \times R = 0.06$

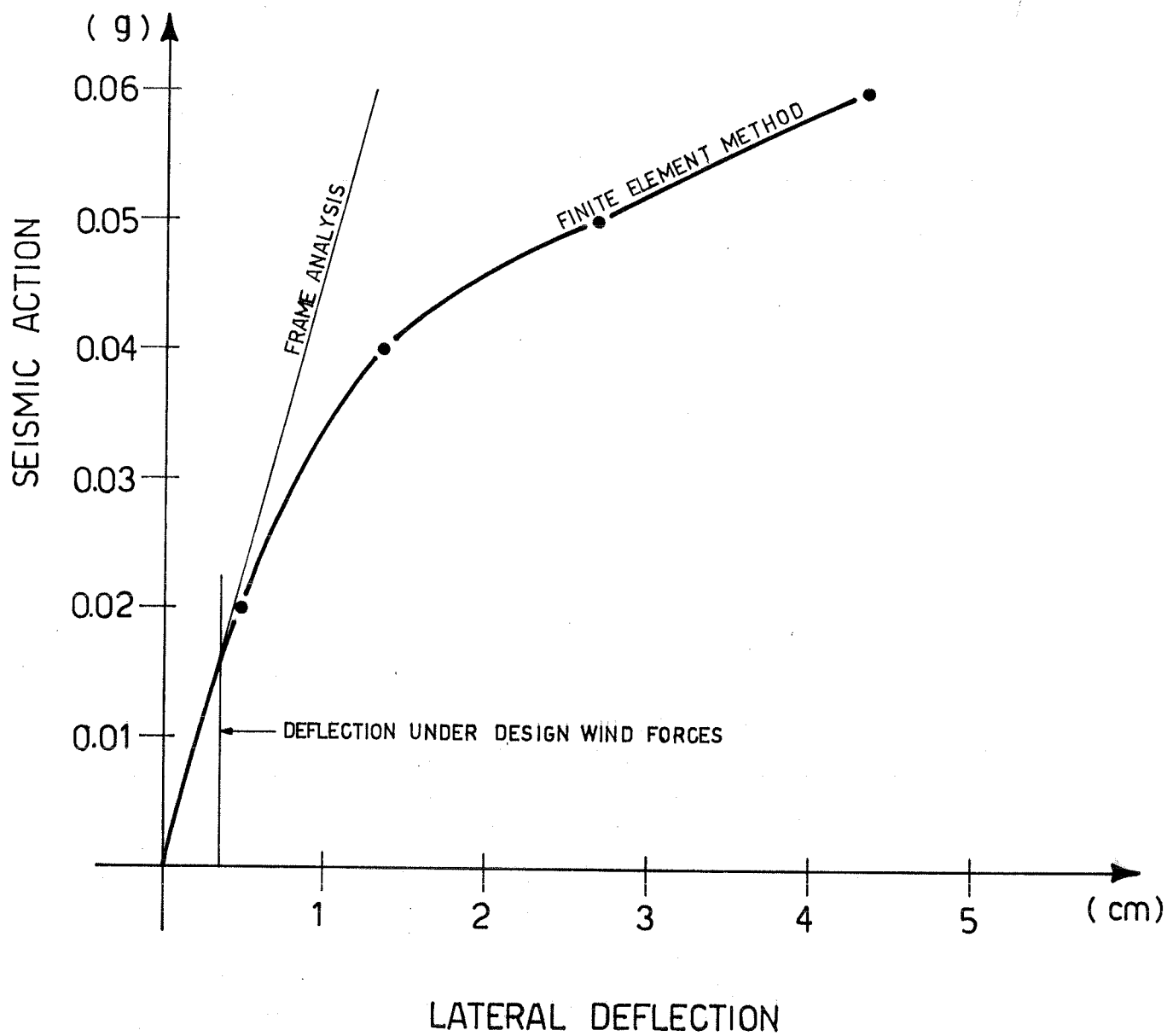


Fig. 4

- Lateral deflection of the top of the bottom part of the shear wall for increasing values of lateral forces

LOW CYCLE BEHAVIOR AND STRENGTH OF PRECAST CONNECTIONS

Alex ASWAD

Stanley Structures, Inc.
Denver, Colorado U.S.A.

SUMMARY

This paper presents some of the test results related to common precast member connections. The testing program was conducted on full-size panels at Stanley Structures (Denver plant) in 1977.

Due to drastic space limitation the description herebelow will be limited to six connections. Testing consisted of static, monotonic, or cyclic loading to failure. The number of full cycles was limited to three and the duration of each cycle was approximately ten minutes.

The results are summarized in tabular form and provide information on the maximum force attained, secant stiffness and material strengths. No attempt has been made here to derive a general analytical model, but comments are included to allow a better understanding of connection behavior and strength. It is found that connection capacities were higher than the values obtained from current conservative methods since plate bearing (when available) and mesh contribution were usually neglected.

RESUME

Cette contribution présente quelques résultats des essais de charge sur connections du type "sec" effectuées sur panneaux en béton à la Compagnie Stanley Structures (Denver) en 1977.

Vu l'espace restreint les descriptions ci-dessous sont limitées à six types de connections. Le chargement était du genre statique, monotone ou cyclique jusqu'à rupture. Le nombre des cycles entiers était limité à trois et la durée de chaque cycle était d'environ dix minutes. Aucun modèle analytique n'est proposé, mais les résultats en forme de table et commentaires sont inclus pour permettre une meilleure compréhension du comportement et de l'estimation de la capacité des connections généralement employées aux Etats Unis. Les résultats obtenus montrent des capacités supérieures aux valeurs normalement admises qui négligent l'appui sur béton et la présence des treillis métalliques.

INTRODUCTION

The precast/prestressed industry has experienced a phenomenal growth in the past few years. Parallel to this volume growth a refinement in the stress and strength analysis of monolithic structures was pursued and the pertinent state-of-the-art reached a satisfactory degree of precision.

Precast panel type structures are desirable from an economic point of view; however, the presence of (non-grouted) vertical and horizontal joints was always a reason for concern in lateral load situations, either in roof/floor diaphragms or in shear walls. Finding the most effective and reliable method to connect prestressed or precast members is one of the most important problems facing the industry today. Since the floor and wall assemblies are expected to act as diaphragms or shear walls in lateral load resistance, there is a need to know connection capacities, their failure modes and also their stiffness under service loads. However, available information on commonly used welded "dry connections" is lacking in many respects although proper modeling of shear walls and diaphragms require this kind of information. A conservative capacity can often be estimated but stiffnesses or failure modes are generally not available.

In this report a few of the findings of the test program on connections conducted at Stanley Structures (Denver) are presented.

TEST PROGRAM OBJECTIVES

The test program had several objectives:

- a. To derive the failure capacities for common connections.
- b. To derive the connection stiffness under service loads.
- c. To investigate biaxial loadings (shear and pullout).
- d. To observe the failure mode and to optimize the design.
- e. To recommend improved design values for the capacities.

SCOPE

All tests were run on full-size (8'-0" wide) panels and connections, each produced using regular materials and production methods. The tests described below are divided into two main categories:

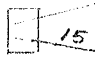
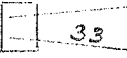
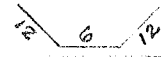
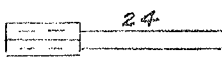

- Category I - Connections for double tees (2" flange thickness).
- Category II - Connections for precast wall panels, 6" thick.

Loading was statically applied. In the majority of cases the load was cycled three times between $+P_0$, where P_0 is a value smaller than the actual maximum load, and then the connection brought to failure. In the following pages the words "connection" and "plate" will often be interchanged.

Plates description is detailed in Table 1 and Figure 1. Although D-34 is shown with inclined rebars, it had parallel rebars during the tests.

Average concrete strength and rebars' yield strength were 4,900 psi and 57,000 psi, respectively.

Table 1: Connections Description

| Plate No. | 3/8" Steel Plate Size | Rebars | Studs |
|-----------|---|---|--------------------|
| D-34 | 2-1/2" x 6" | (2) #3 ;  | None |
| D-36 | 4" x 6" | (2) #4 ;  | None |
| D-40 Tie | None | #4 ;  | None |
| P-3 | 5" x 10" | None | (4) 1/2"x8" H.A.S. |
| P-8 | See Fig. 1 | (2) #5 ;  | None |
| P-9 | Note: Angle size is 3"x3"x6" long | #5 ; angle  | None |

CATEGORY I: DOUBLE TEE CONNECTIONSTest Results

Force versus displacement relationship for connection D-34 is displayed in Figure 2. The one for D-40 is shown in Figure 3.

Connection D-34 exhibited a brittle failure at 11.9 kips. This was due to the lack of "truss action" by the rebars. Although the failure load was about double the previous recommended ultimate strength, it was decided to change the design so that the bars will be placed at an angle of 60° with the tee edge as detailed. This connection is being used in vertical joints.

Connections D-36 and D-40 exhibited good ductile behavior and stiffness. It is worthy of note that the application of 1.0 kip pullout force normal to the panel caused the D-40 to lose about a third of its ultimate capacity. This latter type of pullout forces whose magnitude is not well known are generated during elevation adjustment of double tees at erection time. Consequently it is desirable to assume a conservative value for the rated capacity. The latter two plates are used in horizontal members connections.

CATEGORY II: PRECAST WALL CONNECTIONSTest Results

Figures 4 to 6 display the experimental force/displacement relationships for this category.

The P-8/P-3 combination is a standard connection used in horizontal joints. The ultimate capacity was substantially larger than the previously rated capacity of 14.9K. In test "a", hairline cracks initiated around the studs in P-3 at a shear force of 35.7 kips. When the force reached 37 kips brittle weld failure occurred. In test "b", however, a large slip occurred at a level of 35K (due to compression bearing spalling) followed by a high residual force. In both tests no cracks or signs of distress showed up around P-8.

Other combinations P-8/P-3 were tested in a biaxial force situation of shear and in-plane pullout. Under pure pullout, hairline cracking started at 17.8K and maximum force reached was 23.4K while final failure occurred by stud fracture. Under the combined force situation a simultaneous shear of 29.5K and pullout of 20.4K were attained before stud fracture occurred. An elliptical shear/pullout intersection curve was found to safely represent this combination's behavior.

The P-9/P-9 combination is widely used in vertical joints. Several premature weld failures occurred when undersize field weld plates (2"x3") were intentionally tried. 3" x 4" x 3/8" weld plates allowed the monotonic failure load to reach 32.7K. Under cyclic loading ($P_0 = 16.5K$), no cracks appeared and maximum load attained was 25.2K when weld failure occurred. In the last test the weld plate was bent to accommodate a 1/2" elevation difference.

CONCLUSIONS

- a) When the force applied to a plate was simple shear, ultimate capacities were higher than the ones listed in Ref. 2(1977) by up to 100% in some cases. The extra capacity was on the high side whenever the connection included a 3/8" thick plate which increased the bearing portion of the capacity.
- b) Ductility of the standard plates tested was good to excellent except for the D-34 with straight rebars, although its actual capacity was much superior to the recommended one in Ref. 2(1977).
- c) Rebars' anchorage lengths were sufficient to develop ultimate capacities.
- d) Plates subjected to cycled loads showed no major stiffness deterioration after three cycles.
- e) Pullout forces normal to panel surface substantially decrease ultimate capacity in shear. Moderate in-plane pullout forces acting simultaneously with shear do not noticeably affect ultimate shear capacity of precast connections, although they reduce the connection stiffness.
- f) Size of field weld plates is critical in wall panel connections if premature weld failure is to be avoided.

Table 2 below lists recommended values for plate capacities assuming $\phi = 1.0$ for the capacity reduction factor, $f'_c = 5,000$ psi and $f_y = 48,000$ psi. These values are derived from the test data after proper adjustment for nominal strengths and number of tests.

In general we can conclude that these and other properly detailed connections allow significant inelastic deformation. They could safely be used in Seismic Zones 1, 2 and possibly 3 of the Uniform Building Code. The data base was large enough to reach the conclusion that rebars are a significant factor in obtaining a high ductility level. When joint forces are evaluated accurately, a $\phi = 0.85$ is recommended.

Table 2: Capacities Summary

| Plate No. | Force Type | Maximum Test Force in KIPS | Recommended Rated Capacity ($\phi=1$), in KIPS |
|-----------|----------------------------|----------------------------|---|
| D-34 | Shear | 11.9 | 7.5 |
| D-36 | Shear | 16.1 | 14.0 |
| D-40 | Shear | 12.3 | 8.0, incl. pull \perp to panel |
| P-8/P-3 | Shear | 36.0 | 29.0 |
| P-8/P-3 | Shear and in-plane pullout | 29.5 & 20.4 | 20 (shear) and 16 (pullout); or 12 (shear) and 20 (pullout) |
| P-9/P-9 | Shear | 32.7 | 24.0, with 3"x4"x3/8" weld plate |

SELECTED REFERENCES

1. Anon., "Standard Plates Book", published by Stanley Structures, Denver, June 1977.
2. Anon., "Calculated Ultimate Load Capacities for Standard Plates - A preliminary Report". Stanley Structures, June 1977.
3. Zeck, U. I., "Joints In Large Panel Precast Concrete Structures", Publication PB-252 852 by U. S. Department of Commerce (N.T.I.S.), January 1976.

INDUSTRY LITERATURE

1. Ruden, S. J., "Report on Embedded Plate Pullout Tests on Precast Concrete Members", published by Prestressed Concrete of Colorado, (Stanley Structures, Inc.) in Denver, September 1971.
2. Rath, Rath & Johnson, Inc., "KSM Structural Engineering Aspects of Headed Concrete Anchors and Deformed Bar Anchors in the Concrete Industry", published by KSM Welding Systems, 1974.

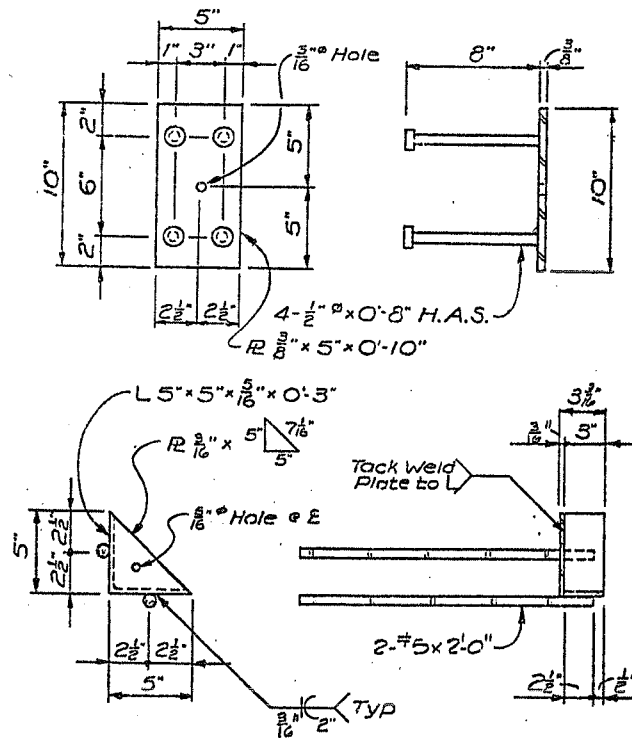


FIGURE 1 -- PLATES P-3 (TOP) AND P-8 (BOTTOM)

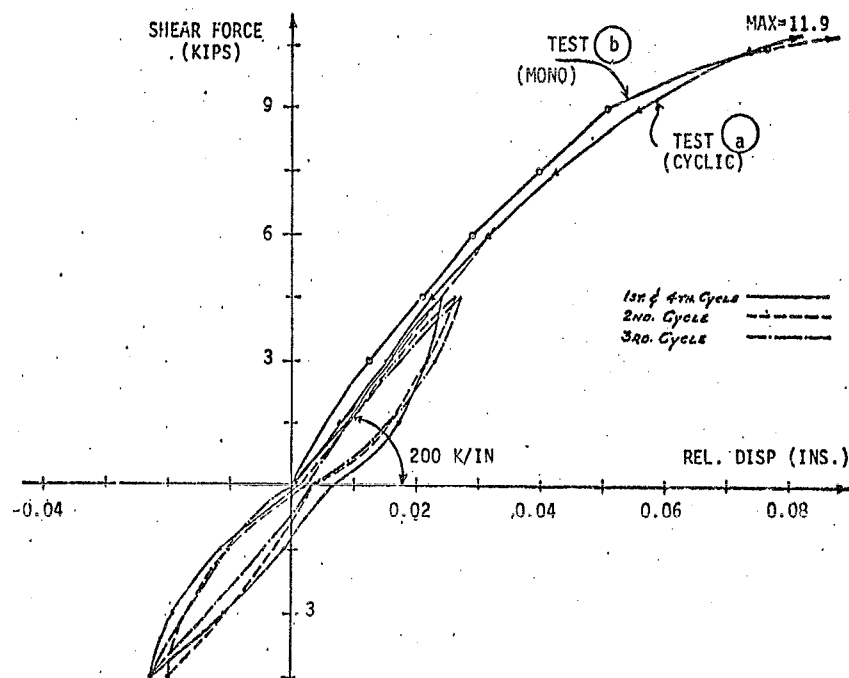


FIGURE 2 -- CYCLIC BEHAVIOR OF D-34/D-34 COMBINATION

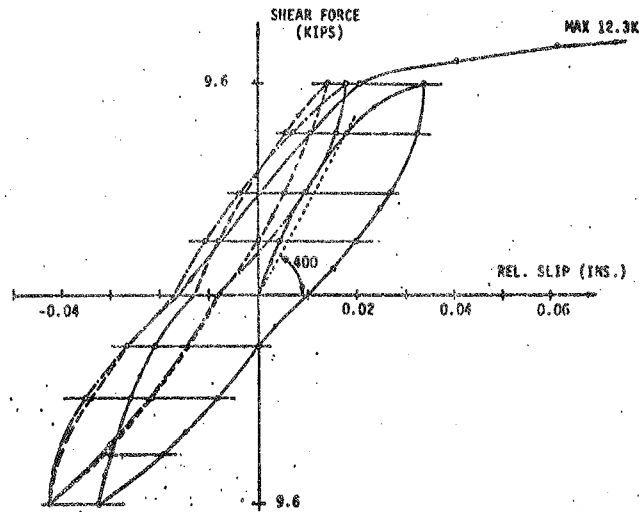


FIGURE 3 -- CYCLIC SHEAR FORCE VS. SLIP FOR D-40/D-40 TIES

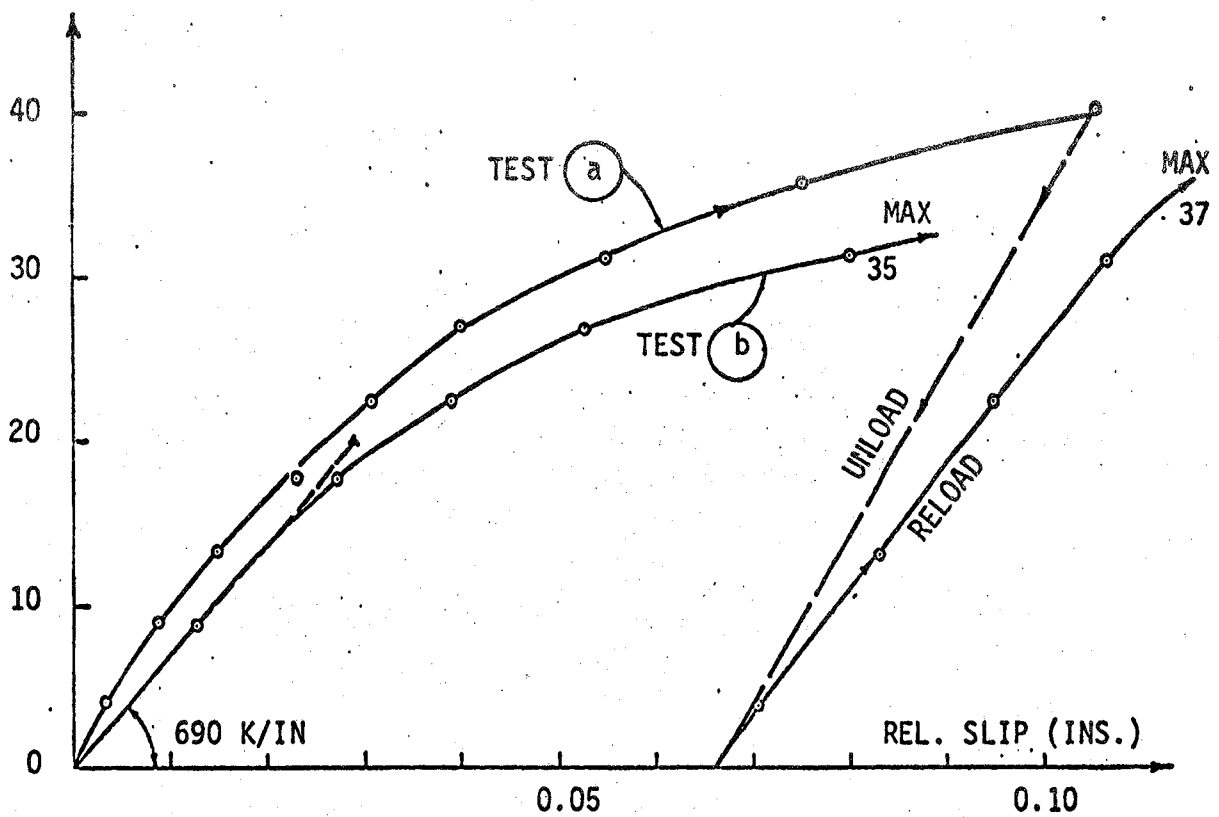


FIGURE 4 -- SHEAR FORCE VS. SLIP FOR P-8/P-3 COMBINATION

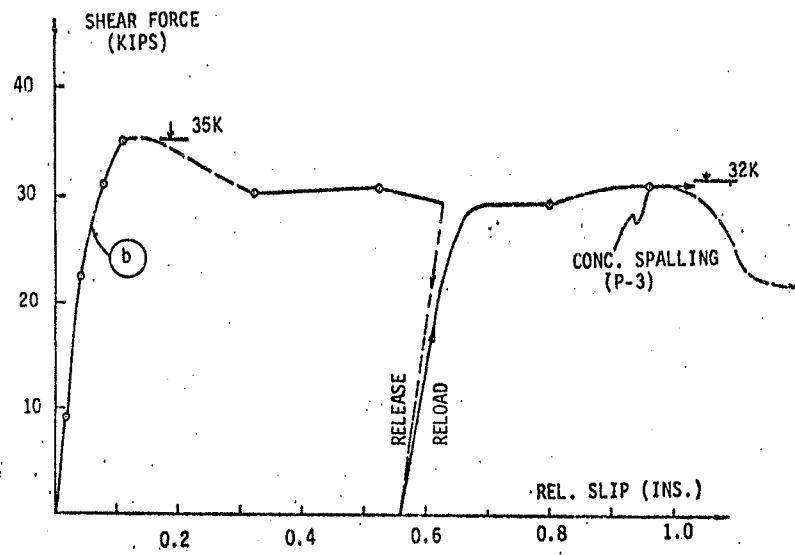


FIGURE 5 -- FORCE VS. SLIP FOR P-8/P-3,
INCLUDING DESCENDING BRANCH

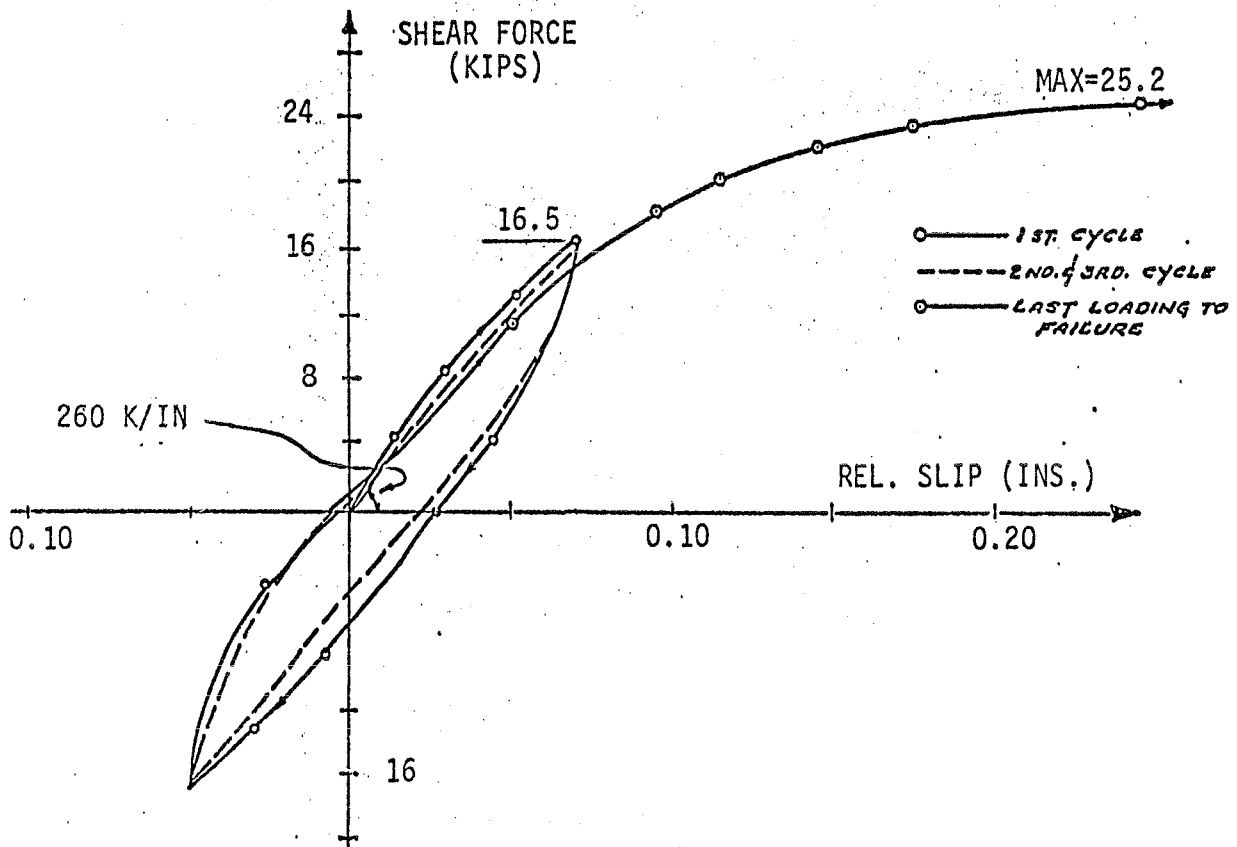


FIGURE 6 -- CYCLIC SHEAR VS. SLIP FOR P-9/P-9 COMBINATION

ENERGY DISSIPATION IN PANELIZED BUILDINGS USING LIMITED-SLIP BOLTED JOINTS

A.S. PALL

Concordia University
Montreal, Quebec
Canada

C. MARSH

Concordia University
Montreal, Quebec
Canada

SUMMARY

The paper proposes the use of limited-slip bolted joints for integrating precast concrete panels, an alternative to structural grouted joints. Preliminary results of research into energy dissipating capability of such joints are reported. Under strong earthquake excitations, the limited slip-page of joints allow for a considerable energy absorption without serious permanent deformations. This is a desirable mechanism for arresting seismic forces and a key factor in the survival of the structure. The Reserve Energy Technique, suitably modified for panelized buildings, has been used.

SUMMAIRE

L'article suivant propose une utilisation des joints à coulisse avec glissement limité pour les panneaux de béton pré-usiné soit une alternative au joint de structure nécessitant un remplissage. Les résultats préliminaires concernant la capacité de dissipation d'énergie de ces joints y sont présentés. Sous une grande excitation sismique le glissement limité des joints permet une absorption très grande d'énergie ainsi qu'une affaiblissement de la structure portante sans aucun sérieux problème de déformation permanente. Ce mécanisme est désirable pour diminuer les forces sismiques et pour garder l'intégrité de la structure. La technique de "Réserve d'énergie" a été modifiée convenablement pour les bâtiments à panneaux pré-fabriqués et est présenté dans cette étude.

INTRODUCTION

When a strong motion earthquake excites a structure, kinetic energy is fed into the structure. To survive, the structure must, without undue damage, absorb all the energy imparted to it. Elastic strain energy is often a small part of the energy demand, so the balance must be dissipated by work done in inelastic deformations and friction, etc. It is thus well recognised that energy dissipation is a key factor in explaining the survival of structures in unexpected seismic disturbances.

By the very nature of the construction process, the joints are considered to be weak links in panelized buildings. Under severe ground motions these natural planes of low stiffness and weakness are mainly responsible for introducing a non-linear behaviour to the overall system, the panels themselves remaining in the elastic stage. Thus, the connection re-

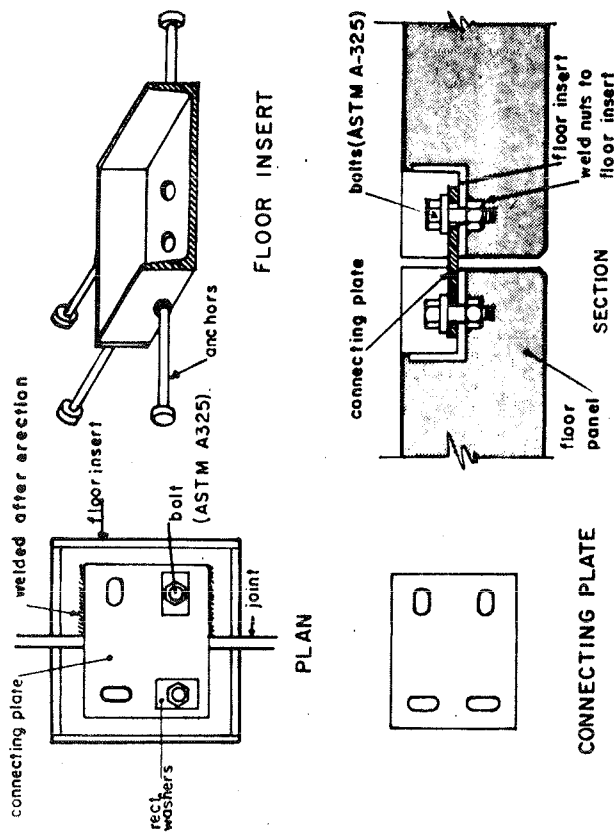


FIG. 1 FLOOR-TO-FLOOR-OR WALL-TO-WALL JOINT

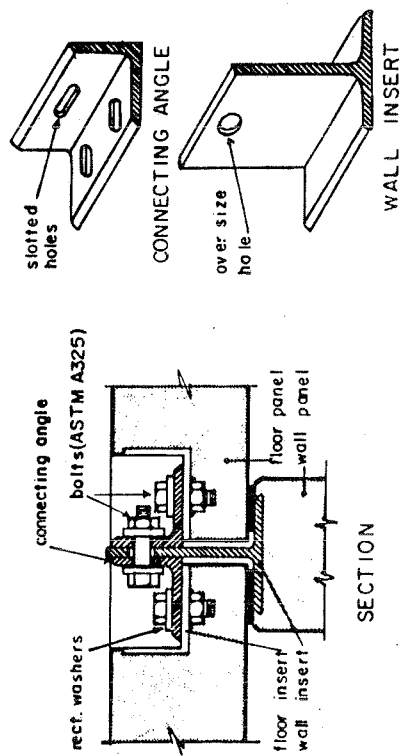


FIG. 2 FLOOR-TO-WALL JOINT

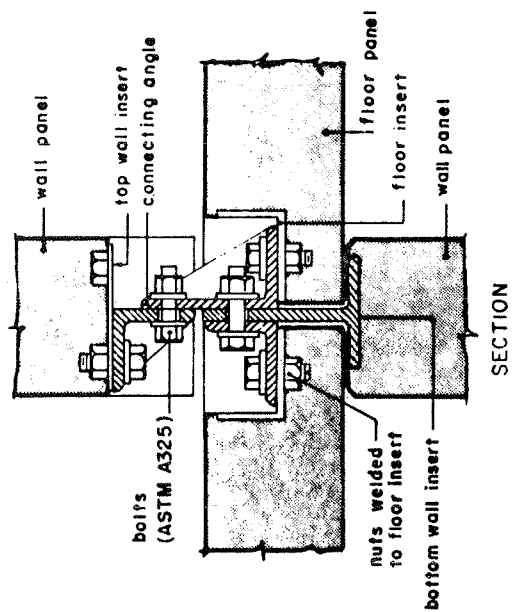


FIG. 3 FLOOR-TO-WALL JOINT

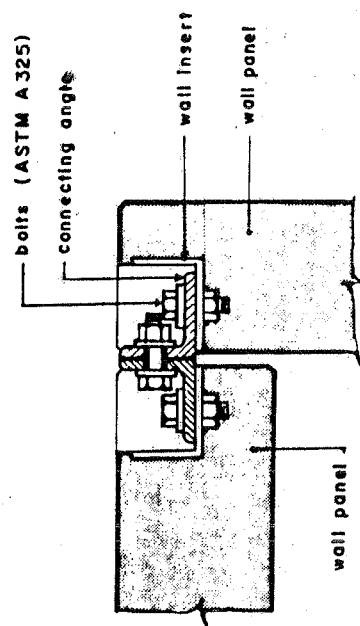


FIG. 4 CORNER WALL-TO-WALL JOINT

gion can be the location of the energy absorbing mechanism. Hence, these very planes of weakness, if properly harnessed, could be used for improving the seismic resistance of panelized buildings. The challenge, therefore, lies in maximizing the energy dissipating mechanism of the joints. To rationally satisfy the seismic demands, limited-slip bolted joints are proposed as an alternative to the usual structural grouted joints.

LIMITED-SLIP BOLTED JOINTS

Limited-slip bolted joints, hereafter referred to as LSB joints, consist of steel plates or sections with slotted holes which are friction bolted to steel inserts anchored into concrete panels. Figures 1 to 4 show the details for slab and wall joints. The length of slot accommodates the normal fabrication and erection tolerances with an additional clearance to absorb energy by slipping. At the same time the slip is not to be too large as to distort the structure beyond acceptable limits.

With LSB system, the horizontal joints in the wall will be grouted or dry packed after, say, three storey levels have been erected. The vertical joints are the ones expected to slip under severe seismic action. These joints will not be grouted but sealed by other appropriate means. Floor slab joints will be grouted or otherwise sealed. The grouting process is independent of erection operation and can proceed uninterrupted, sheltered from the weather.

Using this system, mechanization is extended to the jointing process so that the entire construction operation is totally industrialized. Fabrication of panels is already considered to be industrialized.

Several static and dynamic cyclic tests have been conducted on connection specimens having different faying surface treatments to evaluate basic design properties (Pall, Marsh, Fazio, 1979). Load-deformation curves and hysteresis loops for wall to wall connection, using 12.7mm dia. high strength bolts (ASTM A325), are shown in Figures 5 and 6 respectively. In general, up to the point of slipping the connection behaves elastically after which the slippage absorbs energy, simulating plastic behaviour. As the bolt reaches the end of slot hole, it goes into bearing, giving an ultimate load much higher than that causing slip. Appropriate surface finish can be selected based on strength and economy considerations.

ANALYSIS

At peak seismic demands, feed-in kinetic energy less feedback from the structure into the soil layer must balance elastic strain energy plus energy lost in friction and work done in non-linear deformations.

Most of the multistorey panelized buildings fall in the intermediate range of frequencies, for which the principle of constant energy input applies (Newmark and Hall, 1973), i.e. energy input elastically or inelastically remains the same. So it is possible to calculate kinetic energy fed into the building, considering only elastic behaviour.

The force-deflection diagram of a structure is used as a measure of total work capacity. The diagram is plotted for some trial deflections until the energy demand and energy capacity of the structure are reconciled.

The Reserve energy technique (Blume, 1961), originally developed for

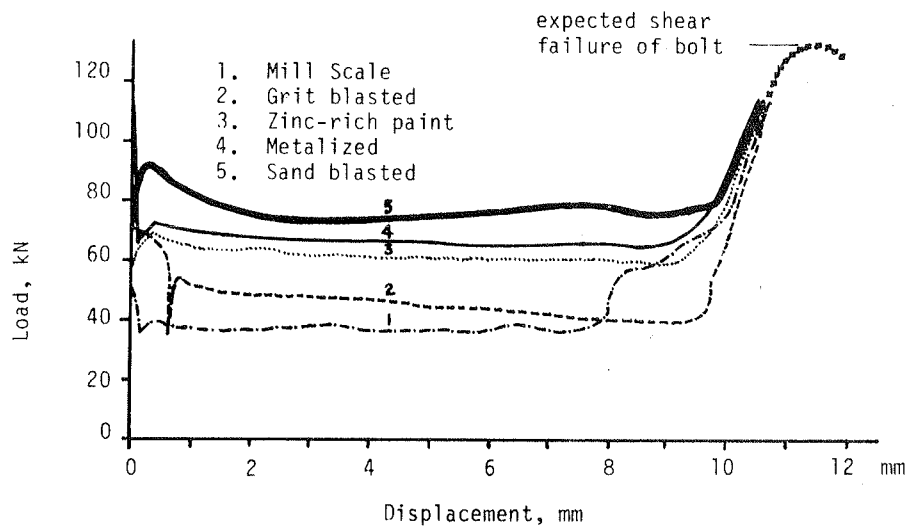


FIG. 5 LOAD DISPLACEMENT CURVE, WALL-TO-WALL JOINT

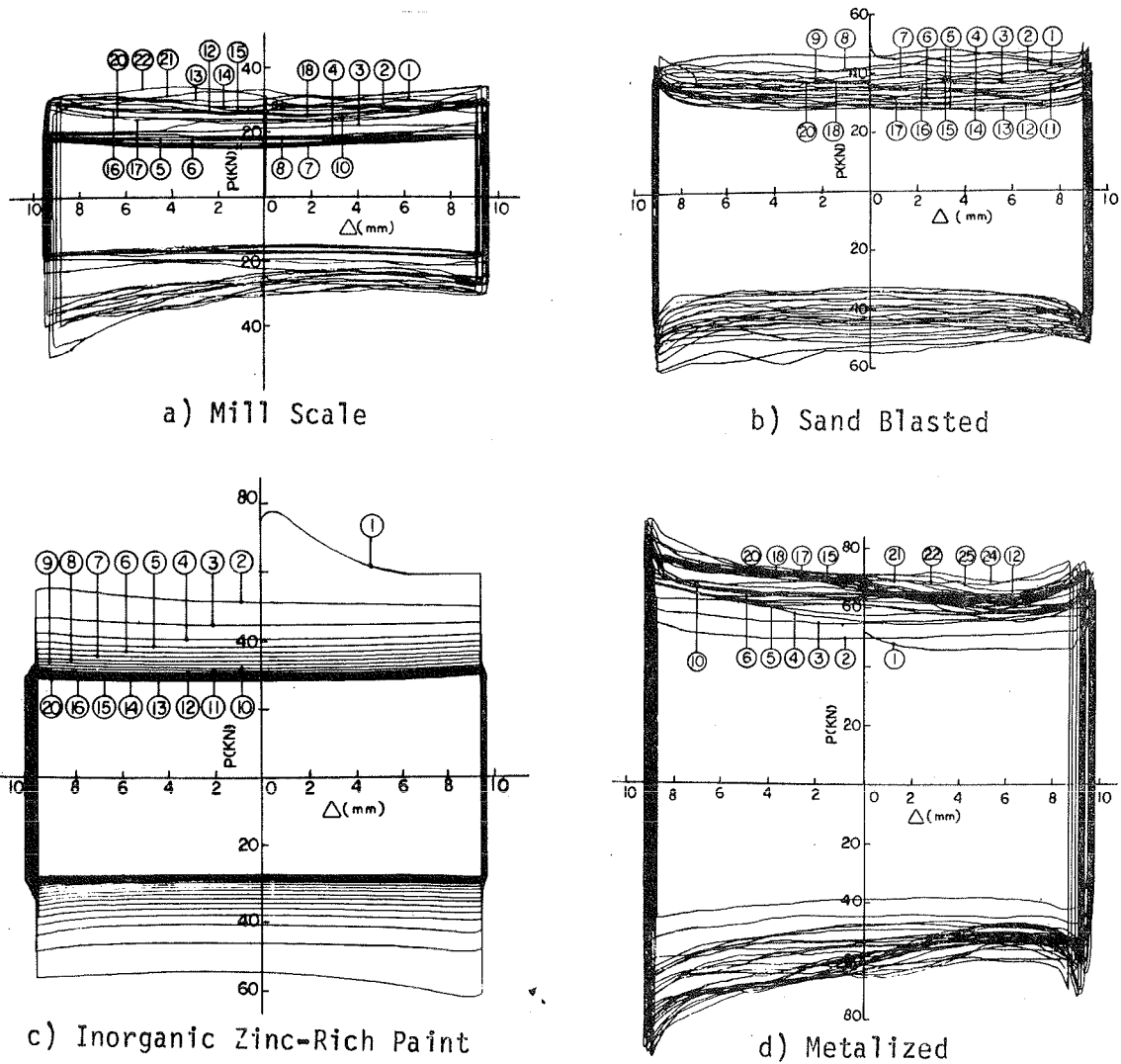


FIG. 6 HYSTERESIS LOOPS, WALL-TO-WALL JOINT

framed buildings, has been used for panelized buildings with the following modifications:

- a) Since the mode of deflection is basically flexure, possibility of failure is most likely at the base of the wall, so it is sufficient to reconcile the energy demand only at the lower most storey.
- b) The deterioration factor (γ) accounts for the reduction in work capacity after several excursions, due to the degradation of the properties of the panels and the joints. In the present case, it is taken as 0.3.
- c) Since the structural rigidity is constant over the height and fewer modes are excited than in the framed buildings, the participation of other storeys in draining energy (α) is considered to be 75% instead of 50% assumed for framed buildings.
- d) Since panelized walls essentially deform in the bending mode, the work done is predominantly due to the primary moments with a small contribution from shear forces.

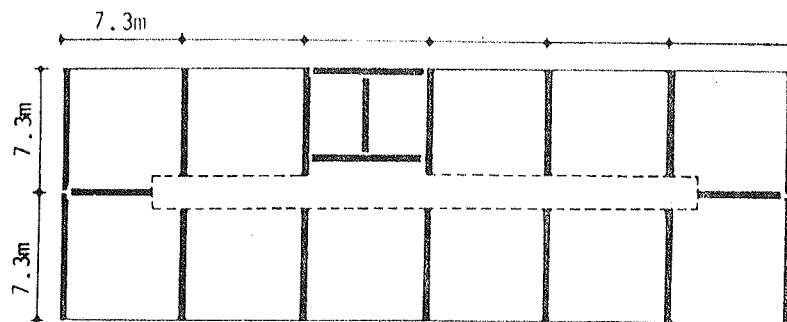


FIG. 7 TYPICAL PANELIZED BUILDING

Typical Example

In order to investigate the energy absorbing capabilities of proposed joints, typical apartment buildings (Fig. 7) of 10 and 15 storeys were studied. The buildings are considered to be located in zone 3 (NBC, 1977) which has a peak ground acceleration of 0.08g for a probability of one in 100 years and 0.25g for a probability of one in 200 years. Probability of return of the latter earthquake during the life of the building is very low but the design could ensure the safety of structure even in this extreme case. Analysis is made for only exterior end walls having vertical joints. Structural idealization and properties of these walls are shown in Fig. 8. The following assumptions are made in the analysis:

- a) Floor diaphragm is infinitely rigid in its own plane and flexible out of plane (Unemori, 1978).
- b) Each interior cross wall is considered as two individual isolated walls.
- c) Vertical panel walls are considered as continuous elastic cantilevers. Although each cantilever wall includes horizontal joints, for the present analysis it is assumed that gravity loads (or post-tensioning, if necessary for higher seismic accelerations) produce sufficient friction to prevent any shear slip or rocking. Additional energy dissipation is, however, expected

in these joints (Becker, 1978).

- d) The initial damping for elastic vibrations is assumed to be viscous and is taken as 5% of the critical value (Brankov, 1977).
- e) Foundations are rigid and 10% energy radiation is assumed from the structure into the soil layer (Blume, 1961).
- f) The panels, being large, remain in the elastic range.
- g) The stiffness of the connection is a function of the load on the connection and the relative displacement of the connected parts (Fig. 8).

It is realised that the above assumptions may not be truly realistic, however, at this preliminary level, they allow the examination of the basic behavioural mechanism.

Response spectrum analysis using elastic response spectra (NBC, 1977), was carried out on a computer (TABS, 1973), for peak ground accelerations of 0.08g, 0.10g, 0.15g, 0.20g and 0.25g. Root mean square combination was employed for the first three modes only. Probable elastic shears and quasi-static design shears for the 15 storey building are shown in Fig. 9.

Analysis of the wall (Fig. 8) for static lateral loads was carried out by displacement method using a plane frame computer program (MAP, 1975). Shear deformations were taken into account. Due to slipping of connections in vertical joints, the analysis involves step by step integration of short load increments, assuming the stiffness properties of connection remain constant during each increment but changing in accordance with the load deformation state existing at the end of increment.

Force-displacement diagrams for each storey were prepared for panel walls as well as for joints for different trial deflections (Fig. 10). The sum of the areas of these diagrams represent the total work capacity of the storey.

Curves were plotted for reconciliation of energy demand at the lowest storey (Fig. 11). Intersection of these curves with code design coefficient \bar{C} is the point up to which the building must deform to balance the energy demand.

DISCUSSION OF RESULTS

- a) It is seen from the analysis for 10 and 15 storey buildings that both the buildings are capable of resisting 0.08g seismic level within elastic range, but at higher ground accelerations the joints slip and force the overall building into non-linear behaviour.
- b) As the connections slip, redistribution of the forces in the joints takes place until they become almost uniform throughout the height. Had the connections been elastic, the forces would be distributed as shown by the dotted lines in Fig. 12. One of the effects of slipping joint is, therefore, to provide a limit to load and to allow the capacities of all the standardized connections to be utilized.
- c) Energy absorption capacities of the proposed joints are shown in Figs. 13 and 14. It is seen that at higher seismic levels, nearly 25% of the

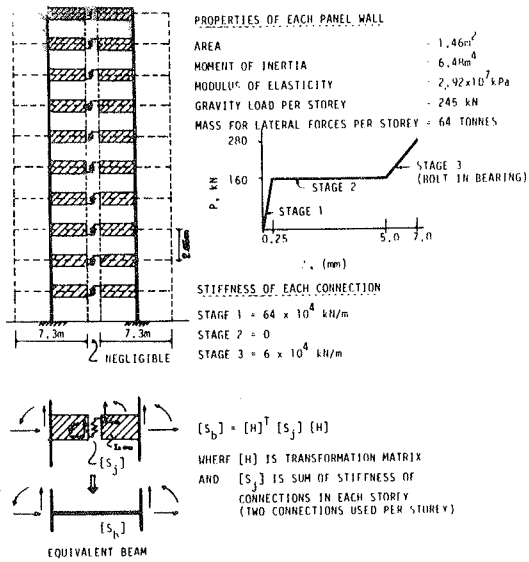


FIG. 8 STRUCTURE IDEALISATION

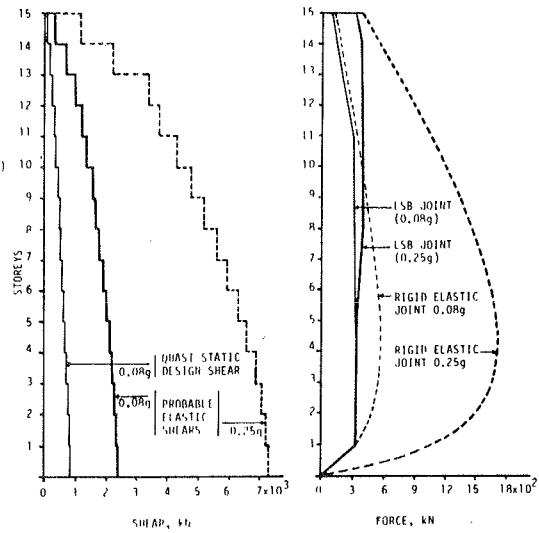


FIG. 9 STOREY SHEARS

FIG. 12 FORCES IN JOINTS

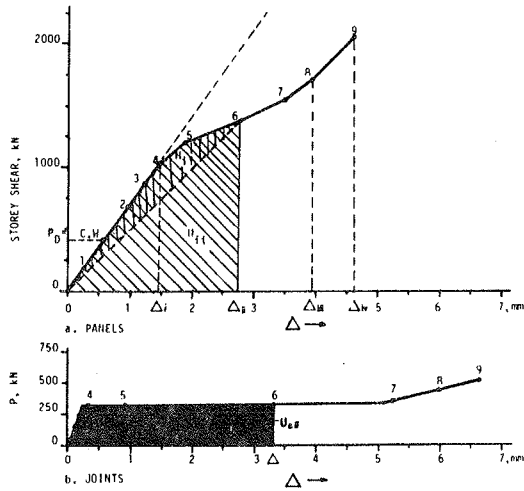


FIG. 10 LOAD-DISPL. DIAGRAM, 11th STOREY, 15 STOREY BUILDING

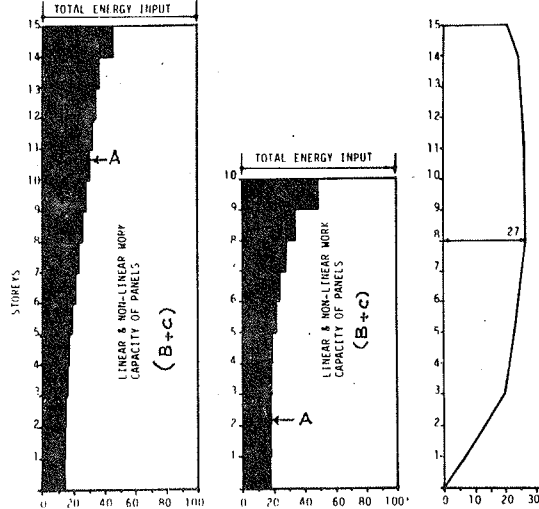


FIG. 13 ENERGY DISSIPATED BY JOINTS, 0.25g

FIG. 15 DUCTILITY IN JOINTS

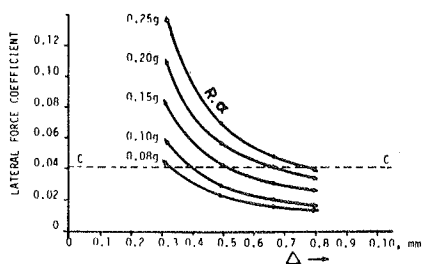


FIG. 11 ENERGY RECONCILIATION AT FIRST STOREY, 15 STOREY BLDG

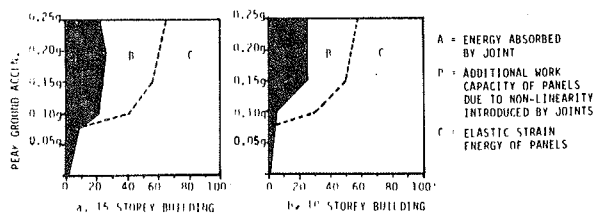


FIG. 14 TOTAL ENERGY DISSIPATED BY JOINTS

total energy is absorbed by the joints in friction alone. Furthermore, the joints have contributed indirectly in softening the structure by introducing non-linearity to the otherwise elastic panels. Thus, LSB joints act as friction dampers and are the main source of energy dissipation.

d) The need for the building to deform into the non-linear range places high ductility demands on the joints. Ordinary grouted joints with reinforcing loops cannot meet such a demand without permanent damage. The term "ductility", although incorrect for the proposed joints, is purposely used to be commonly understood. For the present joints, it is the ratio of final displacement of the connection after slip to its elastic deformation before slip. There is no yielding of material involved in the proposed joints which is desirable from the point of view of damage or repairs.

e) After the earthquake, the stored elastic strain energy of the panels will restore the connections nearly to their original position and the building will be ready to face future earthquakes.

CONCLUSION

Limited-slip bolted joints seem to extend the benefits of industrialization of panels to the erection procedure.

Preliminary analysis shows that such joints dissipate sufficient energy to improve significantly the response of panelized buildings when subjected to severe ground motions. Furthermore, due to softening of the structure, caused by slipping joints, the effective periods of vibration are prolonged which is also beneficial in attracting less seismic accelerations. To this end, rigorous non-linear dynamic analysis is in progress to study the seismic performance of panelized buildings using such joints.

REFERENCES

1. Becker, J.M., Rosset, J.M. and Llorente, K., "The Seismic Response of Precast Concrete Panel Buildings Considering Connection Behaviour", Sixth European Conf. on Earthquake Engineering, Dubrovnik, Yug., 1978.
2. Blume, J.A., Newmark, N.M. and Corning, L.H., "Design of Multistorey Reinforced Concrete Buildings for Earthquake Motions", P.C.A., Skokie, Ill., U.S.A., 1961.
3. Newmark, N.M. and Hall, W.J., "A Rational Approach to Seismic Design Standards for Structures", 5 W.C.E.E., Rome, 1973.
4. Brankov, G. and Sachanski, S., "Response of Large Panel Buildings for Earthquake Excitations in Non-Linear Stage", 6 W.C.E.E., New Delhi, 1977.
5. MAP - Matrix Analysis Program, by Ha, H.K., Centre for Building Studies, Concordia University, Montreal, 1975.
6. National Building Code of Canada, NBC-1977, Commentary on Part 4, National Research Council of Canada, Ottawa, Canada.
7. Pall, A.S., Marsh, C. and Fazio, P., "Limited-Slip Bolted Joints for Large Panel Concrete Structures", Behaviour of Building Systems and Building Components, Vanderbilt University, Nashville, Tenn., 1979.
8. Unemori, A.L., Rosset, J.M. and Becker, J.M., "Effect of Inplane Floor Slab Flexibility on the Response of Crosswall Bldg.", M.I.T., Cambridge.

THEME IV

SEISMIC BEHAVIOUR OF CONCRETE STRUCTURES: OBSERVATION OF
ACTUAL STRUCTURES AND LABORATORY TESTS

COMPOTEMENT SISMIQUE DES STRUCTURES EN BETON: OBSERVATIONS
"IN SITU" ET ESSAIS EN LABORATOIRE

Reporter
Rapporteur

Giuseppe GRANDORI
Polytechnic of Milan
Italy

STUDY ON HYSTERETIC BEHAVIOUR OF STATICALLY
INDETERMINATE PRESTRESSED CONCRETE FRAME STRUCTURE
SUBJECTED TO REVERSED CYCLIC LATERAL LOAD

Hiroshi MUGURUMA

Kyoto University
Japan

SUMMARY: To investigate the lateral load-deflection hysteretic characteristics of prestressed concrete frame structure, reversed cyclic loading tests were carried out on two portal frame specimens consisting of prestressed concrete beam and ordinary reinforced concrete solumns. Test results were discussed in terms of the lateral deflection ductility of frame itself and the rotating ductility of constituent member sections. The lateral load-deflection hysteresis curves were calculated on the basis of idealized moment-curvature relations of constituent member sections. Measured hysteresis curves agreed well with calculated ones.

RESUME: Pour préciser les caractéristiques de l'hystérèses de flexion de charge latérale des charpentes en béton précontraint, furent effectués les examens de charge latérale à cycles alternatifs sur deux portiques formés de poutres en béton précontraint et de colonnes ordinaires en béton armé. Les résultats furent traduits en termes de ductilité de flexion latéral du portique même, et de ductilité rotative des éléments constitutifs. La courbe de l'hystérèse de flexion de charge latéral de la charpente fut calculée à partir de la moyenne ideale des relations entre moments et courbures dans les différents éléments constitutifs. La courbe de l'hystérèse mesuré s'avéra correspondre avec celle de l'hystérèse calculée à priori.

1. INTRODUCTION

In the seismic response analysis of structures the restoring force characteristics under cyclic lateral load should be adequately assumed on the basis of experimental or theoretical elasto-plastic deformation behaviours of constituent members or structure itself. As the prestressed concrete frame construction concerns, a few experimental works under lateral load had been presented in the past¹⁾⁻⁴⁾, but the knowledges on lateral load-deflection characteristics are not always sufficient for estimating the ductility or energy absorption capability. In this study, the reversed cyclic lateral loading tests were carried out on statically indeterminate portal frame consisting of prestressed concrete beam and ordinary reinforced concrete columns. The lateral load-deflection hysteresis obtained were compared with the calculation based on the moment-curvature relation of constituent member section. And further, the relation between the ductility factor obtained from lateral deflection of frame and that from rotating curvature at critical section of constituent members were discussed.

2. TEST SPECIMENS

Two portal frame specimens were tested by applying the lateral load. The frame of 4.2 m long and 1 m high consists of prestressed concrete beam and ordinary reinforced concrete columns as shown in Fig. 1. The dimensions of cross section are 16 cm in width and 21 cm in depth for both prestressed concrete beam and ordinary reinforced concrete columns. Throughout the whole length of beam, uniformly distributed prestress was transferred into the concrete section by 2- $\phi 11$ mm dia. prestressing steel bars. The column was reinforced by 4-D16 mm and 4-D13 mm dia. ordinary deformed bars with $\phi 9$ mm dia. closed stirrups in a pitch of 6.5 cm. The reinforcements in columns were anchored mechanically on the top surface to prevent the slippage of reinforcement from beam-column joint. Mechanical properties of prestressing steel bar and ordinary reinforcements are listed in Table 1.

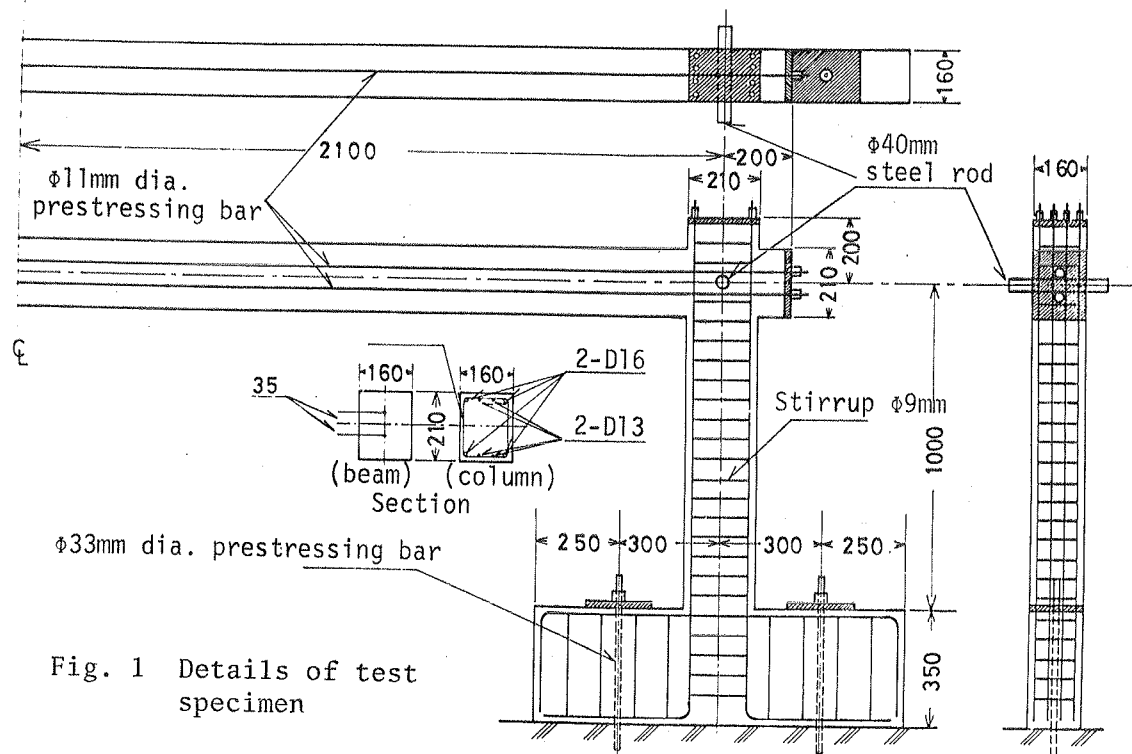


Fig. 1 Details of test specimen

The frame specimens were cast in monolithic in the vertical position. Normal portland cement, river sand and river gravel with maximum size of 20 mm were used in the concrete. Mix proportion of concrete was 1:1.64:2.13 by weight with water-cement ratio of 0.45. After casting,

the specimens were wet-cured until at the age of 28 days. At 28 days, the prestressing force of 18.6 tons in nominal was transferred into the beam section and neat cement paste with the water-cement ratio of 0.45 was injected into the ducts for prestressing steel bars. After that, the specimens were stored in air until the test age of 3 months. In Table 2, properties of con-

Table 1 Mechanical properties of prestressing steel bar and ordinary reinforcement

| | Prestressing steel bar | Longitudinal reinforcement | | Hoop reinforcement |
|---|------------------------|----------------------------|-----------|--------------------|
| Diameter (mm) | $\phi 11$ | D 16 | D 13 | $\phi 9$ |
| Sectional area (cm) | 0.95 | 1.99 | 1.27 | 0.64 |
| Yielding stress (kg/cm ²) | 14,800* | 3,786 | 3,502 | 3,182 |
| Tensile strength (kg/cm ²) | 15,300 | 5,578 | 5,315 | 4,609 |
| Modulus of elasticity (kg/cm ²) | 2,104,000 | 1,920,000 | 1,720,000 | 2,050,000 |

* 0.2 % off-set stress

crete are summarized. Also, in Table 3, initial prestressing force actually transferred and effective prestressing force at the test age are listed.

Table 2 Properties of concrete

| Test specimen | At prestress transfer (at 28 days) | | | At the age of loading test (3 months) | | |
|-------------------------|------------------------------------|---|-----------------|---------------------------------------|---|-----------------|
| | Comp. strength | Tens. strength (kg/cm ²) | Elastic modulus | Comp. strength | Tens. strength (kg/cm ²) | Elastic modulus |
| Frame No. 1 | 386 | 31.2 | 255,000 | 421 | 38.6 | 275,000 |
| No. 2 | 387 | 28.1 | 244,000 | 429 | 30.6 | 215,000 |
| Control beam and column | 369 | 26.2 | 265,000 | 432 | 28.3 | 237,000 |

In addition, control beam and column specimens were made with frame specimens for obtaining the moment-curvature relations and reversed cyclic loading tests were carried out prior to lateral loading tests on frames.

Table 3 Prestressing force transferred into beam section

| Specimen | Initial prestressing force transferred (tons) | Effective prestressing force at the test age (tons) | Effective ratio (%) |
|--------------|---|---|---------------------|
| Frame No. 1 | 18.53 | 17.36 | 93.7 |
| Frame No. 2 | 18.71 | 17.82 | 95.2 |
| Control beam | 17.61 | 16.51 | 93.7 |

3. TEST PROCEDURES

At the age of 3 months lateral loading tests were carried out. For providing the fixed column foot, the column bases of the specimen were connected rigidly on the concrete testing floor by prestressing. Two hydraulic jacks with servo-valve for cyclic loadings were connected to the steel rods previously cast into both column-beam joints. The lateral load was applied to the frame by means of pulling by one jack at one end and simultaneously pushing by remaining jack at another end. By such means, the occurrence of axial force in beam or twisting of frame during the lateral loading can be avoided.

In this study, Frame No.1 was loaded monotonically in one direction for obtaining the lateral load-deflection skeleton curve, while Frame No.2 was tested under reversed cyclic loadings, where any vertical load was not applied to the frame. The lateral deflection of frame was measured at exterior face of both column-beam joints by linear transformer.

4. TEST RESULTS AND DISCUSSIONS

(a) Moment-Curvature Relations of Constituent Member Section

Load-deflection relation of frame can be calculated primarily by using the moment-curvature relations of constituent member sections. In this study, the moment-curvature relations were measured from control beam and column specimens under reversed cyclic loadings. The results are shown by dotted lines in Fig. 2(a) and 2(b), respectively. Also, moment-curvature relations idealized by using the values of resisting moment and corresponding curvature at the critical points such as at initial cracking, crack re-opening, tensile steel yielding and ultimate flexural loading capabilities are shown in the Figure by solid lines. These values were calculated in this study by applying the following idealized stress-strain curves for concrete and steels and by assuming the linear strain distribution overall the section.

Concrete⁵⁾ : For $0 \leq \epsilon_c \leq \epsilon_{cu}'$

$$\sigma_c = E_c \epsilon_c + (f_c' - E_c \epsilon_{cu}') \epsilon_c^2 / \epsilon_{cu}'^2 \quad (1)$$

$$\epsilon_{cu}' = (0.0013 f_c' + 1.299) \times 10^{-3} \quad (2)$$

$$E_c = 2.31 \times 10^5 \sqrt{f_c' / 200}$$

For $\epsilon_{cu}' \leq \epsilon_c \leq 0.004$

$$\sigma_c = \frac{f_c' - 150}{\epsilon_{cu}' - 0.004} \epsilon_c + \frac{150 \epsilon_{cu}' - 0.004 f_c'}{\epsilon_{cu}' - 0.004} \quad (3)$$

For $\epsilon_c \geq 0.004$

$$\sigma_c = 150 \text{ kg/cm}^2 \quad (4)$$

ϵ_c : Concrete strain, σ_c : Compressive stress in kg/cm²

f_c' : Cylinder strength in kg/cm², E_c : Elastic modulus

Prestressing steel bar and ordinary reinforcement: Ideal elasto-plastic relation having elastic modulus and yield strength listed in Table 1.

The results of calculations are summarized in Table 4.

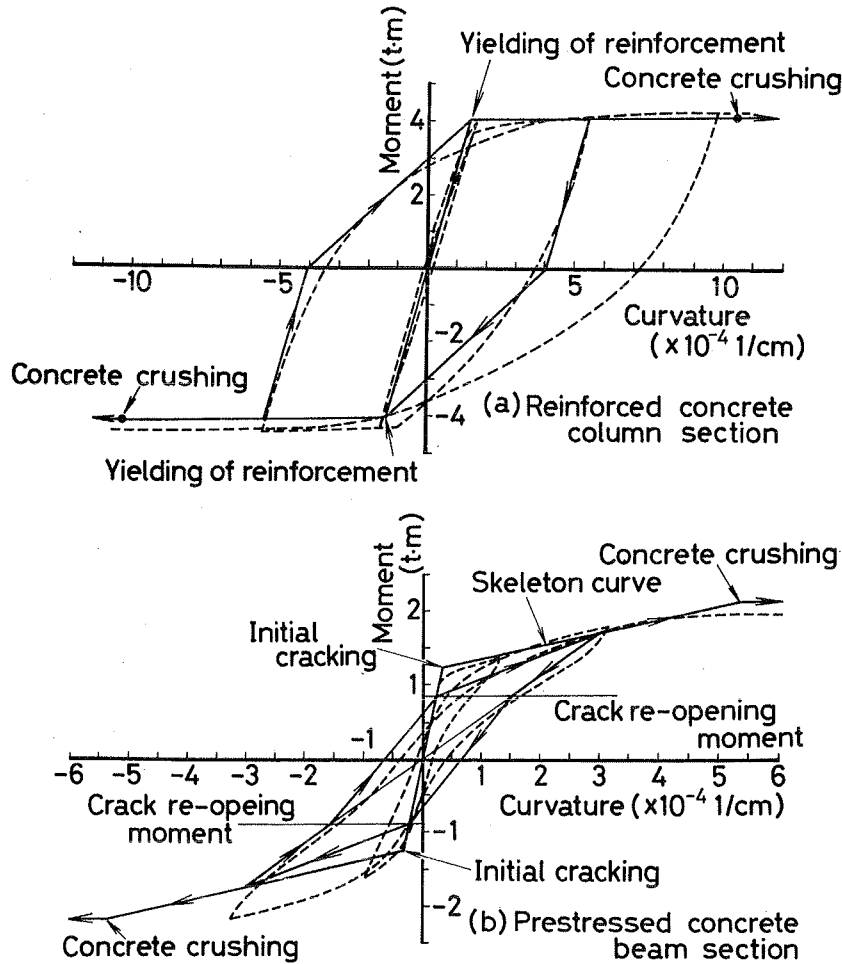


Fig. 2 Measured and idealized moment-curvature relations of constituent member sections.

Table 4 Calculated results on moment and corresponding curvature of constituent member sections at critical loading stages for idealizing the moment-curvature relation

| | Critical loading stage | Moment (t.m) | Curvature ($\times 10^{-4} 1/cm$) | Comp. fiber strain of concrete (%) |
|----------------|-------------------------------|--------------|-------------------------------------|------------------------------------|
| Beam section | Initial cracking | 1.24 | 0.36 | 0.035 |
| | Concrete crushing* (ultimate) | 2.18 | 5.34 | 0.289** |
| | Crack re-opening | 0.88 | — | — |
| Column section | Initial cracking | 0.75 | 0.20 | 0.020 |
| | Tensile steel yielding | 4.05 | 1.40 | 0.091 |
| | Concrete crushing* (ultimate) | 4.21 | 10.35 | 0.289** |

* The ultimate flexural moment is assumed as the moment at which the compressive fiber strain of concrete attains at the strain that the average stress in stress-strain curve of concrete becomes maximum, that is, the strain at which the stress block coefficient, k_1k_3 , becomes maximum.

** The value of 0.289 % is calculated from Eqs.(1) ~ (3) in accordance to above described definition.

(b) Lateral Load-Deflection Skeleton Curves and Ductility of Frame

In Fig. 3, lateral load-deflection skeleton curve measured from Frame No. 1 is illustrated by solid line. The initial flexural crack took place at both column foot sections at the lateral load of 2.25 tons (Point A in Fig. 3) and followed at both end sections of beam at 4 tons (Point B). When applied load is 10.1 tons, the yielding took place at both column foot sections (Point C) and after that the large elasto-plastic lateral deformation was observed because of the formation of plastic hinge at column foot sections. At the load of 12.3 tons the crushing of concrete took place at both end sections of beam (Point E) and the frame becomes failure mechanism with considerable post-crushing plastic deformation. Thus, in this study, the deflection at crushing

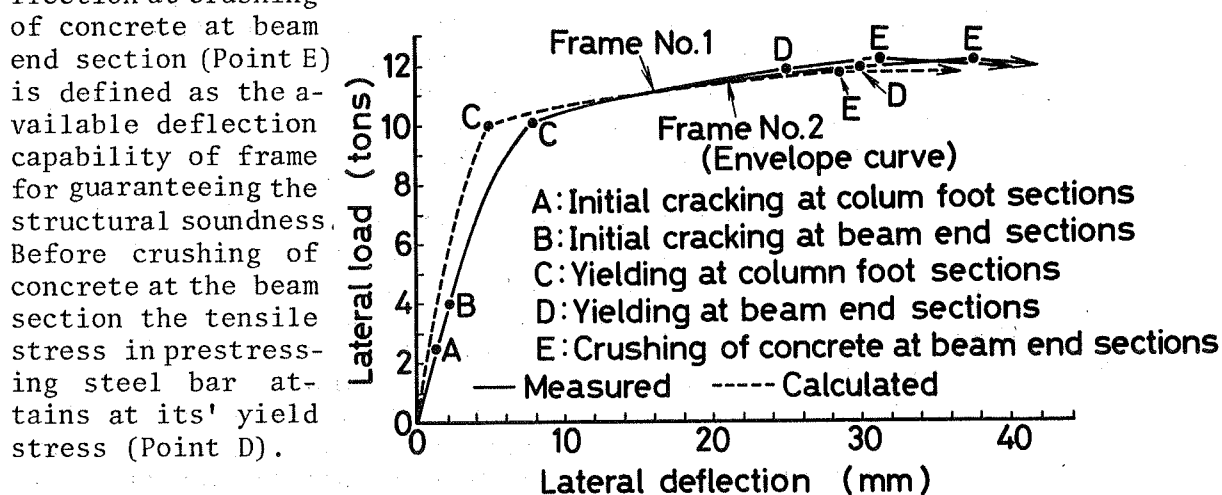


Fig. 3 Measured and calculated lateral load-deflection skeleton curves of frame

Lateral load-deflection skeleton curve of frame can be calculated by using the idealized moment-curvature relations of constituent member sections shown in Fig. 2 (a) and 2 (b), respectively. The method of calculation is described in Section 4 (d). The result is plotted in Fig. 3 by dotted line. The calculated curve agrees fairly well with measured ones.

(c) Ductility Factor of Frame and Rotating Ductility Factor at Critical Section

The measured deflections at the yielding of column foot sections (Point C in Fig. 3) and at the crushing of concrete at beam end sections (Point E) are summarized in Table 5 with calculated ones. In this study, available ductility factor of frame is defined as the ratio of lateral deflection at failure mechanism to that at the yielding of column foot sections. These values are also listed in Table 5. Obtained value of $\mu_f = 3.930$ or $\mu_f = 4.709$ in Table 5 seems to be sufficient for ensuring the seismic safety, considering the large post-crushing deflections after failure mechanism as shown in Fig. 3.

Table 5 Summary of measured and calculated lateral deflections of frame specimens and corresponding moment-curvature values at critical sections

| Loading stage | | At the yielding of column foot sections (Point C in Fig. 3) | At the crushing of concrete at beam end sections (Point E in Fig. 3) |
|----------------------------------|--|---|--|
| Frame No. 1 (Measured) | Load (tons) Lateral deflection (mm) Ductility factor | $\delta_y = 10.1$ 7.97 $\mu_f = \delta_u / \delta_y = 3.930$ | $\delta_u = 12.3$ 31.36 |
| Frame No. 2 (Measured) | Load (tons) Lateral deflection (mm) Ductility factor | $\delta_y = 10.1$ 7.98 $\mu_f = \delta_u / \delta_y = 4.709$ | $\delta_u = 12.1$ 37.58 |
| Frame (Calculated) | Load (tons) Lateral deflection (mm) Ductility factor | $\delta_y = 10.0$ 4.72 $\mu_f = \delta_u / \delta_y = 6.117$ | $\delta_u = 11.7$ 28.87 |
| Column foot section (Calculated) | Moment (t.m) Curvature (1/cm) Conc. fiber strain (%) Ductility factor | $c\phi_y = 4.05$ 1.40×10^{-4} 0.091 $\mu_c = c\phi_u / c\phi_y = 6.036$ | $c\phi_u = 4.21$ 8.45×10^{-4} 0.252^* |
| Beam end section (Calculated) | Moment (t.m) Curvature (1/cm) Conc. fiber strain (%) Ductility factor | $b\phi_y = 2.17$ 3.20×10^{-4} 0.190 $\mu_b = b\phi_u / b\phi_y = 1.669$ | $b\phi_u = 2.18$ 5.34×10^{-4} 0.289 |

* The compressive fiber strain of concrete does not attain at the crushing strain of 0.289 % when crushing of concrete takes place at beam end sections.

For guaranteeing the large available ductility in frame, the yielding section of constituent member before the frame becomes failure mechanism should continuously rotate without considerable decrease of resisting moment. From such consideration, calculated resisting moments and curvatures at critical sections are listed in Table 5 in corresponding to the yielding and failure mechanism of frame. As can be seen in Table 5, the curvature of $c\phi_y = 1.40 \times 10^{-4}$ 1/cm at column foot section at frame yielding increases to $c\phi_u = 8.45 \times 10^{-4}$ 1/cm when the frame becomes failure mechanism. Thus, it can be concluded that in the frame used in this study column foot section should have rotating ductility factor more than $\mu_c = c\phi_u / c\phi_y = 6.036$ for guaranteeing the ductile post-prak lateral deflection behaviour in frame. On the contrary, at failure mechanism of frame the curvature at beam end sections becomes $b\phi_u = 5.34 \times 10^{-4}$ 1/cm, while at yielding of column foot section it is $b\phi_y = 3.20 \times 10^{-4}$ 1/cm. Therefore, it may be noted that the plastic deflection of frame after yielding of column foot section is mainly owing to the plastic rotation of column foot sections.

(d) Lateral Load-Deflection hysteretic behaviours

In Fig. 4, lateral load-deflection hysteresis curve obtained from reversed cyclic loading tests on Frame No. 2 is shown by solid line. As can be seen from Fig. 4, good spindle shaped hysteresis loops with large energy dissipation capability are observed. In this study, the reinforcements in column of frame specimen were anchored mechanically on the top surface of column for preventing the bond slippage of reinforcements from beam-column joint. This may results in the good spindle shape in hysteresis loops.

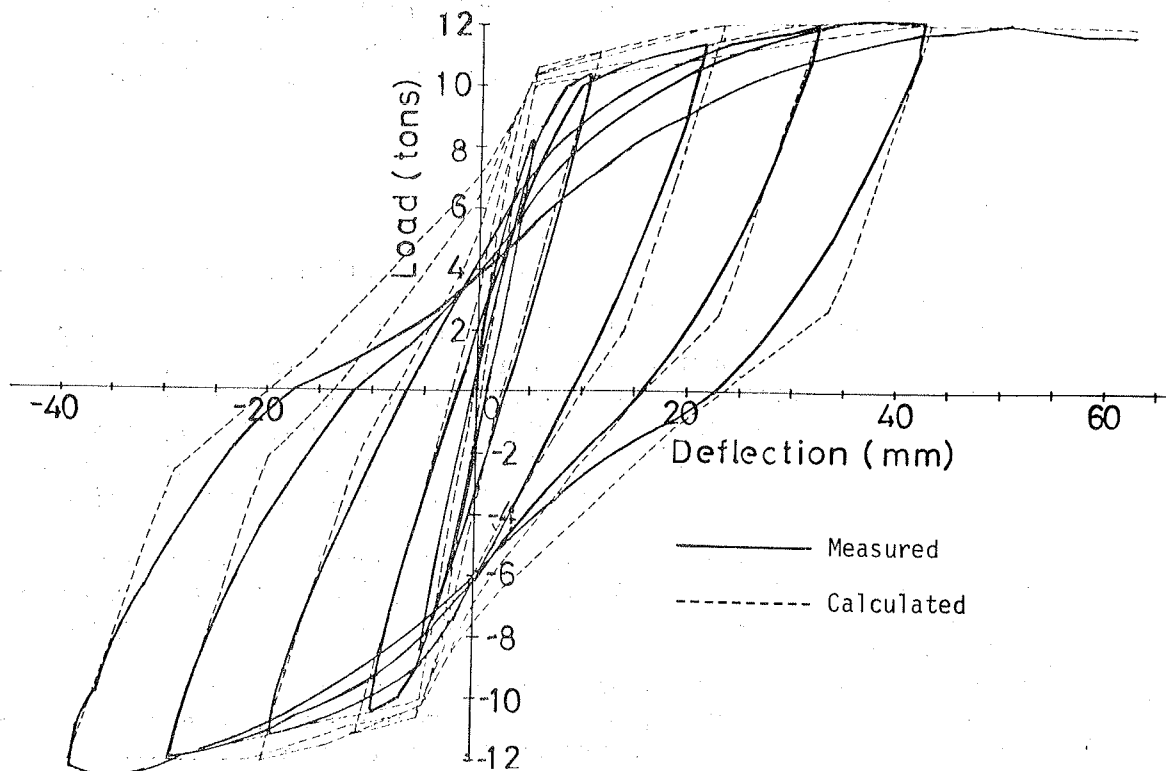


Fig. 4 Measured and calculated lateral load-deflection hysteresis loops on Frame No. 2

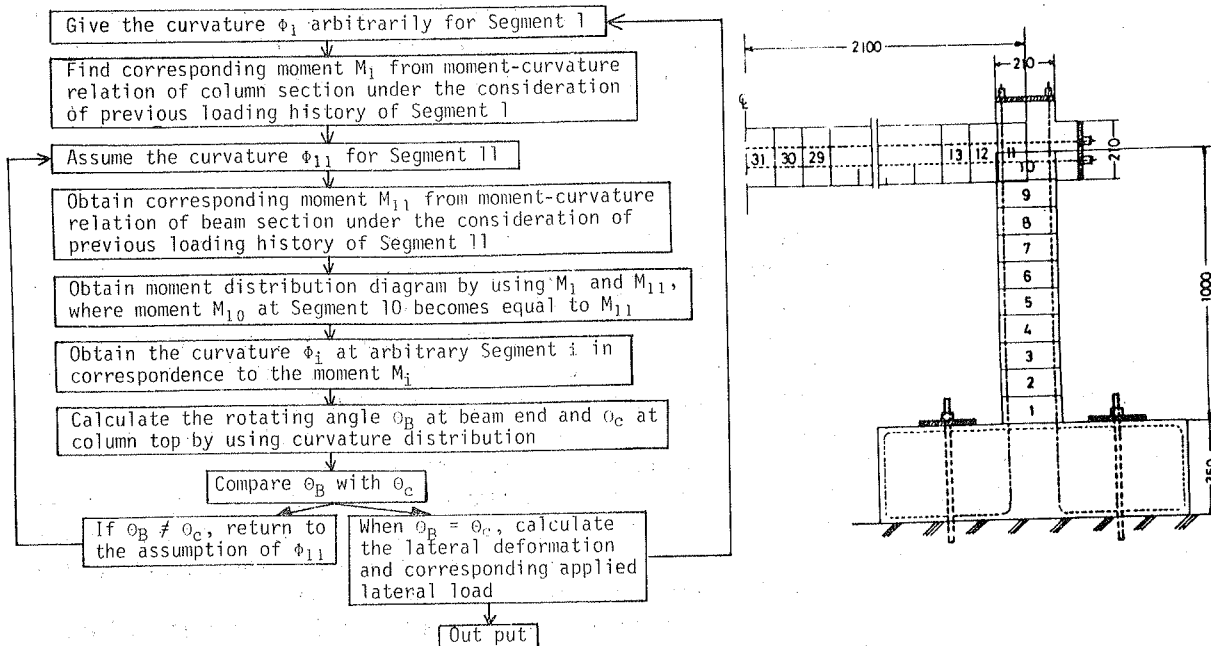


Fig. 5 Flow chart for calculating lateral deflection hysteresis loops of frame

The calculation of hysteresis curves was carried out by dividing the frame into 62 segments shown in Fig. 5, where the idealized moment-curvature relations of constituent member sections illustrated in Fig. 2 (a) and 2 (b) were applied to each segment. The calculating procedure by trial and error method is also indicated in Fig. 5 in a form of flow chart. The calculated results are plotted by dotted line in Fig. 4. As can be seen in Fig. 4, the calculated hysteresis curve agrees well with measured one. Thus, it can be concluded that the restoring force diagrams of prestressed concrete frame structure necessary for dynamic response analysis can be predicted primarily on the basis of idealized moment-curvature hysteretic curves of constituent member sections proposed in this study.

5. CONCLUSIONS

From the test results obtained and theoretical calculations carried out in this study, following conclusions can be derived.

(1) Considerable plastic lateral deflection can be observed in the frame after yielding of column foot sections. Available ductility factor of frame defined as the ratio of lateral deflection at failure mechanism to that at the yielding of column foot sections is 3.930 for Frame No. 1 and 4.709 for Frame No. 2. Considering the large post-crushing deflections after becoming the failure mechanism, these values seem to be sufficient for ensuring the seismic safety.

(2) Good spindle shape hysteresis loops were observed in frame until final stage of reversed cyclic loadings. This may be owing to preventing the bond slippage of column reinforcements by mechanical anchoring on top surface of beam-column joint.

(3) The restoring force diagrams of prestressed concrete frame structure can be predicted primarily by using idealized moment-curvature hysteretic curves of constituent member sections proposed in this study.

(4) For guaranteeing the large available ductility in frame, the rotating ductility at the critical section of constituent member yielding before the frame becomes failure mechanism should be discussed in contrast to the ductility of frame itself. In this study, the rotating ductility factor at column end sections necessary to obtain the available ductility factor of frame, $\mu_f = 3.930$ or $\mu_f = 4.709$, was predicted as $\mu_c = 6.036$.

REFERENCES

- 1) S. Inomata & A. Watanabe, Experimental study on prestressed concrete frame constructions, Journal of Japan Society for Testing Materials, Vol. 8, No. 69, pp.528-539, June 1959 (in Japanese).
- 2) K. Nakano, Experiments on behavior of prestressed concrete four-story model structure on lateral force, Proc. of the 3rd World Conference on Earthquake Engineering, Vol. III, pp.572-590, Jan. 1965.
- 3) Architectural Institute of Japan, Design essential in earthquake resistant buildings, pp.186-200, Elsevier Co., New York, 1970.
- 4) S. Okamoto and Y. Yamazaki, Structural behaviour of a two story precast prestressed concrete building under horizontal static and dynamic loading, journal of Japan Prestressed Concrete Engineering Association, Vol. 20 Extra Number for 8th FIP Congress, pp.79-85, May 1978.
- 5) H. Muguruma & E. Nagai, On the extreme compressive fiber strain of concrete at flexural failure of reinforced or prestressed concrete member, Review of the 30th General Meeting, The Cement Association of Japan, pp.217-219, June 1976.

WAFFLE FLAT PLATE-COLUMN CONNECTIONS UNDER ALTERNATING LOADS

Roberto MELI
National University of
Mexico

Mario RODRIGUEZ
National University of
Mexico

ABSTRACT

Five waffle flat plate-column connections were tested under a constant gravity load and cycles of alternating unbalanced moments. Strength, stiffness, modes of failure and hysteresis loops were studied for different types of reinforcement. Failure was governed by shear stresses in the solid head or in the ribs. Despite the nature of the failure, rather ductile behavior was obtained specially when proper transverse reinforcement was placed; nevertheless the hysteresis loops were always narrow indicating low capacity of energy dissipation through inelastic deformations. Based on the experimental results some recommendations are given about the seismic design of structures of this type.

RESUME

Cinq unions entre dalles nervurées et poteaux ont été soumises à des essais d'application d'une charge verticale constante et de cycles de moments fléchissants alternés. L'étude a porté sur la résistance, la rigidité, les mécanismes de rupture et les cycles d'hystérésis pour différents systèmes d'armatures. La rupture a été provoquée par effort tranchant dans le massif qui entoure les poteaux ou dans les nervures. Malgré le type de rupture, un comportement assez ductile a été obtenu, spécialement quand des armatures transversales convenables ont été utilisées; néanmoins les cycles d'hystérésis observés sont toujours étroits, ce qui indique une faible capacité de dissipation d'énergie par déformations inélastiques. À partir des résultats expérimentaux, certaines recommandations relatives à l'analyse et au dimensionnement de structures de ce type soumises à des sollicitations sismiques sont également présentées.

INTRODUCTION

The structural system studied is a flat plate where part of the concrete in the tensile zone has been eliminated, giving rise to a rib grid with a solid head around the columns. In some countries, building codes severely restrict the use of these structures as lateral load resisting systems, whereas in others it is a common practice to use the frame action of flat plate and columns to withstand earthquake forces in medium to high rise buildings.

One objection to the earthquake performance of flat plate-column structures is their low lateral stiffness, but the main shortcoming pointed out is their inability to behave

in a ductile manner before failure. Modern seismic codes allow important reductions in design forces for ductile structures that can dissipate large amounts of energy through the rotation of plastic hinges, as in ductile concrete frames designed to permit formation of failure mechanisms through plastic hinges in properly detailed beam ends. An equivalent mode of failure in a flat plate structure would involve the formation of negative and positive moment yield lines, as in fig 1. Commonly, failure mechanisms of a more brittle nature take place before these bending yield lines can be fully developed. Either a column failure occurs due to shear or to bending and axial load, or a local failure of the slab takes place around the columns, caused by its inability to resist the shear stresses due to the unbalanced moments transmitted by the columns. Failures by shearing off or crushing of column ends and by punching of the slab around the column have been repeatedly observed in flat plate structures after strong earthquakes.

Flat plate-column structures are usually idealized as equivalent frames where the slabs are replaced by beams whose stiffnesses are those of an equivalent slab width. Criteria proposed to calculate the equivalent width for the purpose of a lateral load analysis, give rise to widely differing results and the validity of the equivalent width concept has been objected. Stresses in the connection are calculated assuming that a fraction α of the unbalanced moment resulting from the analysis is equilibrated by a linearly varying distribution of shearing stress (fig 2). Following the ACI-77 code α is 0.40 for square columns and the shear stresses due to the unbalanced moment have to be added to those due to the vertical loads in a prescribed critical section and compared with a maximum resistant stress of $0.33\sqrt{f'_c}$ (in MPa). According to that code, when stresses are due to unbalanced moments, strength cannot be increased through use of shear reinforcement.

Experimental studies of the seismic behavior of flat plate-column structures have dealt exclusively with solid thin slab reinforced with upper and lower reinforcement meshes. Results reported by Hawkins et al (1977), Islam and Park (1976) and Kanoh and Yoshizaki (1975) clearly demonstrate that the best way to provide ductility and to avoid rapid deterioration under repeated loads is to embed in the connection zone a wide beam with closely spaced stirrups.

Two peculiar features of waffle plate systems deserve an independent study of their seismic behavior:

- a) The longitudinal reinforcement is concentrated in beams; a heavily reinforced beam can be placed in the column line to resist a major portion of the unbalanced moment. Some shear reinforcement is commonly placed in the beams.
- b) Shear failure of the ribs in the periphery of the solid region can occur; it has not been proven that this mode of failure can be checked with the same criterion as for the solid head around the column (fig 3).

Due to the former considerations and to the wide use of these systems in Mexico and Latin America, an experimental program was performed to verificate if the behavior and the design criteria for solid slabs could be extrapolated to waffle slabs, to find methods to check against a shear failure outside the solid zone and to find types of reinforcement that can provide good ductility and energy dissipation.

TEST PROGRAM

Tests were made on five specimens modeling the region between inflection lines of an interior waffle slab-column connection under gravity and earthquake design loads, for the second floor of a seven storey high office building with 7.5 m spans. Specimens were reduced at 1:4 scale and were built with microconcrete having nominal compressive strength of $f'_c = 25$ MPa and reinforced with commercially produced small diameter deformed bars that were annealed so as to obtain a yielding plateau at a stress of about 300 MPa. Stirrups were built with galvanized wire that was deformed and annealed to show a stress strain curve similar to that of the longitudinal reinforcement. Results from previous experimental studies demonstrated that with the scale and experimental technique used, a satisfactory similitude is obtained with the behavior of the prototype, even in the post-elastic range and under repeated loads.

Specimen and loading systems are shown in fig 4. The column was postensioned to the design axial force; the design gravity load was applied on the slab and held constant during tests. Alternating loads were applied at the ends of the slab to produce unbalanced moments in the connection; column ends were hinged and restrained against lateral displacements. The deflection configuration of the slab and the strains in some bars at the section on the face of the column were measured. The alternating loads produced displacement of the same magnitude and in opposite directions at both ends of the slab; two or three cycles were applied for each displacement level and lateral displacements were progressively increased to reach the failure in approximately ten increments.

Slab depth was governed by deflection limitations and the shear strength of the connection was slightly higher than that needed to resist the design loads. Upper layer longitudinal reinforcement was that required for the design negative moment, and 68% of that amount was located in the lower layer as positive reinforcement. With that reinforcement the unbalanced moment required for a flexural mechanism was 30% higher than that required to cause shear failure of the connection, according to the ACI code. Specimen E1 was designed with the afore mentioned criterion and without any shear reinforcement; in specimen E2 independent stirrups were located in each beam at half-depth spacing. In the next specimens a beam of width equal to the column size plus once the slab depth was embedded in the solid region; that beam was formed by six-leg stirrups including the reinforcement of the rib intersected by the column axis plus additional reinforcement at the corners of the stirrups. In specimen E3 stirrups at half-depth spacing were placed in the wide beam. In specimen E4 the flexural and shear strength of the solid region were increased and no stirrups were located in the ribs outside this zone, in an attempt to provoke shear failure in the ribs. In model E5 the size of the solid region was further reduced with the same purpose. The arrangement of the reinforcement is shown in fig 5 and main properties of the five specimens are summarized in table 1.

EXPERIMENTAL RESULTS

All specimens showed similar cracking patterns and failure modes. The gravity load produced a slight negative bending cracking that was increased in one side by the alternating loads. From a given load level, positive moment cracks began to appear in the lower side. Flexural cracks never formed a complete yield line across the width of the slab. For higher loads shear cracks appeared in the lateral faces of the solid zone; gradually a complete diagonal crack formed starting from the originally positive bending crack on the column face in the lower side of the slab and reaching the end of the solid zone in

the upper face of the slab. Cracks of much lower width formed in the opposite diagonal. Finally a complete inverted frustum was formed and the capacity to resist unbalanced moment decreased fastly; nevertheless even for very high displacements and widely open inclined cracks, the specimens could sustain the design vertical load. Small width cracks in the ribs appeared in all the specimens, but only in E5 the failure was governed by the shear failure of the rib intersected by the column axis.

Experimental results are summarized in table 2. Maximum unbalanced moments resisted are reported together with the shear stresses caused by vertical load and the maximum moment, assuming a linear variation of stresses according to ACI-77 criteria. Experimental strength is compared with theoretical values in the same table. It can be appreciated that the unbalanced moment required for the flexural failure mechanism was always higher than the maximum attained in the test. Also shown are the moment that causes the maximum concrete shear strength ($0.33\sqrt{f'_c} M_{pa}$) and the moment that causes a shear stress of $0.17\sqrt{f'_c} + p_v f_y$, that is, the theoretical strength that includes the contribution of the stirrups, with a ratio of transverse reinforcement p_v and a yield stress f_y , according to the specification of ACI-77 for punching shear under vertical loads only.

It can be appreciated that the experimental strength is close to the calculated by shear ignoring the contribution of the reinforcement; (the average of the ratio between calculated and measured strength is 0.99 and the coefficient of variation is 0.12). The effect of the reinforcement on the strength is not very clear; specimens E4 and E5 with higher amounts of longitudinal and transverse reinforcement showed higher strength than E3; nevertheless, strength of E4 was significantly lower than that predicted considering the contribution of the reinforcement. The eighth column of table 2 shows the unbalanced moment that causes a shear stress of $0.33\sqrt{f'_c} M_{pa}$ at half-depth outside the solid region, calculated with the same criteria as for the critical region around the column; that moment was significantly exceeded in specimen E5 in which the failure occurred outside the solid region.

The load-deflection behavior is described by the relation between the applied unbalanced moment and the rotation of the connection, defined as the sum of the displacements at both ends of the slabs divided by their distance. The envelopes of that relation for the initial and final cycles are shown for some specimens in fig 6. It can be appreciated that after an almost linear initial segment, a sharp decrease of stiffness corresponds to the yielding of the upper bars in the column face for a moment of about one half of that needed to form the complete negative moment yield line. Further decrease in stiffness occurs as new bars reach the yield stress; behavior is rather ductile, specially for specimens with shear reinforcement.

To the total rotation of the connection contribute column and slab bending; the latter can be considered as composed of the general bending of the slab and a local rotation at the column face due to local cracking, yielding and possibly bond slip. The measured contribution of the local rotation to the total deflection of the slab was in the average 40% at first yielding and 60% at maximum load. In Table 2 the measured secant slab stiffness before yielding is reported; despite some dispersion of the results, it can be said that the initial stiffness is in the average 30% of that calculated with the moment of inertia of the gross section at column face and 60% of that calculated with the cracked transformed section.

Also shown in table 2 are the values of the ductility factors defined as the ratio between

the maximum rotation for which the specimen is able to sustain 85% of the maximum load and the rotation that would correspond to the maximum load, had the behavior been linear with the initial stiffness. Even the specimen E3 without any shear reinforcement showed a rather ductile behavior; specimen E2 with independent stirrups in each beam showed lower ductility than specimen E3 and E4 reinforced with the wide beam. The lower ductility of specimen E5 was due to the final shear failure of the ribs without stirrups.

The behavior under cycles of alternating loads was studied through the hysteresis loops shown in figs 7 and 8. Before important shear cracking occurred the loops were very stable, i.e the loop obtained in the first loading cycle was almost exactly reproduced in the following cycles for the same maximum displacement. Near to the maximum load significant differences between the loops of the first and second cycles were evident. The load for the same maximum displacement reduced to about 80% and the area enclosed in the loop of the second cycle was between 50 and 80% of that of the first cycle. For additional cycles the loops did not change with respect to those of the second cycle. After important shear cracking around the column, the loops began to show the peculiar form of the shear failure mechanisms. The initial portion of the curve had a low stiffness, while the cracks due to load in the other direction closed. A segment with higher stiffness followed up to the maximum load. The area enclosed by the loops was much lower than that corresponding to elastoplastic behavior. Reported in table 2 is a parameter, I_{DE} , representing the ratio between the area enclosed by the hysteresis loops at the maximum load and the area corresponding to perfectly elastoplastic behavior with the same initial stiffness, maximum load and ductility. The index has an average value of 0.4 for specimens with shear reinforcement and of 0.3 when the failure occurred in regions without transverse reinforcement.

The described behavior was maintained well beyond the maximum load up to a limit rotation when the strength and stiffness progressively decreased if cycles with the same maximum displacement were repeated. That displacement was considered as corresponding to failure.

CONCLUSIONS

The lateral stiffness of the slab-column system is quite low, specially if some flexural cracking due to gravity load exists. In this case lateral stiffness can be approximately calculated using an equivalent frame whose beam has the moment of inertia of a gross section of the slab in a width equal to the size of the column plus once the slab depth. Such "beam" stiffness will not be sufficient in most cases to produce a frame action with points of inflections of the columns in each floor and to limit lateral displacement to allowable values in medium to high rise buildings. This stiffness is further reduced by yielding of the negative reinforcement in the column face, which can occur for usual distributions of reinforcement at load levels of the order of 50% of the maximum resisting moment.

The ACI-77 method predicts with good approximation the strength of connections of this type under direct shear and unbalanced moment, the resistant shear stress being $0.33 \sqrt{f'_c}$ MPa for square columns. It seems that transverse reinforcement in independent beams or including a wide beam does not contribute to the shear strength. Shear failure of the ribs is unlikely except for a very small solid head. Probably the fraction of the unbalanced moment that is equilibrated by the variation of shear forces is lower in that region. Results on the safe side are obtained if the method used for the critical section around the column is extrapolated to check the section at half slab depth from the periphery of the solid region considering the same resistant shear stress.

Despite the failure was governed by shear, a rather ductile behavior was attained even in models without special shear reinforcement. Nevertheless ductility is significantly increased if transverse reinforcement is used and specially if a wide embedded beam is formed. It seems appropriate an amount of transverse reinforcement such that the shear strength considering the reinforcement equals the uncracked concrete strength ($p_v f_y = 0.17 \sqrt{f'_c}$). The same criterion can be applied to calculate the amount of reinforcement in the ribs.

Under alternating loads stable hysteresis loops were obtained even for very high rotations and after significant shear cracking. Nevertheless the loops were very narrow and enclosed only about 40% of the area of a perfectly elastoplastic system with the same ductility. That means than a flat plate column connection can dissipate during an earthquake less than half as much energy through inelastic deformation as a properly detailed beam section.

In structures of this type it can hardly be avoided that failure be governed by punching shear in the connection, unless column capitals or drop panels are used. To attain a failure mechanism governed by bending it would be necessary to design the connection for the shear stresses caused, not by the design forces, but by an unbalanced moment calculated as the sum of the negative and the positive resistant moments at the sides of the column. Therefore these structures must be designed allowing only small reductions of the earthquake actions due to inelastic behavior. It seems that designing for twice the earthquake forces prescribed for well detailed ductile frames would be appropriate.

To better understand the behavior of these systems additional studies are needed, specially about the effect of different type of reinforcement, the behavior of exterior and corner connections and that of more complex systems with multiple connections.

REFERENCES

- Hawkins, N.M., Mitchell, D. and Symonds, D.W., "Hysteretic Behavior of Concrete Slab to Column Connections", Proc. 6th World Conf. on Earthquake Eng., Delhi, 1977.
- Islam, S. and Park, R., "Tests on Slab-Column Connections with Shear and Unbalanced Flexure" ASCE, Journal of the Struct. Div., vol 102, No ST3, mar 1976.
- Kanoh, Y. and Yoshizaki, S., "Experiments on Slab-Column and Slab-Wall Junctions of Flat Plate Structures" Concrete Journal, Japan Concrete Institute, vol 13, jun 1975.

TABLE 1. PROPERTIES OF SPECIMENS

| Spec No | f' _c | Longitudinal Reinforcement | | | | Vertical stirrups Ø 1.6 mm | | Size of the solid zone | Size of the hollow boxes |
|---------|-----------------|----------------------------|----------------|---------------------|----------------|-------------------------------|----------------|------------------------|--------------------------|
| | | Upper Layer, Ø 5 mm | | Lower Layer, Ø 4 mm | | | | | |
| | | No of bars | f _y | No of bars | f _y | spacing | f _y | | |
| E1 | 25 | 18 | 350 | 18 | 360 | - | 370 | 475x475 | 150x150 |
| E2 | 31 | 14 | 350 | 14 | 590 | 40 | 460 | 475x475 | 150x150 |
| E3 | 26 | 18 | 320 | 18 | 340 | 38 | 390 | 475x475 | 150x150 |
| E4 | 27 | 24 | 330 | 24 | 360 | 23 | 390 | 350x350 | 100x100 |
| E5 | 26 | 24 | 330 | 24 | 360 | 24 | 460 | 312x312 | 100x100 |

Stress in MPa. Dimensions in mm.

TABLE 2. EXPERIMENTAL RESULTS

| Spec No | Experimental strength | | | Calculated strength | | | | Initial stiffness | Ductility factor | I_{DE} |
|---------|-----------------------|----------------|--------------|---------------------|-----------------------------|-----------------------------------|-------------|-------------------|------------------|----------|
| | M_D | shear stresses | | MD for flex failure | M_{D_s} for shear failure | | | | | |
| | | gravity | due to M_D | | $v_u = 0.33\sqrt{f'_c}$ | $v_u = 0.17\sqrt{f'_c} + p_v f_y$ | web failure | | | |
| E1 | 13.2 | 0.41 | 1.11 | 17.2 | 13.5 | 4.3 | 28.0 | 1275 | 4 | 0.30 |
| E2 | 15.2 | 0.41 | 1.28 | 16.9 | 15.7 | 9.4 | 32.7 | 1540 | 6 | 0.40 |
| E3 | 12.4 | 0.41 | 1.04 | 15.6 | 14.1 | 12.1 | 29.2 | 1775 | 8.5 | 0.44 |
| E4 | 14.7 | 0.41 | 1.24 | 21.9 | 14.3 | 17.8 | 17.4 | 1755 | 8 | 0.38 |
| E5 | 18.1 | 0.41 | 1.52 | 22.6 | 14.0 | 18.7 | 9.9 | 2725 | 6.5 | 0.31 |

M_D , maximum unbalanced moment. Stiffness and Moments in KN-m. Stresses in MPa.

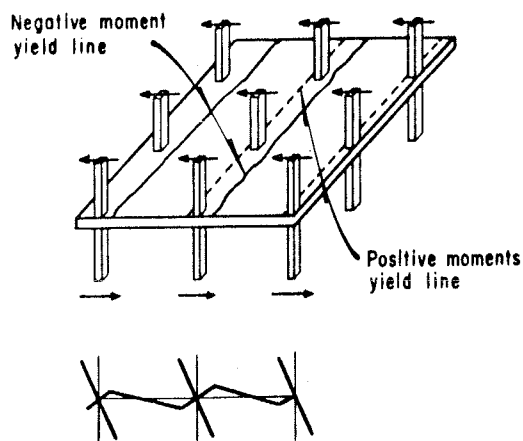


Fig 1. Mechanism of collapse due to bending failure

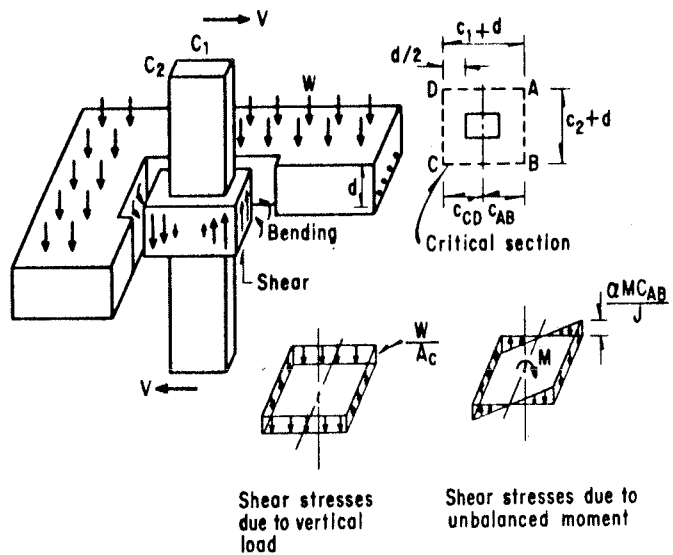


Fig 2. Shear stresses in the critical section according to the ACI-77 code

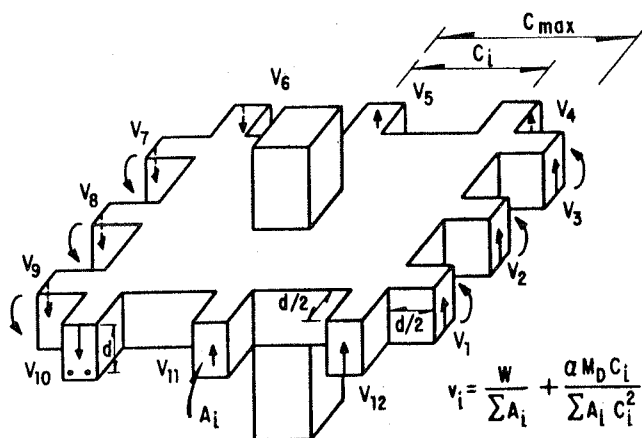


Fig 3. Shear stresses in the beams outside the solid region

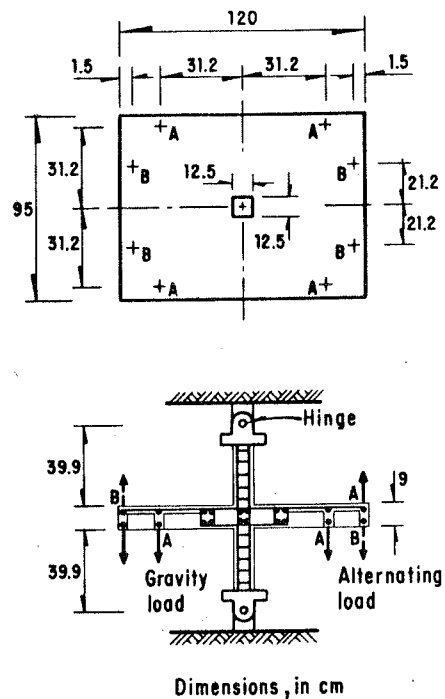


Fig 4. Specimen and test set up

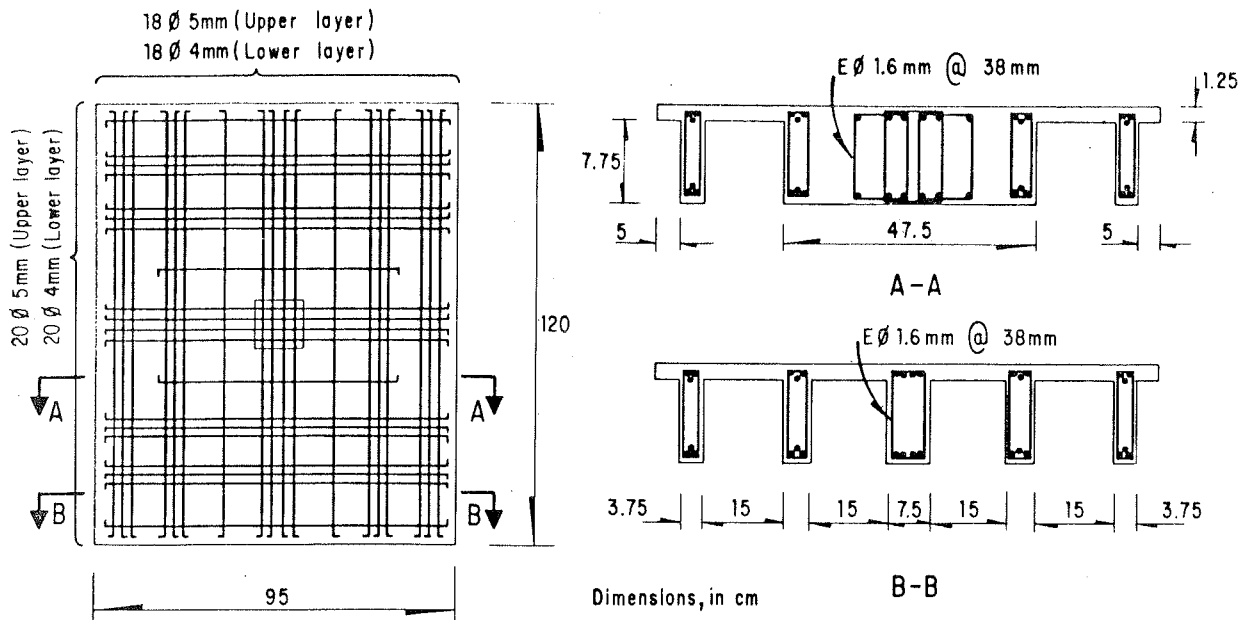


Fig 5. Arrangement of reinforcement (Specimen E3)

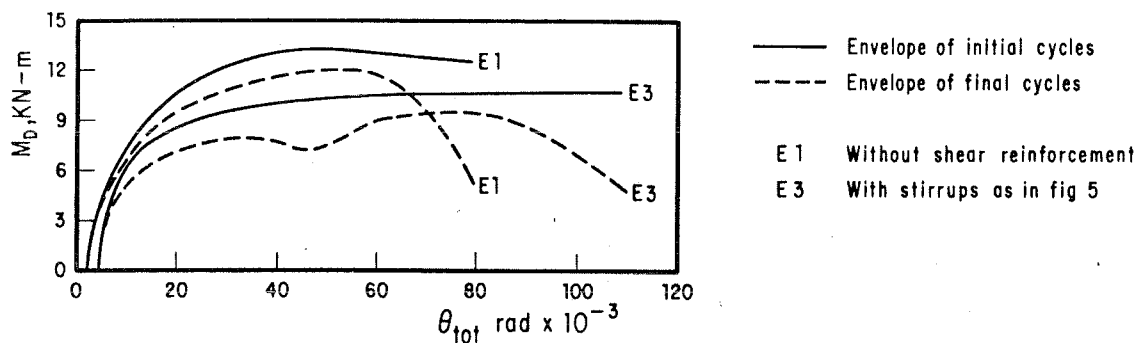


Fig 6. Envelopes of moment-rotation curves

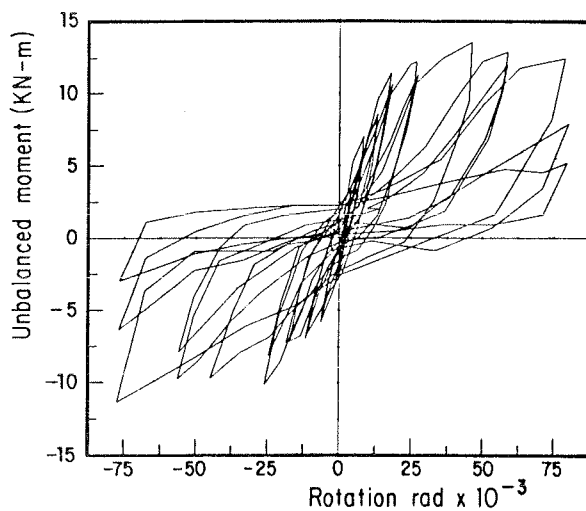


Fig 7. Hysteresis loops for specimen without shear reinforcement

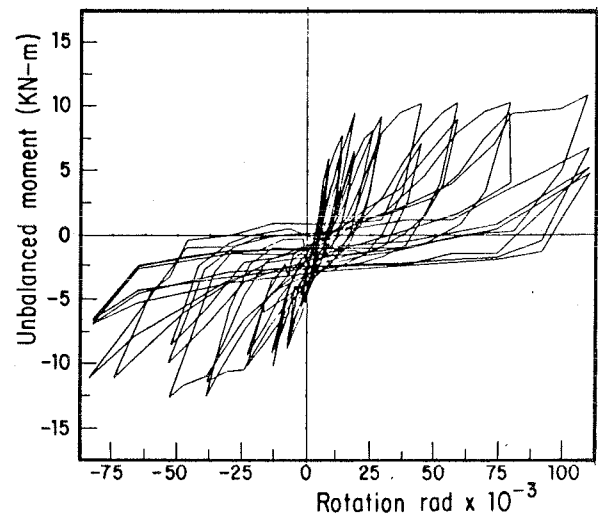


Fig 8. Hysteresis loops for specimen with stirrups as in fig 5

THE SEISMIC ANALYSIS, THEORETICAL AND EXPERIMENTAL, OF THE JOINTS OF PRESTRESSED CONCRETE FRAMES

A. NEGOITA

Polytechnical Institute
Yassy, Roumania

V. HOBJILA

Polytechnical Institute
Yassy, Roumania

SUMMARY

At beginning it presents the considerations concerning the philosophy of some types of precast prestressed concrete frames, built in the latest years.

It exposes in detail the design and performance criteria of the precast prestressed concrete frames assembled by prestressing outside the joints. It presents also the design and performance criteria for the models of the structural elements, which are tested, especially for joints. At the end it presents the results obtained through the experimental research of the structural elements and joints, also some main conclusions, for this kind of structure.

RESUME

Au début on présente des considérations sur la conception de quelques types des cadres préfabriqués en béton précontraint réalisés les années dernières.

On expose en détail l'étude et les performance de conformation pour les modèles des éléments de résistance qui sont expérimentés, en particulier pour les joints.

Enfin, on présente les résultats expérimentaux des éléments de résistance et des joints et quelques conclusions principales pour ce type de structure.

A. On some Prefabricated Prestressed Concrete Frames in Seismic Areas

The use, in seismic areas, of some precast frames which are assembled by means of prestressing imposes to satisfy the resistance requirements, local and general stability ones, those of ductility of the compounding members, of the joints which are realised by prestressing as well as of the whole structure.

One analyses the breacking-up of frames both into joints and outside the joints, by taking into account the mechanic criteria of seismic behaviour as well as the technologic requirements for mounting, the possibilities to realise the assembly by prestressing in areas intensely/moderately stressed.

The division in fragments in the even areas of joints corresponds satisfactory to the mounting technology; the assembling of beams and columns is realised by pretensioning the steel rods introduced into channels of the lateral threshold that have resulted by cutting-out of the central superior of the beams, assuring the stresses taking-over for all the loadings acting after assembling phase (fig.1). The assembling

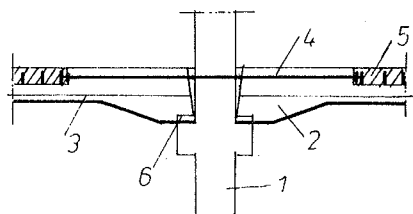


Fig.1-Prestressed beam-column-beam connection

- 1-reinforced or prestressed concrete column;
- 2-beam;
- 3-pretensioned reinforcement;
- 4-post-tensioned rod;
- 5-initially cut-off zone;
- 6-metallic elements.

and prestressing in the joint areas of the frames, in negative bending moments, presents certain difficulties depending on both the realisation in situ of some initial stresses of high values and the use of some active reinforcements as thick post-tensioned rods or rectilinear or curve wire-bundles of relatively short lengths. The columns are realised either of a single piece or of two pieces along the structure, of reinforced or prestressed concrete /Inemata, 1977/, /Mihul, 1978/.

The general assembly, outside the joints, by prestressing the small sized elements the relatively large subassemblies by using flexible rectilinear wire-bundles on the horizontal-line and thick post-tensioned bars on the vertical line, may assures the prestressing and continuity of the joints placed in moderate stressing-areas for all the loading, acting after the assembly.

One can mention, as first phase, the singlestoried prestressed concrete frames realised in R.S.România, in Bucharest, since 1954, of arch-bricks assembled by prestressing with rectilinear post-tensioned wire-bundles (fig.2a), having rigid joints for all the loadings.

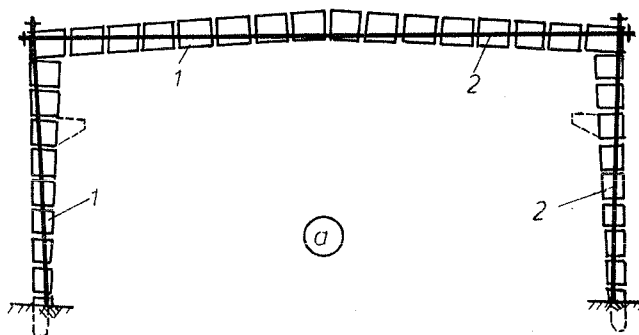


Fig.2a-Portal frames realised in Bucharest

- 1-arch brick;
- 2-post-tensioned wire-bundles;
- 3-column;
- 4-prestressed concrete beam

Another type of singlestoried structure (fig.2b) has its prestressed concrete beam assembled with reinforced concrete columns by means of prestressing, by means two short curve wire-bundles. Both of the singlestoried structures behaved roughly well during the 4 March 1977 earthquake.

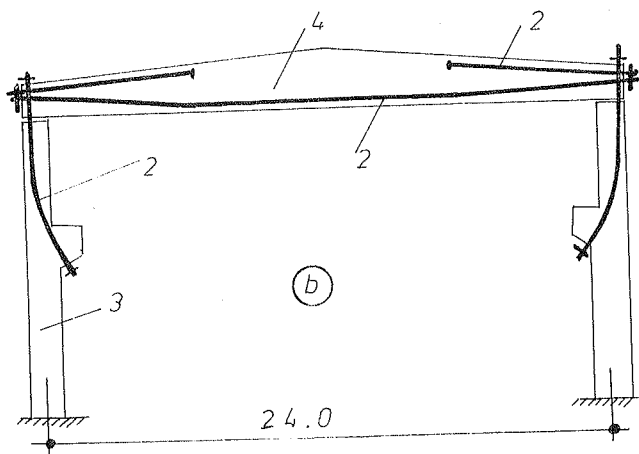


Fig. 2b-Portal frame
realised in
Bucharest

B. Prestressed Concrete Frames of Prefabricated Parts Assembled by Prestressing Beyond the Joints

The breaking-up of the frame beyond the joints, which is advantageous of the mechanical point of view, leads to a more attentive technology of the mounting; the space frames are realised of space-subassemblies that maintain the structure point carried out and prestressed in the initial phase into the factory with pre-tensioned adherent reinforcements, in order to receive the negative bending moments, as well as of intermediary elements for the general assembly on vertical and horizontal line (fig. 3).

The columns with constant section along the structure height are provided with 4 longitudinal channels located at the cross-section corners, in view to assemble them on the vertical direction with thick post-tensioned PC90 type bars, rendered continue at the middle of the story depth (fig. 3d).

The tapered beams, from the + shape on the support to the + in span, allow the members to support on the floor-ribbed slabs prestressed into two directions - at their bottom.

Located in moderate stressing areas, the beam-beam joints (fig. 3b) and column-column respectively (fig. 3c) are realised by prestressing, by directly passing the wire-bundles, and post-tensioned bars. In the beam-beam joints are also foreseen passive reinforcements, connected by welding in view to increase the ductility in these areas /Mihul, 1978/, /Negoiță, 1977/.

Alongside the structure assembling in the site, one assures, by prestressing, the limitation of plastic displacements into columns in the conditions of an exceptional earthquake. One assures the formation and development of plastic hinges into the beams; after the seism has ceased, by maintaining the prestressing, the temporary opened cracks are closing or maintaining with limited openings so that the volume of repairing to be minimal.

The pretensioned reinforcements are initially obtained on the basis of a linear elastic analyse; to satisfy the ductility and cracking requirements determines the final sections of the active reinforcements; by the division in fragments con-

ception of the presented structure the cracking criteria is easily realised into the joining areas.

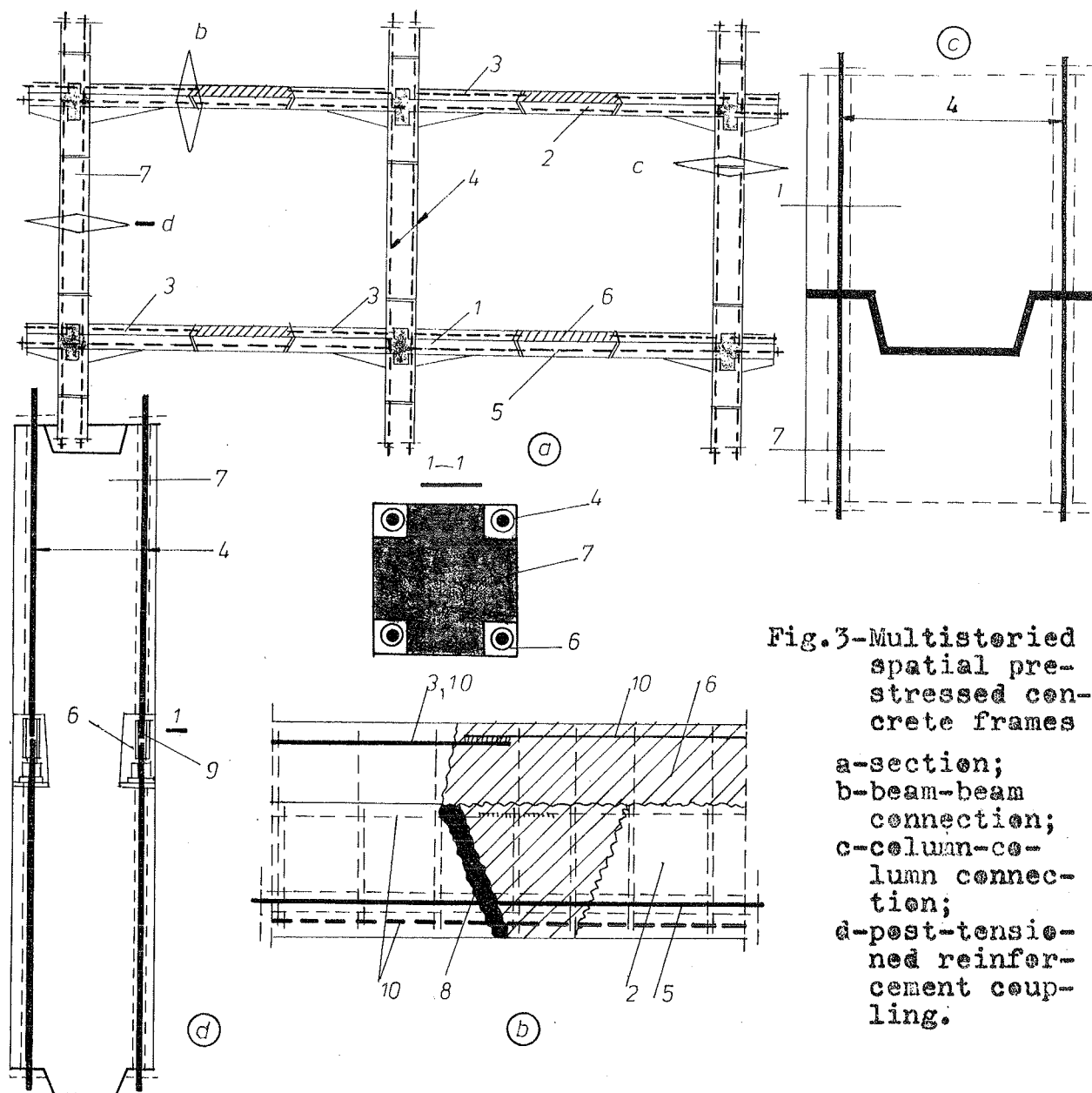


Fig.3-Multistored spatial prestressed concrete frames

a-section;
b-beam-beam connection;
c-column-column connection;
d-post-tensioned reinforcement coupling.

1-space element; 2-horizontal connection element;
3-pretensioned reinforcement; 4-post-tensioned bars;
5-post-tensioned wire-bundles; 6-in situ cast area;
7-vertical connection element; 8-fibre-reinforcement mortar; 9-bar-coupling; 10-passive reinforcement.

C. Testing Concerning the Joint Behaviour Column-Column and the Structural Joints

One has performed testings on plane models (1:3) of marginal subassemblies in lightweight prestressed concrete rendered continue by means of prestressing with thick post-tensioned non-injected bars, after interposing a vertical tying member, watching their response in displacements and strains,

for the beams concurring in the marginal joint as well as for the columns realised of segments, after the properly assembling phase.

The members of \perp -type that maintain the structure joint, realised in lightweight (granulite) B400 concrete, are pre-stressed with 4x3 $\varnothing 3$ SBP II ($R_s = 13600 \text{ daN/cm}^2$) for taking the negative moments and with 3 $\varnothing 8$ OB37 ($R_s = 2100 \text{ daN/cm}^2$) in the opposite area. The column elements longitudinally reinforced with 3 $\varnothing 6$ and cross-wardly with $\varnothing 6$ OB37 stirrups at 8 cm distance, are assembled by prestressing by means of 4 post-tensioned $\varnothing 12$ mm PC90 rods ($\sigma_{s,2} = 7300 \text{ daN/cm}^2$, $\sigma_r = 9300 \text{ daN/cm}^2$).

The realising the continuity of post-tensioned bars has been performed at the half-height of the column by tapped joinings.

The geometric elements and the loading scheme of the experimental assembly are presented in fig.4; in this phase of

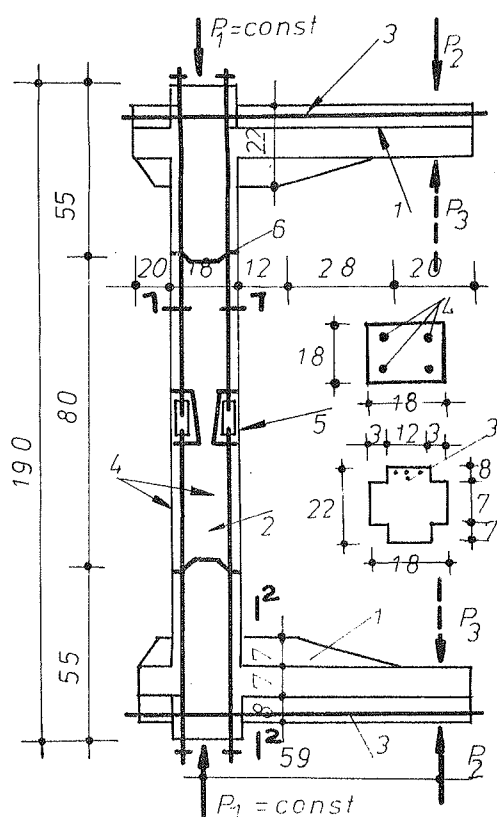


Fig.4 - Geometrical elements and the loading scheme of the experimental assembly

- 1-subassembly;
- 2-column element;
- 3-pretensioned reinforcement;
- 4-post-tensioned bars;
- 5-couplings;
- 6-column-column pre-stressed connection

researches one has pursued its failure to happen by plastic hinge formation into the column. By alternative repeated static loading we pursued to establish the resistance characteristics and deformability and how much the experimental assembly stiffness has decreased, all of them necessary for a continue, step by step analyse of the seismic behaviour of the whole structure model.

The obtained results, expressed in free displacements of the lightweight concrete beam-ends, the assembly displacements in the connecting area of the post-tensioned bars into the columns, as well as the strains in column-column joints, are presented in fig.5; 6, 7; the draft of final crackings is presented in fig.8.

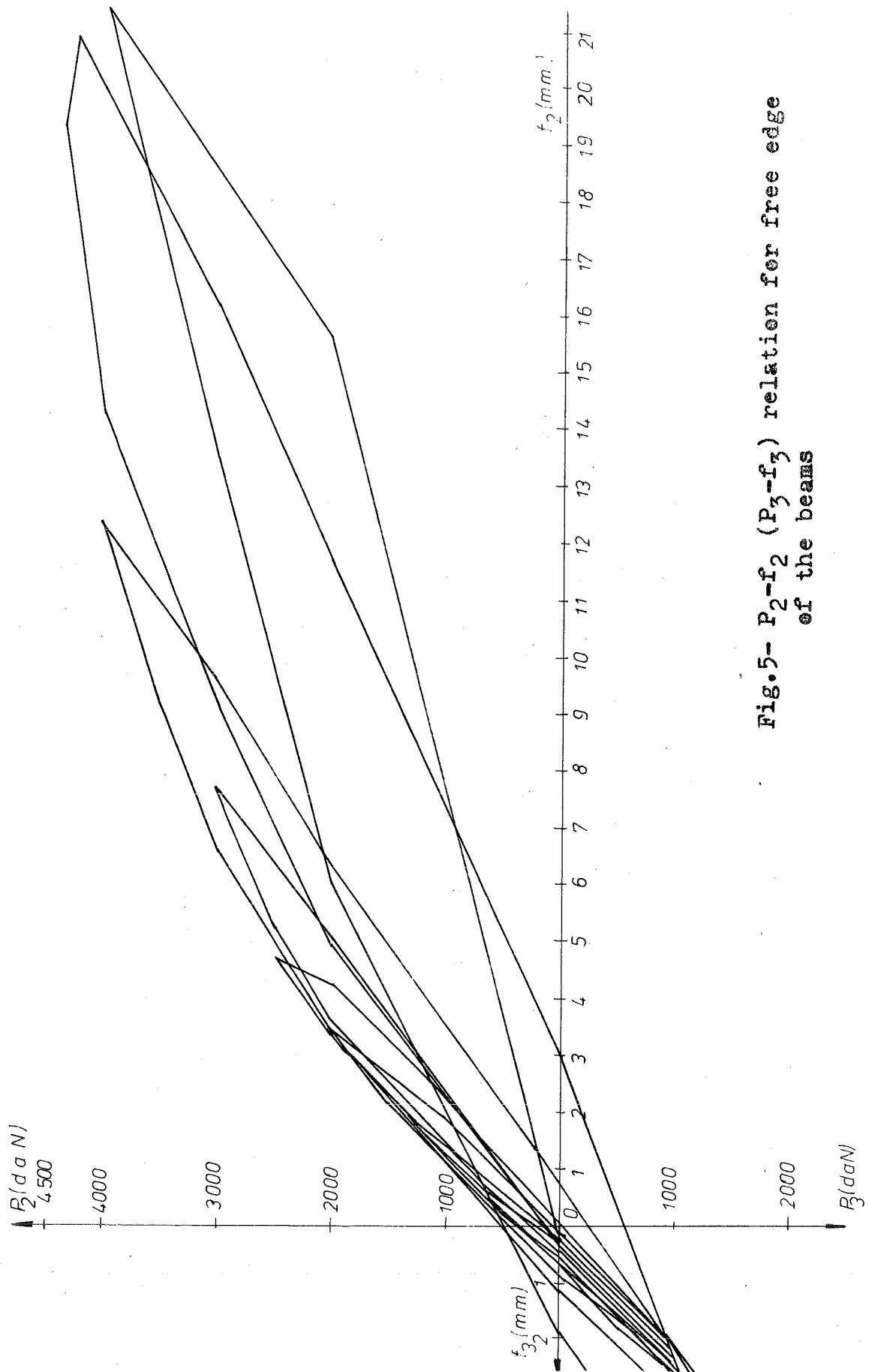


Fig.5- P_2 - f_2 (P_3 - f_3) relation for free edge
of the beams

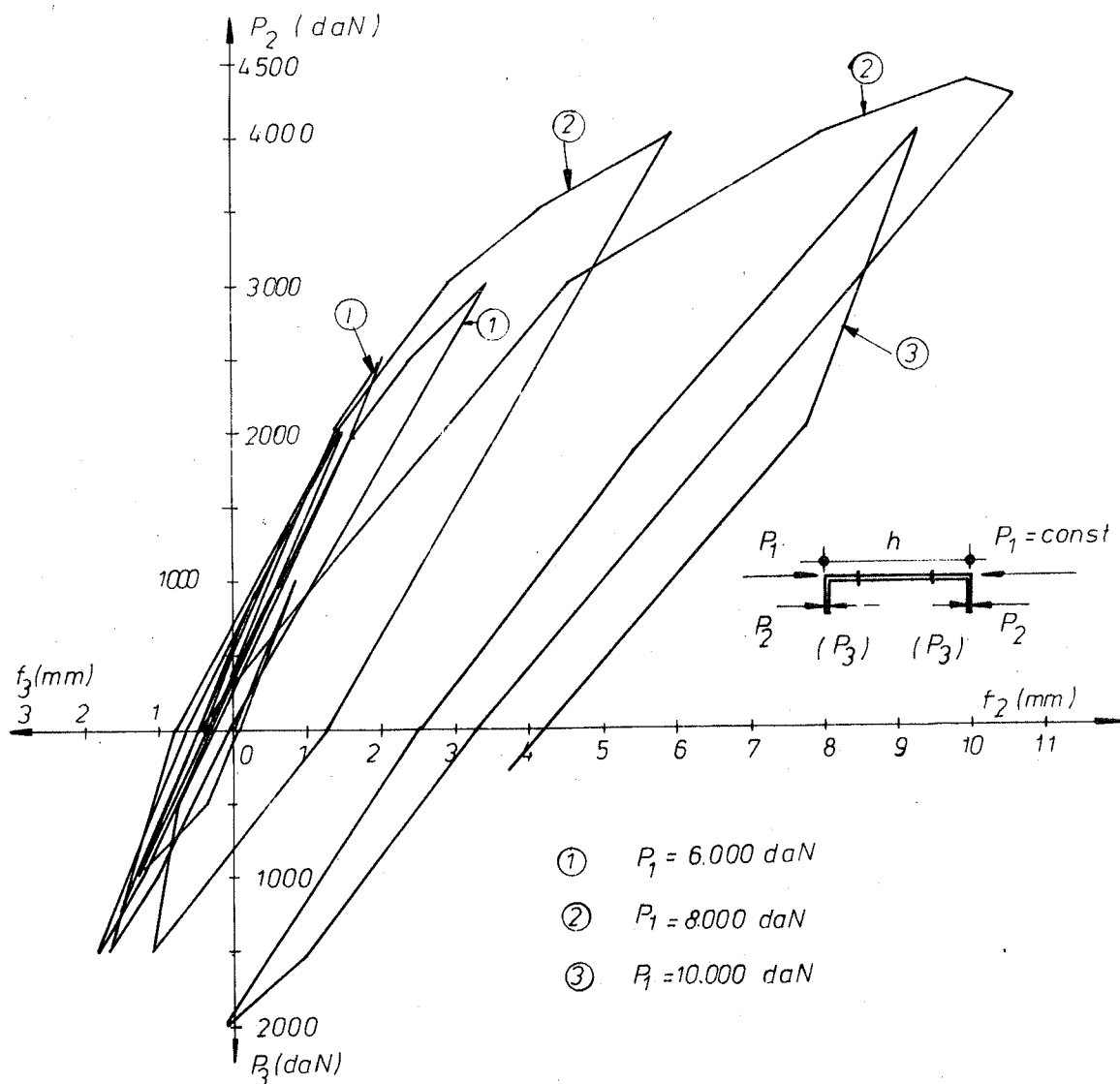


Fig.6- P_2-f_2 (P_3-f_3) relation in middle height section of the experimental assembly

The future researches will have for aim the experimental assembly loading so that the plastic hinge formation to produce on the prestressed concrete beams.

By analysing the experimental results that are synthesised in the $P-\Delta$ and $P-\varepsilon$ curves respectively one finds a good behaviour of the experimental assemblies, of the column-column joints and of the coupling areas of post-tensioned bars respectively; a total continuity is realised into the joinings alongside the assuring of some corresponding ductilities.

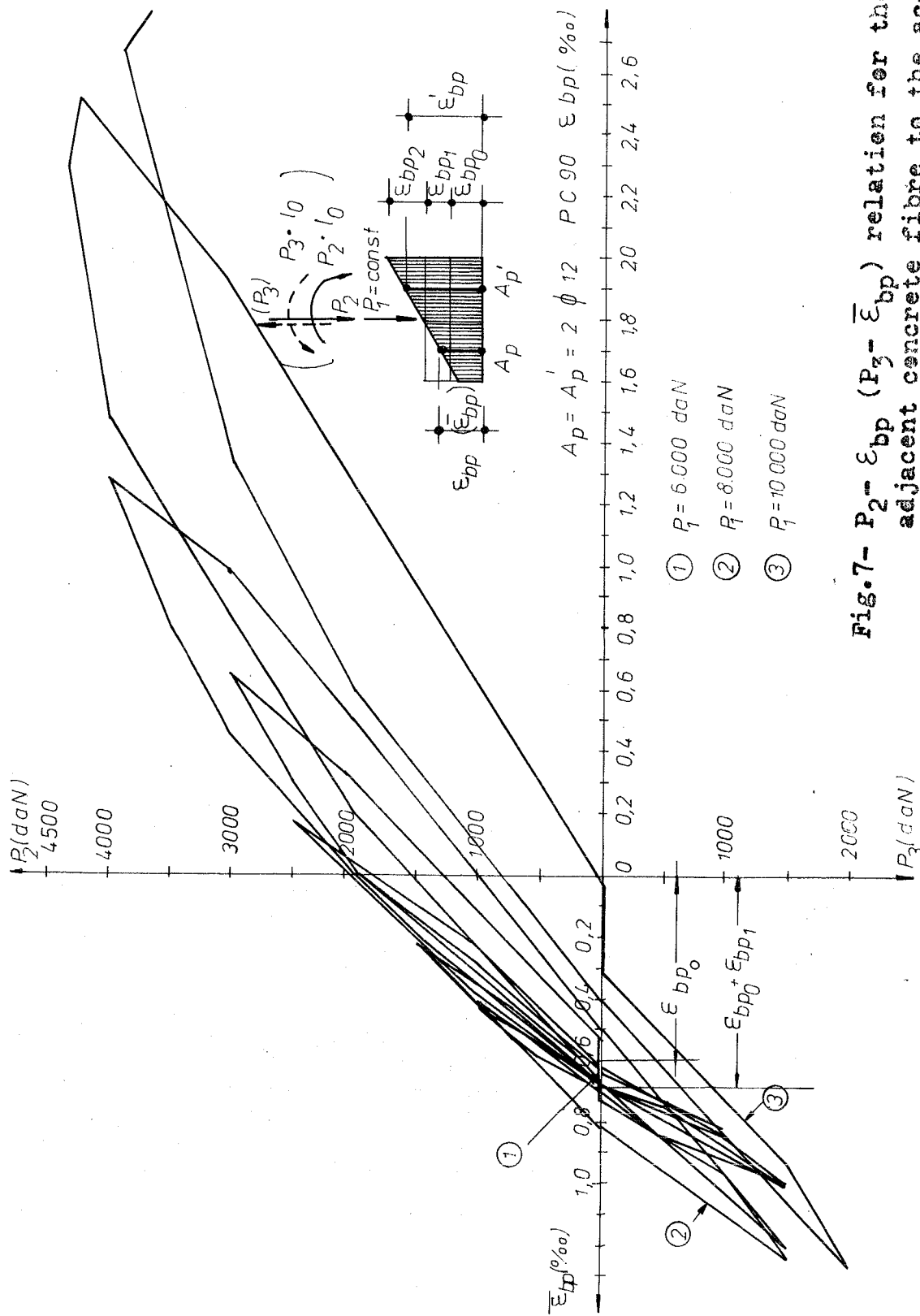


Fig.7- $P_2 - \epsilon_{bp}$ ($P_3 - \epsilon_{bp}$) relation for the adjacent concrete fibre to the active reinforcement A_p , in the column-column connection

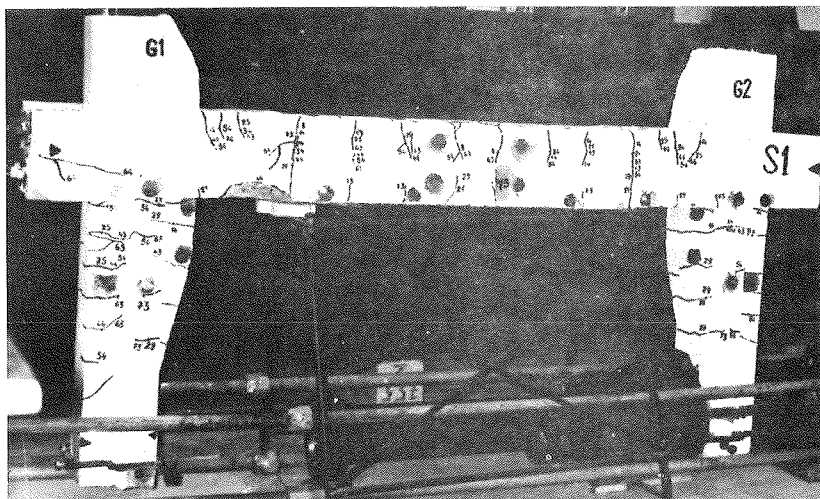


Fig.8- General view of the experimental assembly after failure

REFERENCES

- /1/ Sh. Inemata FIP-Commission On Seismic Structures,
Exemples of Joints for Precast Prestressed Concrete
Structures in Seismic Region, nov., 1977
- /2/ A. Mihul, C.Leonte, V.Hobjilă,
Industrializarea execuției halelor etajate,
Conferința națională de beton, oraș Gh.Gheorghiu-Dej,
R.S.România, oct., 1978
- /3/ Al.Negoită, M.Dumitraș, I.Negoită, V.Hobjilă,
Aspecte specifice privind proiectarea antiseismică
a structurilor din beton precomprimat,
Simpozionul de beton precomprimat, Cluj-Napoca,
R.S.România, 1977.

LE COMPORTEMENT SISMIQUE "IN SITU" DES HAUTS BATIMENTS AVEC UN
NOYAU CENTRAL ET DES PORTIQUES PERIPHERIQUES

I. NEGOITĂ

Polytechnical Institute

Yassy, Roumania

A. NEGOITĂ

Polytechnical Institute

Yassy, Roumania

I. OLARIU

Polytechnical Institute

Yassy, Roumania

RÉSUMÉ

On présente le comportement sismique d'une structure réalisée en béton armé avec un noyau central en diaphragmes et des portiques périphériques (des poteaux et des poutres de cadre), d'un haut bâtiment administratif, situé en Bucarest - Roumanie, sous l'action du séisme de 4.03.1977, considéré comme un séisme extraordinaire. On analyse l'apparition des fissures dans les linteaux du noyau central et dans les poutres de cadre avec l'état des tensions et des déformations, précisés à l'aide du calcul dans le domaine élastique, effectué avec un programme. On a remarqué un bon comportement sismique de la structure, due en général à sa symétrie géométrique et mécanique, aux rigidités à peu près égales dans les deux directions principales, à la conception des articulations plastiques seulement dans les éléments structurels avec une ductilité satisfaisante.

SUMMARY

It presents the sismique behaviour of the reinforced concrete structure with the core wall and the peripheric frames (columns and beams) of the administrative tall building placed in Bucuresti Roumania under the action of the earthquake 4.03.1977, considered like one excessive earthquake. It analyse the appearance of the cracks in the lintels of the core wall and in the beams of the peripheric frames with the strains and stresses state, specified through the calculus in the elastic range, performed with the computer. It had observed the good

behaviour of the structure, due generally to the geometric and mechanical symmetric, to the stiffnesses nearly equals in the two main directions and to the philosophy of the project, which admits the appearance of the plastic hinges only in the structural elements with one satisfactory ductility.

INTRODUCTION

Une forme de structures mixtes en béton armé est représentée par les structures avec un noyau central en diaphragmes et des partiques périphériques, pour les quelles on réalise des planchers en béton armé, monolithe ou en préfabriquées qui avec des mesures spéciales de liaison, peuvent conférer aux planchers une grande rigidité, pour pouvoir être considérés comme diaphragmes horizontales indeformables rigides. Aussi on peut assurer la compatibilité des déformations (déplacements) des éléments verticaux aux divers niveaux de la structure sous l'action des forces horizontales. À la base de la structure, les partiques réduisent les déplacements des diaphragmes (refends), tandis qu'aux derniers niveaux les refends, par leur grande rigidité à la flexion, diminuent les amplitudes des oscillations ou les déplacements sous l'effet des modes supérieures. Les cadres ductiles peuvent contribuer à un bon comportement de la structure en domaine non-élastique en prêtant de la ductilité à la structure [Fintel, 1974:1; Negoită Al., Scharf F., Olariu I, 1975-1978:2,3].

ANALYSE DE LA STRUCTURE

Dans la figure 1 on représente le schéma constructif du bâtiment administratif à 15 niveaux exécuté à Bucaresti - Roumanie en 1965 et avec l'ossature en béton armé monolithe constituée d'un noyau central en diaphragmes verticales et des partiques périphériques dont le comportement au séisme 4.03. 1977 a été étudié. L'analyse a été faite à l'aide d'un programme, mis au point pour l'analyse élastique des structures mixtes dans le domaine élastique [Olariu, 1978:4]. Le programme, écrit en langage FORTRAN, a été vérifié, en testant un modèle d'une ossature à 11 niveaux [Negoită, Olariu 1978:2]. Le modèle mathématique des axes B et C du bâtiment est présenté dans la fig. 2

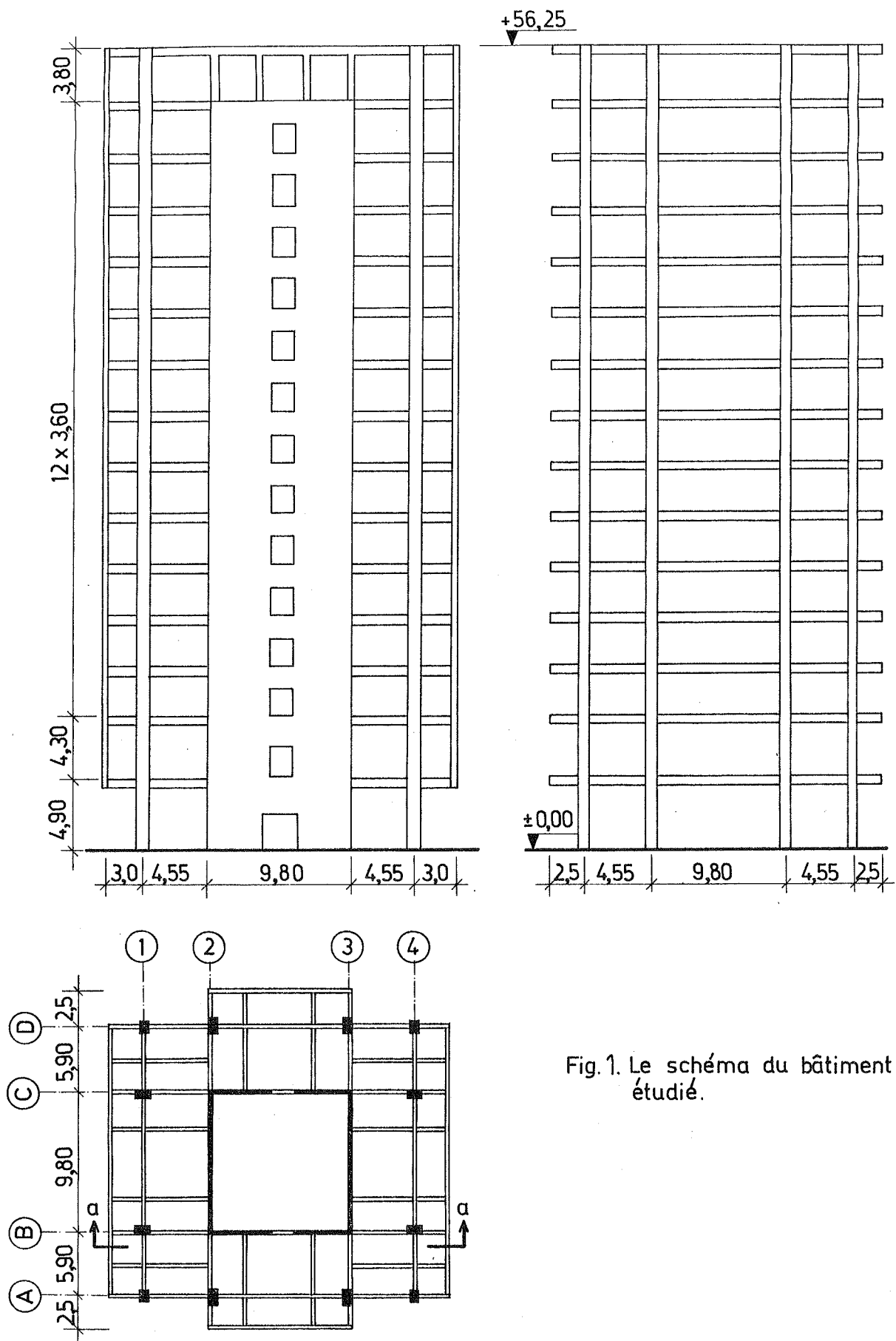


Fig.1. Le schéma du bâtiment étudié.

On a utilisé le spectre des accélérations du séisme roumain de 4.03.1977(fig.3)et dans la fig.4 on voit les premiers modes de vibration en direction x(a),y(b) et pour torsion(c).

La répartition de l'effort tranchant produit par les forces sismiques laterales à chaque niveau entre les éléments résistants verticaux est montré dans la fig.5, en considérant une excentricité supplémentaire due à l'application de l'action sismique à la base du bâtiment avec des valeurs différents à un moment donné($e_g=0,075 B$, ou B est la largeur de la base). Dans la fig.6 on présente les déplacements laterales théoriques pour les divers éléments verticaux en considérant aussi la torsion.

Le calcul élastique effectué met en évidence le fait que les efforts sismiques qui agissent dans le cas du séisme extraordinaire dans les sections de la structure, ont provoqué l'apparition des articulations plastiques, dans les linteaux, dues aux efforts tranchants(fig.7)et considérées d'ailleurs comme la première ligne acceptable de la plastification de la structure après le système. L'armature des linteaux a contribué à la ductilité de l'entière structure. On peut mentionner aussi les fissures apparues dans les poutres de cadre, dans le voisinage du joint avec le noyau central. Les photos(a-f) de la fig.8 montrent la fissuration des linteaux des niveaux(1-6) sous l'action des efforts unitaires principaux.

On n'a pas remarqué des fissures importantes dans les diaphragmes pleins en dehors de quelques fissures, appréciées comme dues au joint du bétonnage. Aussi on n'a pas remarqué des dégradations importantes aux éléments non-structuraux du bâtiment.

QUELQUES REMARQUES

On peut constater donc un comportement acceptable de cette structure mixte sujette aux séismes d'intensité forte, en respectant l'esprit actuel des recommandations techniques. Une attention particulière doit être accordée aux mesures qui dirigent l'apparition des articulations plastiques seulement dans les éléments avec une ductilité possible satisfaisante et aussi aux mesures qui peuvent assurer la ductilité des

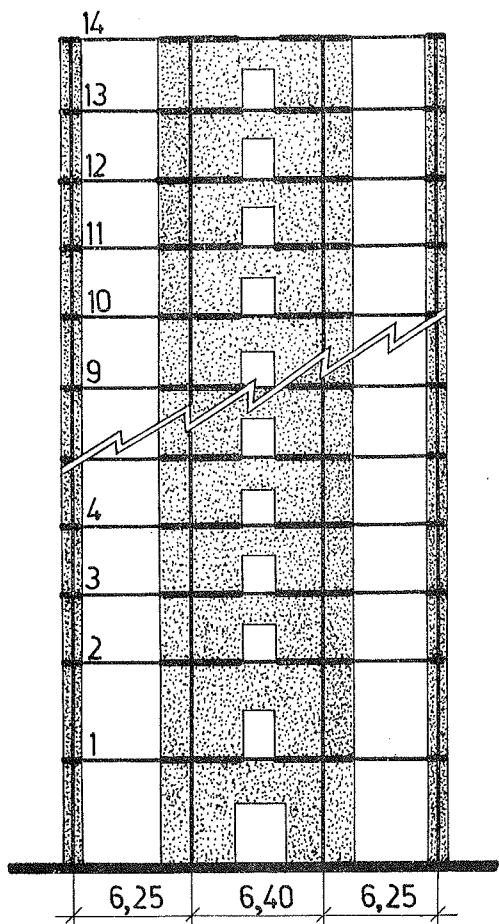


Fig. 2. Le model mathématique des axes B et C.

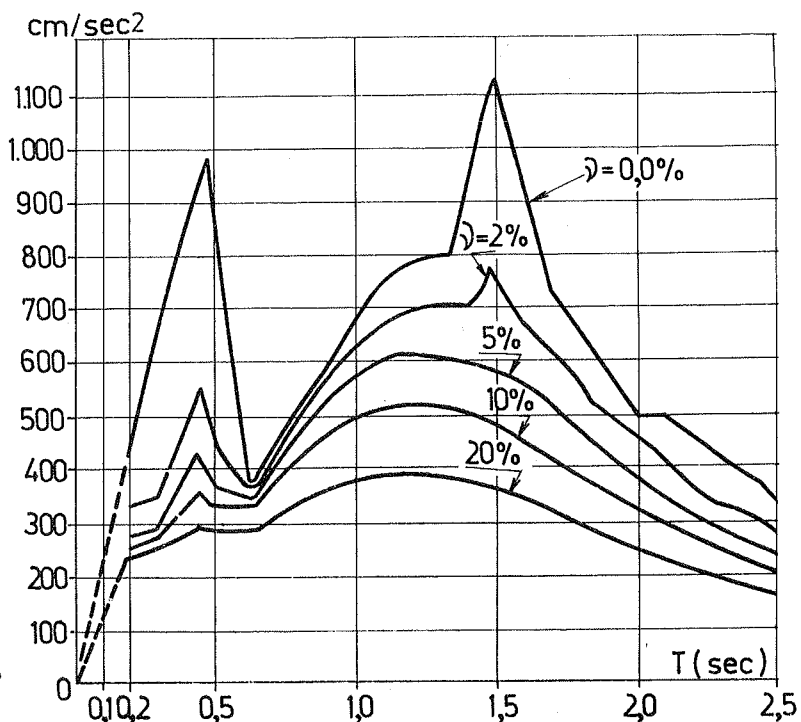


Fig. 3. Le spectre des accélérations du séisme de 4 mars 1977.

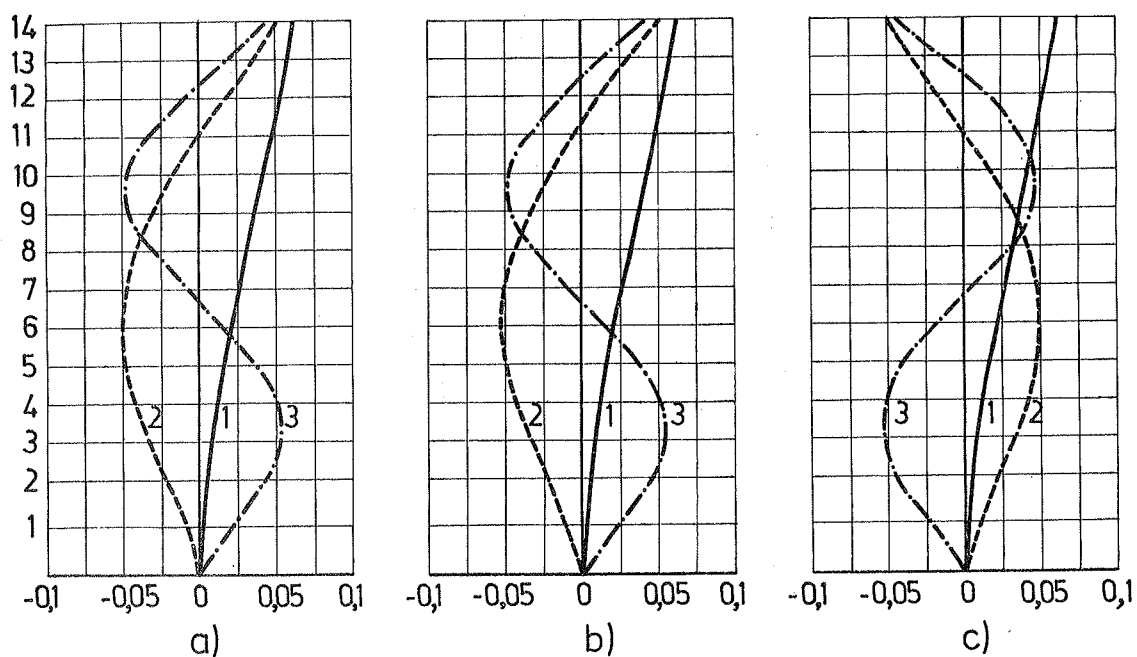


Fig. 4. Les premiers trois modes de vibration en direction x (a), y (b) et pour torsion (c).

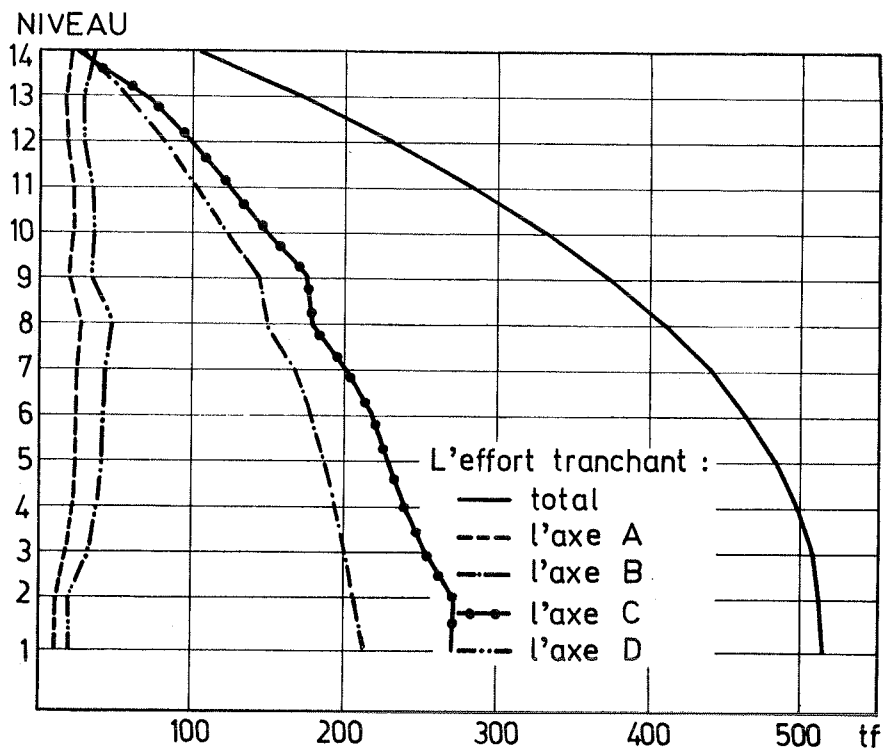


Fig. 5. La répartition de l'effort tranchant entre les éléments résistants verticaux.

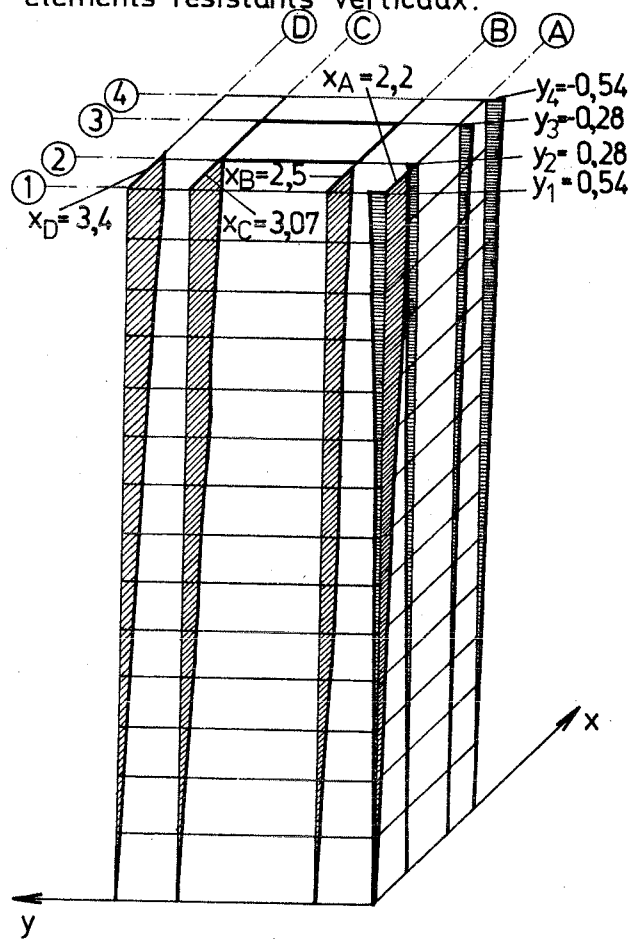


Fig.6. Les déplacements latéraux théoriques de l'ossature.

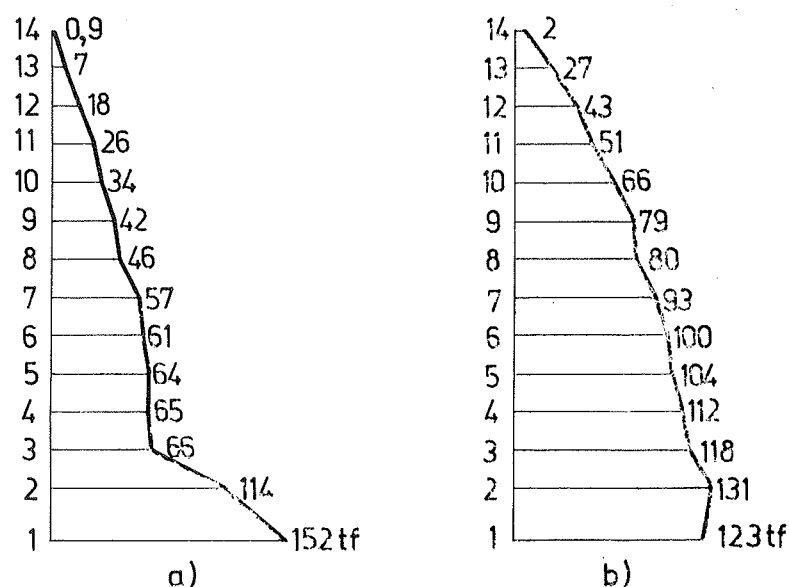
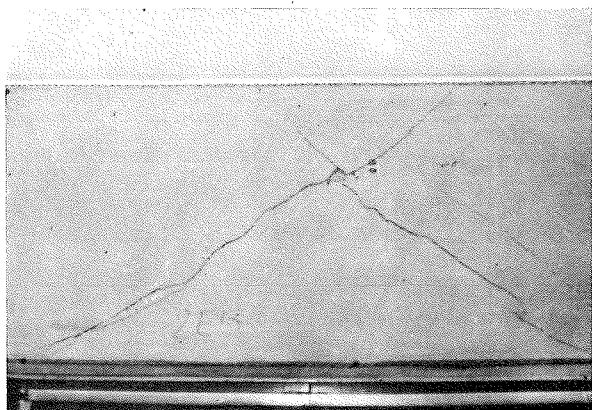


Fig. 7. L'effort tranchant dans les linteaux (a) et dans le refend (b).

linteaux et des poutres de cadre. Il faut réaliser des structures avec des rigidités à peu près égales dans les directions principales et suffisantes pour assurer des déplacements relatifs des niveaux suffisamment petits. Les effets de la torsion dus à l'excentricité conventionnelle doivent être considérés avec grande attention spécialement dans le cas des bâtiments avec grandes dimensions. À présent on recherche l'utilisation de la théorie élastique des noyaux pour exprimer la réponse sismique en tenant compte des expériences sur les plateformes sismiques

BIBLIOGRAPHIE

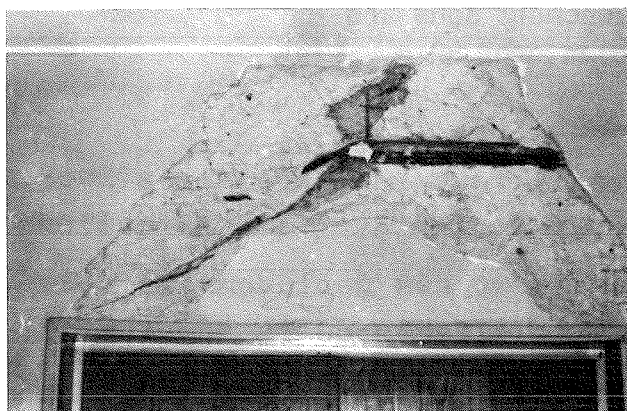
1. Fintel Mark, Ductile Shear Walls in Earthquake Resistant Multistory Buildings ACI-SP-53, 1977
2. Negoită, Olariu I., M. Teodorescu M., Comportarea unei structuri din beton armat cu nucleu central Congres COPISEE București 1978
3. Negoită Al., Scharf F., Structuri mixte Conf. reg. IABSE-ASCE-Tall Buildings, Iași 1975.
4. Olariu I., Structuri mixte solicitate la încărcări seismice. Ser. Inst. politehnic Cluj Napoca 1978



NIVEAU 5.(e)



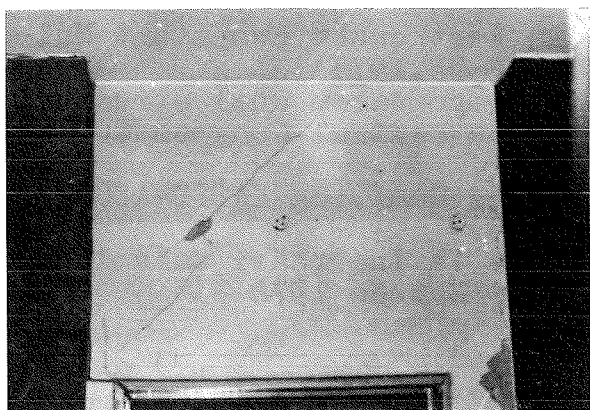
NIVEAU 6.(f)



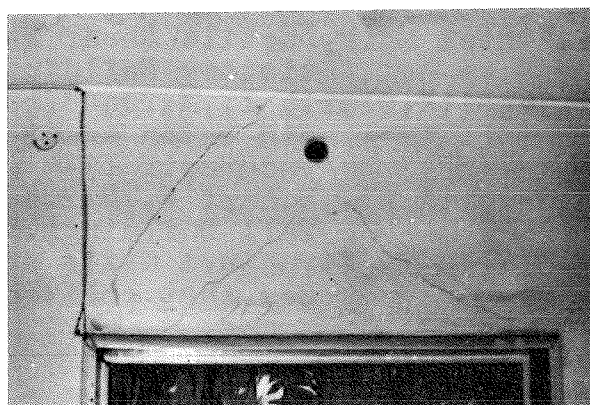
NIVEAU 3(c)



NIVEAU 4.(d)



NIVEAU 1.(a)



NIVEAU 2.(b)

FIG.8. La fissuration des linteaux.

OBSERVED SEISMIC BEHAVIOUR OF VARIOUS CONCRETE STRUCTURES

Yoshio OZAKA
Tohoku University
Sendai, Japan

Masanori IZUMI
Tohoku University
Sendai, Japan

Toshio SHIGA
Tohoku University
Sendai, Japan

SUMMARY

The damage of various types of concrete structures by Miyagi-ken-oki Earthquake (12, June, 1978; $M=7.5$) is investigated and analyzed. An example is a change of dynamic characteristics observed in a university 9 story building, where authors work and the max. horizontal acc. of 980 gals was recorded at the top.

Problems on aseismic design of reinforced concrete structures and the related research works are also discussed.

Les dégâts des structures en béton différents causés par le Tremblement de terre (survenu au 12 Juin 1978) de Miyagi-ken-oki sont investigés et analysés. Le changement des caractéristiques dynamics du bâtiment à 9 étage ou les auteurs travaillent est observé et l'accélération horizontale de 980 gals était enregistrée au sommet.

Les problèmes du calcul para-sismique des structures en béton armé se decrivent, et les recherches sur lesquelles sont aussi discutés.

1. MIYAGI-KEN-OKI EARTHQUAKE AND FEATURES OF DAMAGE

The hypocenter of the Miyagi-ken-oki Earthquake was located at $38^{\circ}09'$ north latitude and $142^{\circ}13'$ east longitude at a depth of 30 km.

In this earthquake much damage of urban nature such as collapses of embankments and buildings, and destruction of electric power, gas, water supply and oil facilities occurred since the hypocenter was close to the city of Sendai (population 600,000) possessing highly urbanized functions, much residential land had recently been developed at a rapid pace in hilly areas in the environs of Sendai accompanying urbanization, and many multi-storied apartment house buildings had been constructed in areas of relatively soft ground. Further, with the Tohoku Shinkansen Line being under construction, there were many structures which had not yet been completed so that much damage was suffered by concrete railroad structures resulting especially in heated debate on earthquake-resistant design of high-speed railroad structures.

2. STRUCTURAL DAMAGE TO REINFORCED CONCRETE BRIDGES AND PROBLEMS OF DESIGN

2.1 Elevated Reinforced Concrete Bridges

At elevated bridges of rigid-frame type (Fig. 2-1), damage was sustained

mainly at tops ((A)) and bottoms ((B), (C)) of columns, and at horizontal beams ((D₁), (D₂)) provided at the middles of columns. However, there were hardly any cases of all of these types of cracks being produced simultaneously in the same viaduct, and in almost all cases there was no more than one type occurring. Fig. 2-2 is an example of damage at the top of a column. In spite of the fact that this is an important part which would be subject to prominent bending and shear during earthquake, it is unavoidable for a construction joint to be provided for reasons of the sequence of concrete placement and reinforcement assembly, and structural defects are liable to be produced. Influences of the defects are evident in the case of this example also. Cross section properties and design section forces of elevated bridge pier which sustained damage are indicated in table 2-1.

Numerous diagonal cracks produced in horizontal beams provided near mid-heights of columns as shown in Fig. 2-3 reached as much as about 1 mm in width, and on performing tension tests on reinforcing bars cut from stirrups at such a part, it was thought that stresses considerably exceeding the yield point had been sustained as shown in Fig. 2-4. The nominal shear of this horizontal beam during earthquake is $\tau = 1.2 \text{ N/mm}^2$, and the shear force which can be carried by stirrups according to the simple truss analogy is of a value corresponding to $\tau = 0.8 \text{ N/mm}^2$. In view of the damage suffered, the design was changed to increase the reinforcement ratio of stirrups at this part to about double the previous ratio.

Fig. 2-5 indicates the results of transverse vibration tests conducted on a viaduct with cracked horizontal cross beams. The natural period of primary vibration was 0.24. This value became 0.25 after repairing by injection of resin in the diagonal cracks of horizontal beams and it may be seen that rigidity of the entire structure had been slightly increased.

2.2 Girder-Type Elevated Structures

At girder-type elevated structures such as shown in Fig. 2-7, much damage occurred such as breakage of cast iron shoes of girders (Fig. 2-6), cracking of heads of piers near shoes, cracking of cantilevered parts supporting electric train power line poles (Fig. 2-7), and bending cracks at bottom parts of wall-type bridge piers.

Further, there were many cases of fairly large movements of girders accompanying damage to shoes.

2.3 Piers of Long Prestressed Concrete Bridges

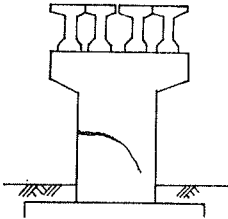
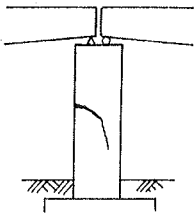
There was considerable damage suffered by massive piers also. Cross section properties and design section forces of piers which sustained damage are indicated in Table 2-1.

Fig. 2-8 is an example of cracking which appeared in a pier of a 4-span continuous bridge of 45 m spans. This cracking was produced from the cross section at which a half of axial reinforcement had been cut off and extended diagonally downward influenced by shear to reach close to the surface on the compression side. Reinforcement continuous at the cross section at which cut-off of axial bars had been performed had been elongated past the yield point by increase in steel stress caused by diagonal cracking and buckled being subjected to earthquake force in the opposite direction (Fig. 2-9).

It is thought that yielding of axial reinforcement had been the direct cause of the heavy damage at this bridge pier.

Fig. 2-10 shows an example of damage to a bridge pier supporting a simple beam of span of 45 m where bending shear cracks are prominently developed as a whole, with many cracks further developed in a complex manner to cause bearing strength of the bridge pier to be lost.

Table 2-1

| Structure | Properties of Cross Section(m ²) Crack Pattern | Action effects (kN or kNm) | Stresses (N/mm ²) | Resistances (kNm or kN) |
|---|---|---|--|--|
| Top End of Elevated Bridge column | $\rho_l = 0.022$ $\rho_w = 0.0021$ $A_c = 1.2 \times 1.2 = 1.44$ See (A) in Fig. 2-1 | $N_{sd} = 530$ $M_{sd} = 2700$ $V_{sd} = 533$ | $\sigma_c = 9$ $\sigma_s = 300$ $\tau = 0.5$ | $M_{rd} = 970$ $M_{Rd} = 5600$ $V_{Rd1} = 730$ $V_{Rd2} = 8700$ $V_{Rd3} = 2000$ |
| Cross Beam of Elevated Bridge | $\rho_l = 0.01$ $\rho_w = 0.0012$ $A_c = 0.85 \times 1.1 = 0.935$ See (D ₁) and (D ₂) in Fig. 2-1 | $N_{sd} = 0$ $M_{sd} = 2000$ $V_{sd} = 730$ | $\sigma_c = 11$ $\sigma_s = 280$ $\tau = 1$ | $M_{rd} = 510$ $M_{Rd} = 2500$ $V_{Rd1} = 530$ $V_{Rd2} = 5600$ $V_{Rd3} = 910$ |
| Bridge Pier of Simple Beam Bridge (NANAKITA-GAWA) | $\rho_l = 0.00095$ $\rho_w = 0.00065$ $A_c = 16.07$  | $N_{sd} = 25000$ $M_{sd} = 53000$ $V_{sd} = 6300$ | $\sigma_c = 8$ $\sigma_s = 130$ $\tau = 0.5$ | $M_{rd} = 67000$ $M_{Rd} = 83000$ $V_{Rd1} = 8200$ $V_{Rd2} = 84000$ $V_{Rd3} = 22000$ |
| Bridge Pier of Continuous Beam Bridge (NATORI-GAWA) | $\rho_l = 0.00143$ $\rho_w = 0.0002$ $A_c = 18.37$  | $N_{sd} = 18000$ $M_{sd} = 42000$ $V_{sd} = 6900$ | $\sigma_c = 9$ $\sigma_s = 250$ $\tau = 0.4$ | $M_{rd} = 43000$ $M_{Rd} = 54000$ $V_{Rd1} = 8400$ $V_{Rd2} = 95000$ $V_{Rd3} = 21000$ |

ρ_l, ρ_w : geometrical percentage of longitudinal and transverse reinforcements respectively.

A_c : Area of Concrete cross section

N_{sd}, M_{sd}, V_{sd} : axial force, bending moment and shear force respectively when considering seismic coefficient $K_h = 0.26$ (dead load, shrinkage, temperature change and earthquake)

σ_s, σ_c, τ : tensile stress of axial bar and compressive and shear stresses of concrete respectively when considering seismic coefficient $K_h = 0.26$ (Straight line theory, modular ratio = 15)

$M_{rd}, M_{Rd}, V_{Rd1}, V_{Rd2}, V_{Rd3}$: calculated value according to method of CEB Model Code

3. DAMAGE TO BUILDING STRUCTURES AND PROBLEM OF DESIGN

3.1 Damage Characteristics of Building Structures

An obvious coincidence was observed in the distributions of weak sub-soil layers and the earthquake damage. Several RC Buildings of three, four storeys without sufficient walls were collapsed and some steel structures were severely destroyed after the rupture of the bracing. Out of twenty seven lives lost in the earthquake, only one was killed under a collapsed house; a wooden temple with a heavy roof. This proves Japanese buildings are generally ductile (Fig. 3-1,2).

3.2 RC(Reinforced Concrete) and SRC(Steel frame and RC Composite) Buildings

Japanese Building Code was revised after Tokachioki Earthquake, 1968 when many pillars were destroyed by sheering forces. Most of damaged RC buildings in the recent quake were constructed before the code-revision, and similar types of cracks were produced in their pillars (Fig. 3-3). A few of new buildings were also damaged inspite that they were designed under the new regulation. An example is IZUMI High School (Fig. 3-4), where hoops of columns were well designed and constructed.

No SRC buildings were collapsed. An example is nine storied university building; where the authors have the offices. Two strong motion accelerographs of three components each were installed δ at the ground and the ninth floor, and latter recorded maximum values of about 1000gals (Fig.3-5,6).

Cracks were produced in the walls and the fundamental natural periods of the building become about 1.5 times longer in microtremor measurement.

3.3 PC(Precast concrete) and Steel Building

No remarkable damage were observed; in an apartment HPC building (large PC pannel and steel frame of H section), concrete was peeled out around the setting base and this might have been produced when heated during the welding in the construction (Fig. 3-7).

Several of long-spaned steel frame structures like storages and gymnasiums were severely damaged. Bracings were insufficient, 'tension members' under the design loads were compressed and buckled, and relative displacements among footings produced stress concentration in the joints (Fig. 3-8,9).

Window glasses, finishings, and curtain walls were broken when they were tightly fixed to the flexible main structures. Furnitures and equipments of the upper parts of the buildings were turn over, and these suggested the necessity of informations on the dynamic characteristics from structural engineers to designers (Fig. 3-10).

4. CONCLUSION

Design seismic coefficients for bridges and building structures in this area are 0.26 and 0.18 respectively but the actually loaded value is estimated to be about two times or so in the average. Consequently simple structures without surplus strength were damaged. Besides, spacial behaviour were neglected in the structural design for calculation-convenience, thus unexpected failure took a place. The effect of soil-structure interaction can not be omitted unless the structure is designed strong enough.

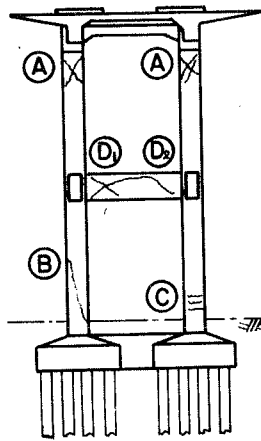


Fig. 2-1
Crack patterns
of Rigid Frame
Viaduct



Fig. 2-2 Damage at the Top of Column

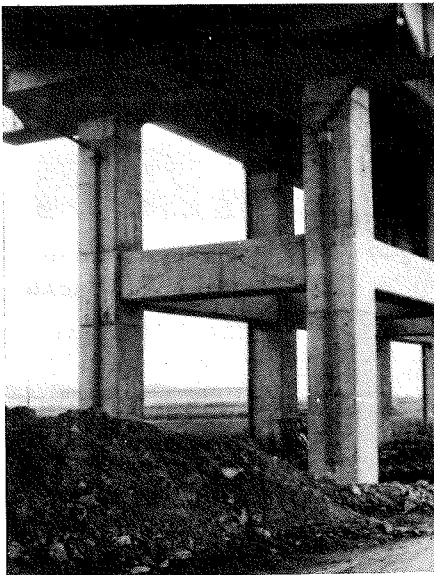


Fig. 2-3 Cracks of Cross
Beam

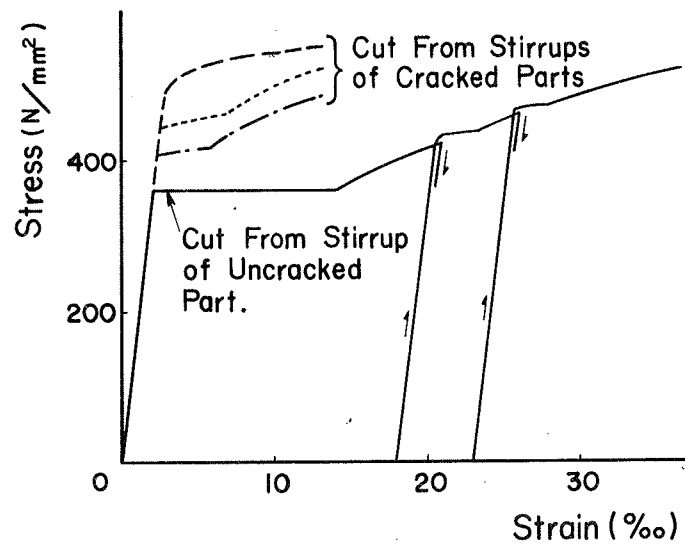


Fig. 2-4 σ - ϵ Diagrams of Reinforce-
ment Cut from Stirrups

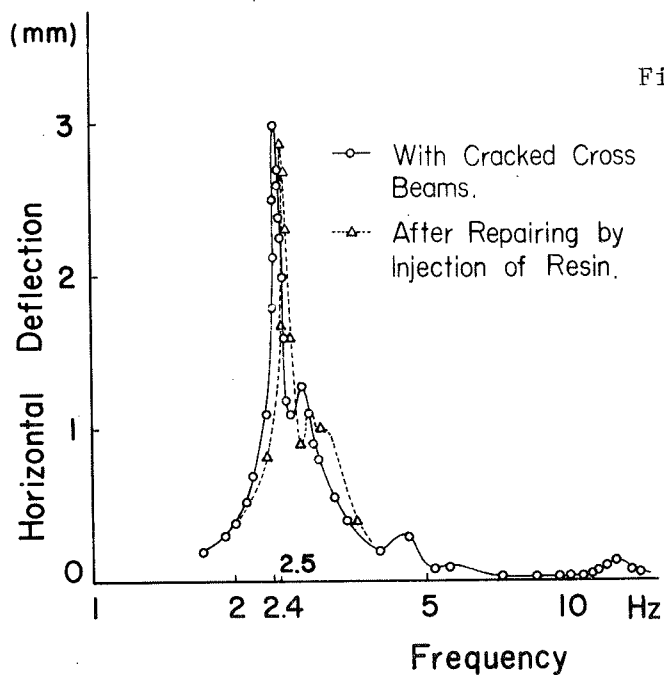


Fig. 2-5 Resonance Curve in
Transverse Direction of
Rigid Frame Viaduct

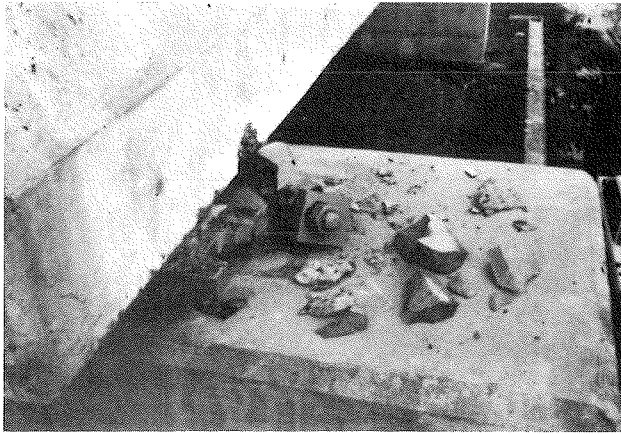


Fig. 2-6 Damaged Cast Iron Shoe

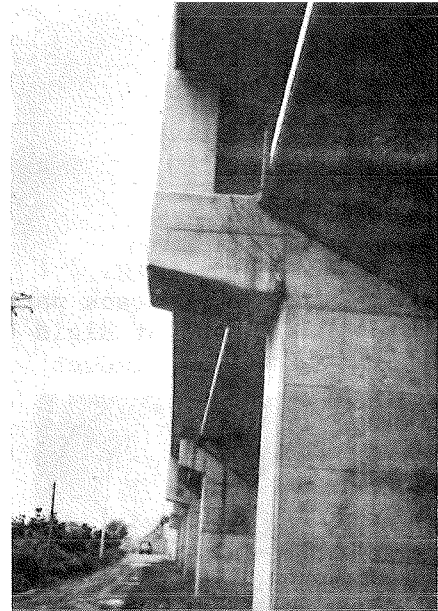


Fig. 2-7 Girder-Type Viaduct and Diagonal Cracks of Short Gasset

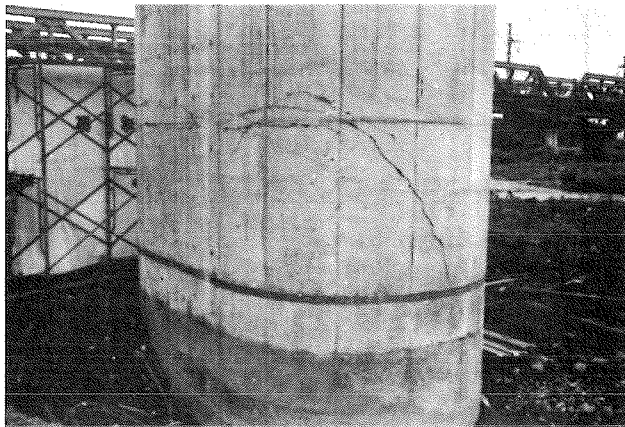


Fig. 2-8 Pier of 4-span Continuous Prestressed Concrete Bridge

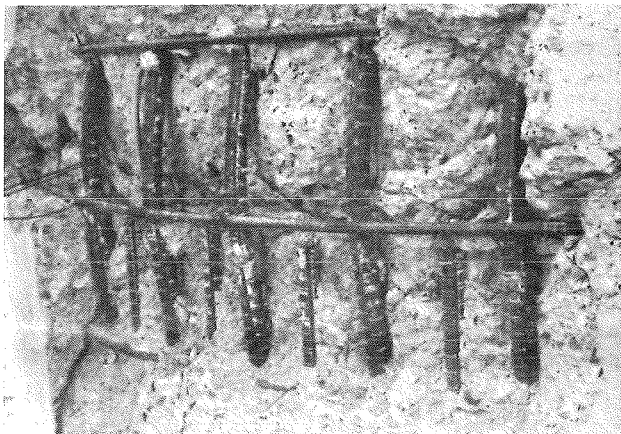


Fig. 2-9 Buckling of Axial Reinforcements of Bridge Pier at the Section of Cut-off

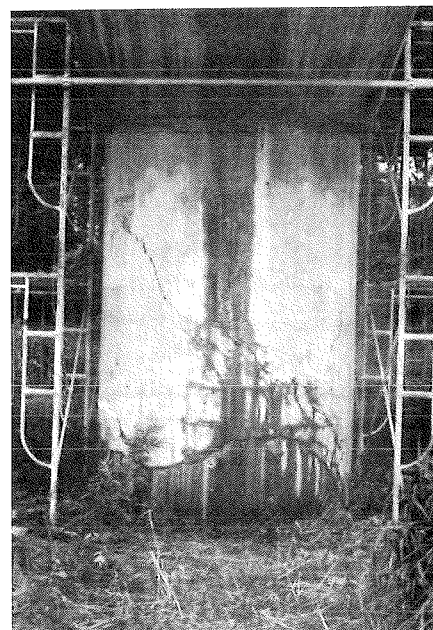


Fig. 2-10 Pier of Prestressed Concrete Simple Girder Bridge

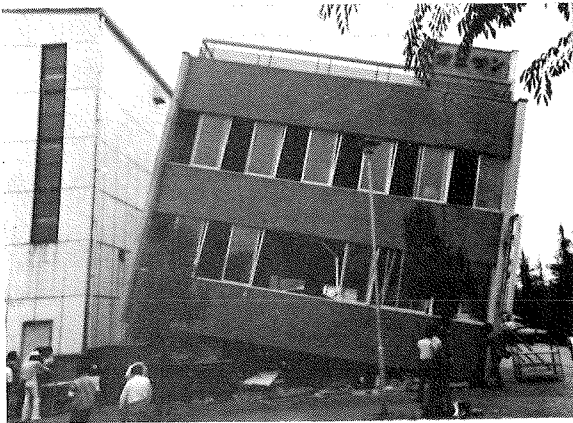


Fig. 3-1 Collapsed RC building



Fig. 3-2 Collapsed wooden house



Fig. 3-3 Damaged Pillar (Designed by Old Regulations)



Fig. 3-4 Damaged Pillar (Designed by New Regulations)



Fig. 3-7 Setting base of a 17 storyed HPC bldg.

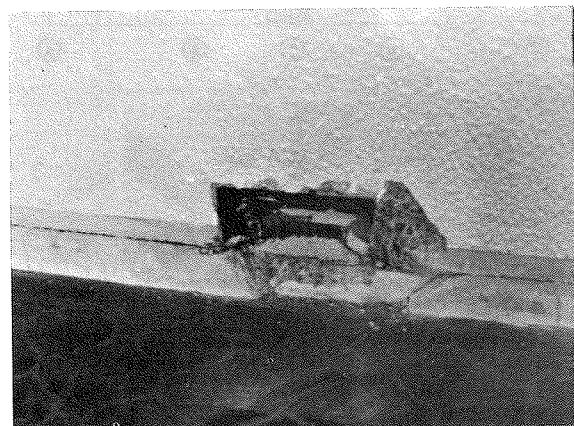


Fig. 3-8 Collapsed steel frame

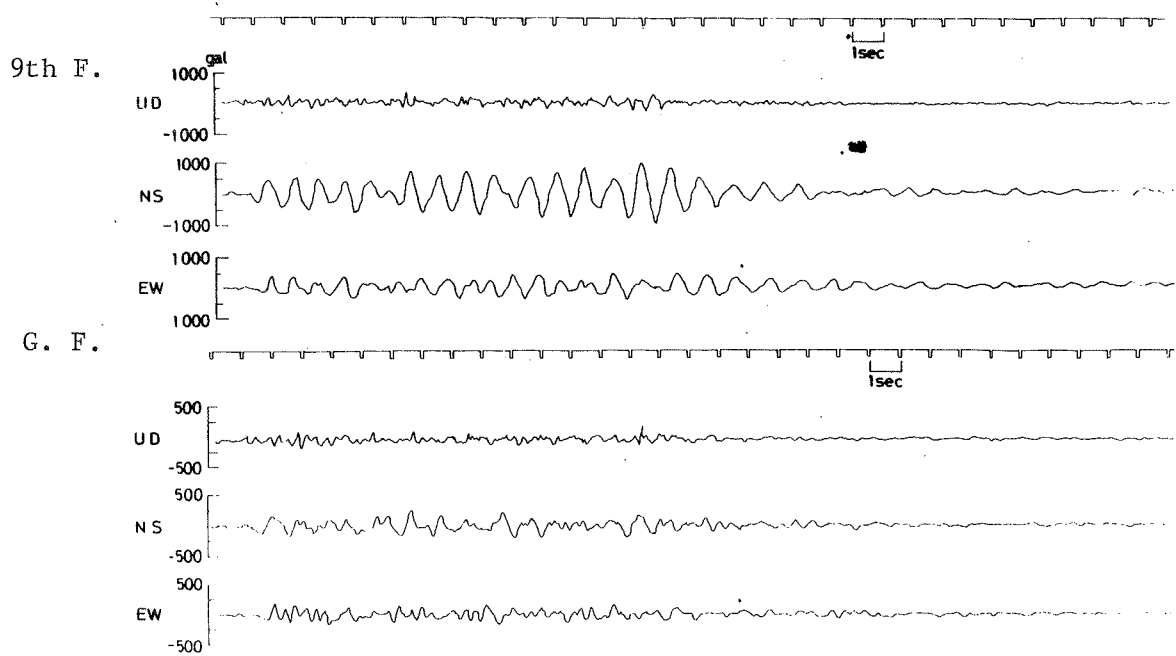


Fig. 3-5 SMAC Recorded obtained at an Univ. bldg.

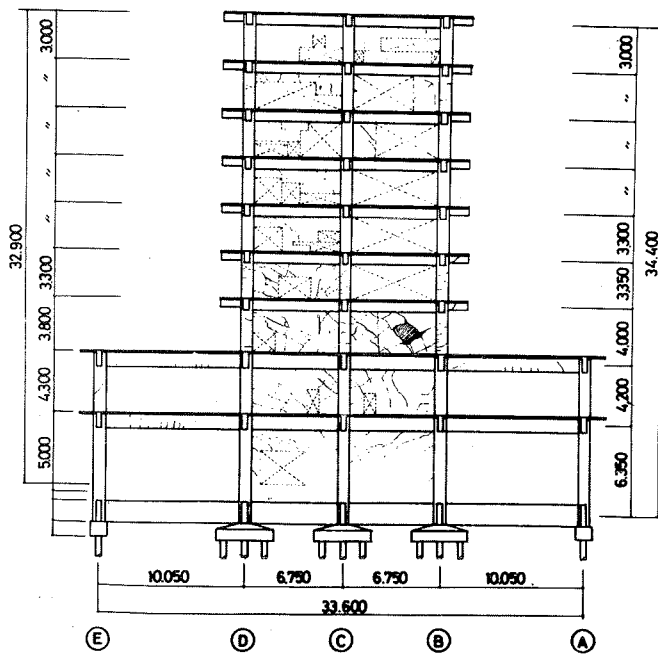


Fig. 3-6 Crack pattern of the Univ. bldg.

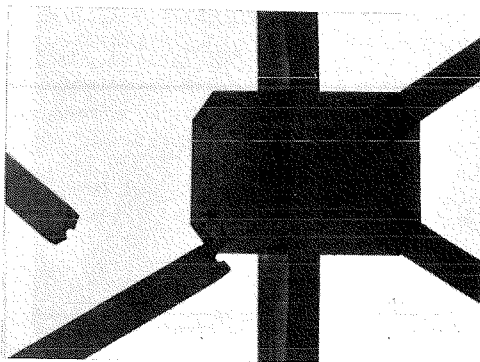


Fig. 3-9 Ruptured bracings

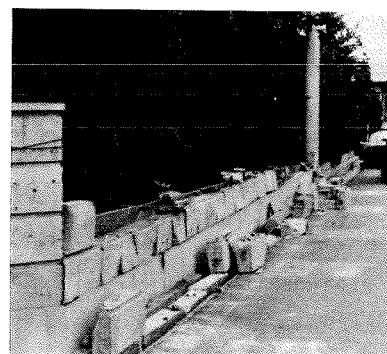


Fig. 3-10 Damaged stone fence

THE MYAGI-KEN-OKI, JAPAN, EARTHQUAKE OF JUNE 12, 1978:

EFFECTS ON REINFORCED CONCRETE STRUCTURES

John A. BLUME

Peter I. YANEV

URS/John A. Blume & Associated, Engineers

URS/John A. Blume & Associated Engineers

San Francisco, Calif. 94105

San Francisco, Calif. 94105

U.S.A.

U.S.A.

Summary--The M 7.4 Miyagi-Ken-oki, Japan, earthquake of June 12, 1978, affected a variety of reinforced concrete structures in the metropolitan area of the city of Sendai. Hundreds of modern structures were subjected to peak ground accelerations in the range of 0.2g to 0.4g. The duration of the strong motion was more than 30 sec. Peak floor-response accelerations in concrete structures reached 1.0g. Although several dozen structures were damaged extensively, the performance of the majority of the structures was excellent. The response of several structures is described; damage is summarized; some strong-motion records are presented; and various causes of damage are examined.

Résumé--Le tremblement de terre japonais de 12 juin 1978 du côté de la préfecture de MIYAGI dont le magnitude Richter était 7,4 a fait vibrer plusieurs types d'édifices modernes en béton armé dans la région de la ville de SENDAI. Les accélérations du sol dans cette région étaient de 0,1g à 0,4g environ et ont affecté certaines des structures. La durée s'est estimée plus de 30 secondes. Les plus fortes accélérations obtenues aux étages supérieurs dans ces édifices en béton ont atteint 1,0g. Lorsque plusieurs douzaines d'édifices s'étaient largement fissurées ou fracturées, la majorité se comportaient sans problème. On décrit ce comportement sismique de plusieurs édifices, en discutant les pourquoi. Aussi, on montre quelques accélérogrammes de ce tremblement de terre.

THE EARTHQUAKE

A major earthquake, identified as Miyagi-Ken-oki (or offshore-Miyagi Prefecture) by the Japanese authorities, struck the northern section of Honshu, the main island of Japan, on June 12, 1978. The shock caused considerable damage in Miyagi Prefecture, particularly in the principal city, Sendai, and its metropolitan area.

The earthquake had a Richter magnitude (M) of 7.4 and a hypocentral depth of about 30 km. It occurred at 08:14:27.0 GMT (17:14 local time). The epicenter was 38.2° N, 142.2° E, about 100 km east of Sendai on the subducting Pacific tectonic plate. In Figure 1, which shows the location of the epicenter, Sendai, and Tokyo, a reversed outline of California has been superimposed over a map of Japan of the same scale (Yanev, ed., 1978). The Japanese Meteorological Agency (JMA) intensity values (0 to 7) for the Miyagi-Ken-oki earthquake are also shown on the map. Figure 2 compares the JMA scale with the Modified Mercalli (MM) scale. In general, JMA intensities were a high 5, which corresponds to MM VIII. More than 100 strong-motion records were obtained in the city of Sendai, peak ground accelerations were generally between 0.20g and 0.40g.

While the epicentral distance to Sendai is about 100 km, the city lies in the down-dip direction of the probable rupture plane, and the surface distance from some sources of the energy release to Sendai could have been as short as 55 km (Yanev, ed., 1978).

Only 27 people were killed by the earthquake (about half of them died because of falling ground-supported walls), a small number of fatalities for such a large earthquake; however, more than 1,000 others were injured. Tsunami effects were negligible, but there was some flooding. Fire was contained locally, and in some places this must have represented heroic efforts. The preliminary total estimated direct building loss (Yanev, ed., 1978) is more than \$830 million (June 1978 U.S. dollars).

Sendai is a large, modern city with a population of more than 615,000 (1975 data). Its metropolitan area contains more than 1.2 million people. Many hundreds of buildings in the city are at least five stories high and are modern high-rise structures. The central downtown area, in particular, has a great many modern buildings in the 10- to 20-story range. A large proportion of them are steel frame; many have concrete shear walls, and others use the Japanese steel-reinforced concrete (SRC) system, in which embedded structural steel shapes, in conjunction with conventional reinforcing steel, constitute the reinforcement.

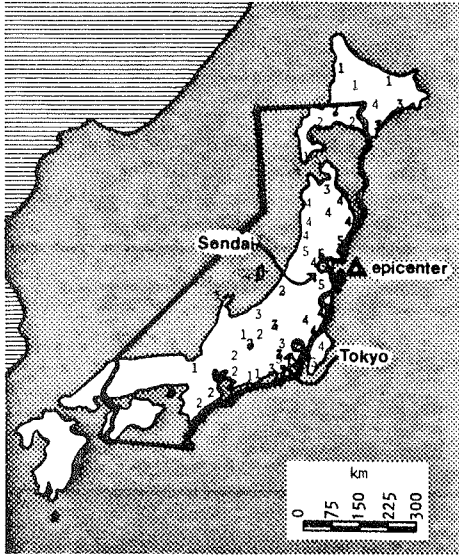


Figure 1 Miyagi-Ken-oki earthquake intensities (Japanese scale: 0-7). Base map data: Building Research Institute, Ministry of Construction, Japan. (Courtesy C. Arnold)

| USA MODIFIED MERCALLI | JAPAN KAWASUMI, 1951 |
|-----------------------------|-------------------------|
| I | 0 |
| II | 1 |
| III | 2 |
| IV | 3 |
| V | 4 |
| VI | 5 |
| VII | 6 |
| VIII | 7 |
| IX | |
| X | |
| XI | |
| XII | |

Figure 2 Comparison of United States (MMI) and Japan Meteorological Agency (JMA) intensity scales

It was difficult, upon entering the city, to believe that a damaging earthquake had occurred. Closer inspection revealed exterior damage, but even that was not widespread; many modern buildings showed no damage to their architectural veneer or glazing. However, upon further investigation, it became obvious that local areas of greater damage, apparently correlated to local geologic and soil conditions, existed throughout the city.

CURRENT SEISMIC DESIGN REQUIREMENTS

The current Japanese Building Code, which was adopted in 1972, specifies the following seismic lateral load criteria for buildings less than 45 m high.

The lateral force f_i at the i th floor is specified to be $f = k \cdot w_i$, where k is the seismic coefficient and w_i is the i th floor mass. The seismic coefficient, k , is given by $k_0 = k Z S$, where:

$$k_0 = 0.2 \text{ for } H \text{ (height)} \leq 16 \text{ m}$$

$$k_0 = 0.2 + i \text{ for } H > 16 \text{ m}$$

$$i = \text{floor increment} = 0.01 \text{ for each 4 m over 16 m}$$

$$Z = \text{zone factor, which varies between 0.8 and 1.0 and is 0.9 in Miyagi Prefecture and Sendai}$$

$$S = \text{soil factor, which varies between 0.8 (rock sites) and 1.0 (soft-soil sites)}$$

Thus, the typical building under 45 m in height is designed for a base shear of about $0.18 W$ to $0.20 W$, where W is the total weight, depending on building height and geological foundation.

Buildings more than 45 m high must be approved by the Examination Board of the Government Building Center of Japan. The Architectural Institute of Japan provides guidelines for the design of high-rise buildings; these have been adopted by the Building Research Institute (BRI) of the Ministry of Construction as general guidelines. Dynamic response analyses are generally performed for high-rise buildings. The design base shear, F , of a building is the product of the base shear coefficient, C_1 , and the total weight, W : $F = C_1 W$, where:

$$C_1 = C_0 Z I$$

$$C_0 = \text{the base shear coefficient, which is dependent on the fundamental period of the building and the geological foundation, varying between 0.20 and 0.085 for periods less than 3 sec}$$

$$Z = \text{zone factor, which varies between 0.8 and 1.0}$$

$$I = \text{an importance factor}$$

REPRESENTATIVE HIGH-RISE BUILDINGS

Two typical high-rise buildings are shown in Figure 3. Many structures like the 6-story rein-

forced concrete Minami Machidori building suffered significant damage; however, there were no collapses despite the high ground acceleration recorded and the long duration of strong motion. The 18-story Sumitomo Life Insurance building is one of the highest structures in Sendai. The structure was designed with the aid of dynamic analyses and was constructed in 1974. The three-floor underground portion of the building is of SRC construction. The 18-story superstructure (and 2-story penthouse) has a steel frame with continuous, full-height, symmetrical concrete shear walls on two sides of the exterior and around the interior elevator core. From in-situ low g-level testing, the natural frequencies of the building in the two horizontal directions are found to be approximately 1.19 and 1.25 Hz; the structure is relatively stiff for its height, probably because of the presence of shear walls.



Figure 3 Two typical high-rise buildings in Sendai. The 6-story reinforced concrete Minami Machidori building, on the left, suffered extensive cracking to its brick veneer facing and shows signs of possible structural damage as well. The 18-story Sumitomo Life Insurance building, shown on the right, suffered cracking at the interior concrete shear walls of its upper stories.

The building was instrumented; records were obtained at the second-basement level (B2F) and at the ninth and eighteenth floors. The following peak accelerations were recorded:

| Earthquake | Floor | Peak Acceleration (g) | | |
|---------------|-------|-----------------------|-----------|---------|
| | | North-South | East-West | Up-Down |
| June 12, 1978 | B2F | 0.26 | 0.23 | 0.12 |
| | 9 | 0.40 | 0.53 | 0.21 |
| | 18 | 0.50 | 0.56 | 0.23 |

The uncorrected basement (B2F) north-south component's time history and its acceleration response spectra at 2%, 5%, and 7% of critical damping are shown in Figure 4. The ground time history of acceleration in the north-south direction is characterized by several excursions above 0.15g, with about 15 sec of motion continuously exceeding 0.10g.

Damage to the building was generally light and was restricted to cracking of the interior shear walls of the upper floors and along construction joints in the stairwell shear walls. The cracking of the walls was sufficient to alter the natural frequency of the building. The post-earthquake frequency is about 0.8 to 1.0 Hz, which is a 20% to 35% drop from the preearthquake condition. There was no apparent damage to other structural or nonstructural elements, including the steel frame.

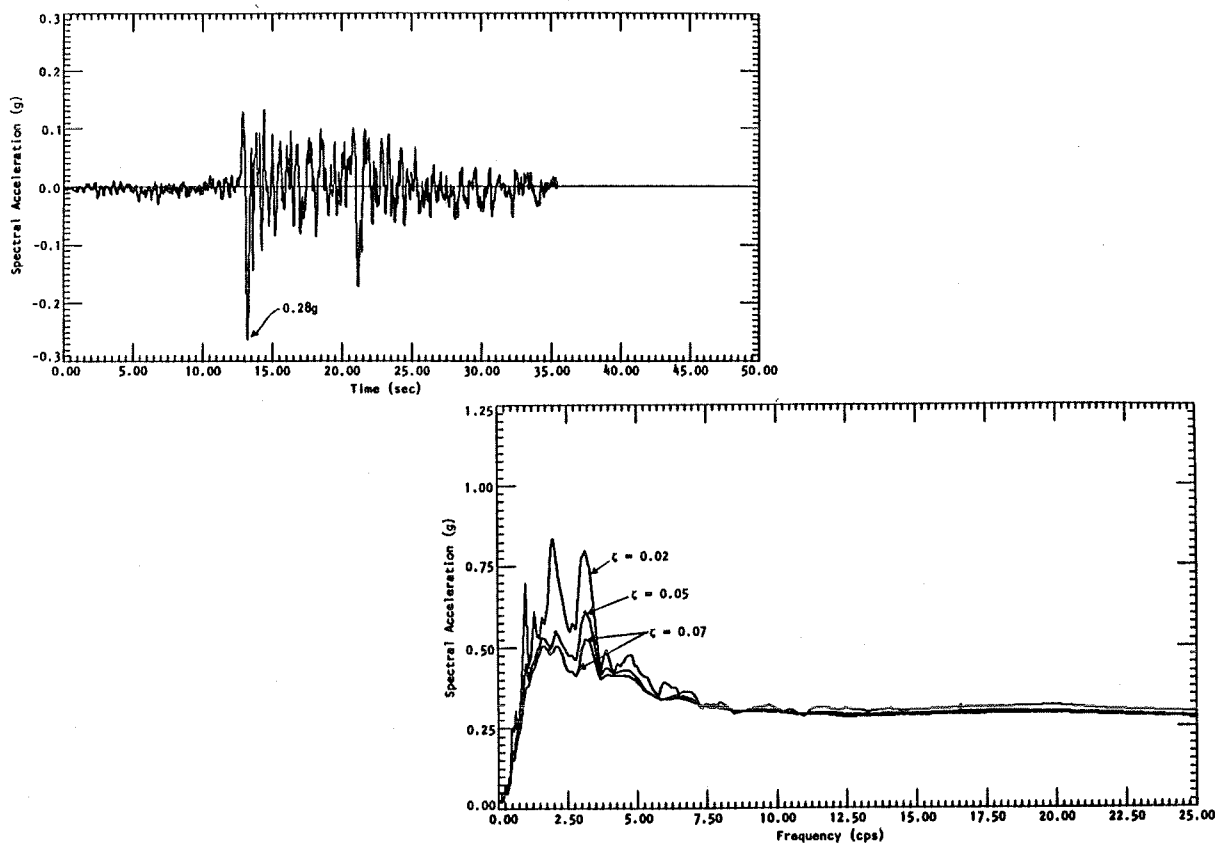


Figure 4 Sumitomo Life Insurance building. The uncorrected basement (B2F) north-south component of the recorded time history and its acceleration spectra at 2%, 5%, and 7% of critical damping.

The reinforced concrete frame Faculty of Engineering building of Tohoku University, founded on a rock outcrop on the outskirts of Sendai, represents a unique case in earthquake engineering. The building (Figure 5) has a 9-story, 34.4-m-high tower surrounded by a 2-story lower structure; the two parts of the structure are interconnected. The tower has continuous transverse shear walls along the entire height and width of the exterior and contains transverse and longitudinal shear walls along the full height of the elevator core. The shear walls vary between 15 and 50 cm in thickness. The building was completed about 1969 and was designed for a total base shear of about 0.20g. As built, its fundamental frequencies in the horizontal directions were both about 2.0 Hz.

The building successfully withstood two strong earthquakes in 1978. The first, an M 6.7 shock, occurred on February 20, 1978, as a foreshock of the June 12, 1978, earthquake. An accumulation of data from previous, smaller earthquakes is also available for the building, which has two SMAC instruments: at ground level (there is no basement) and on the ninth floor. The M 6.7 earthquake apparently caused some damage to the structure (cracking of shear walls, window breakage) and lengthened its period. The June 12, 1978, M 7.4 earthquake amplified that damage: the width of the diagonal cracks in the shear walls increased, and more windows were broken (mostly by falling bookcases and other falling objects). Recorded peak accelerations from the two earthquakes are:

| Earthquake | Floor | Peak Acceleration (g) | | |
|-------------------|-------|-----------------------|-----------|---------|
| | | North-South | East-West | Up-Down |
| February 20, 1978 | 1 | 0.17 | 0.11 | 0.09 |
| | 9 | 0.37 | 0.26 | 0.08 |
| June 12, 1978 | 1 | 0.24 | 0.19 | 0.15 |
| | 9 | 1.00 | 0.49 | 0.31 |

Figure 6 shows the north-south acceleration records from the ground and ninth floors. The east-west records are similar but have lower amplitudes. In the north-south direction, the building experienced about 15 sec of continuous motion at the ninth floor that was between 0.5g and 1.0g and about 20 sec of motion greater than 0.25g. A preliminary analysis (performed by BRI) of the high-amplitude (1.0g) oscillations in the north-south direction at the ninth floor indicates that the displacements involved are about ± 25 cm. Results of spectral analyses by BRI for the east-west component first at the floor are shown in Figure 7.

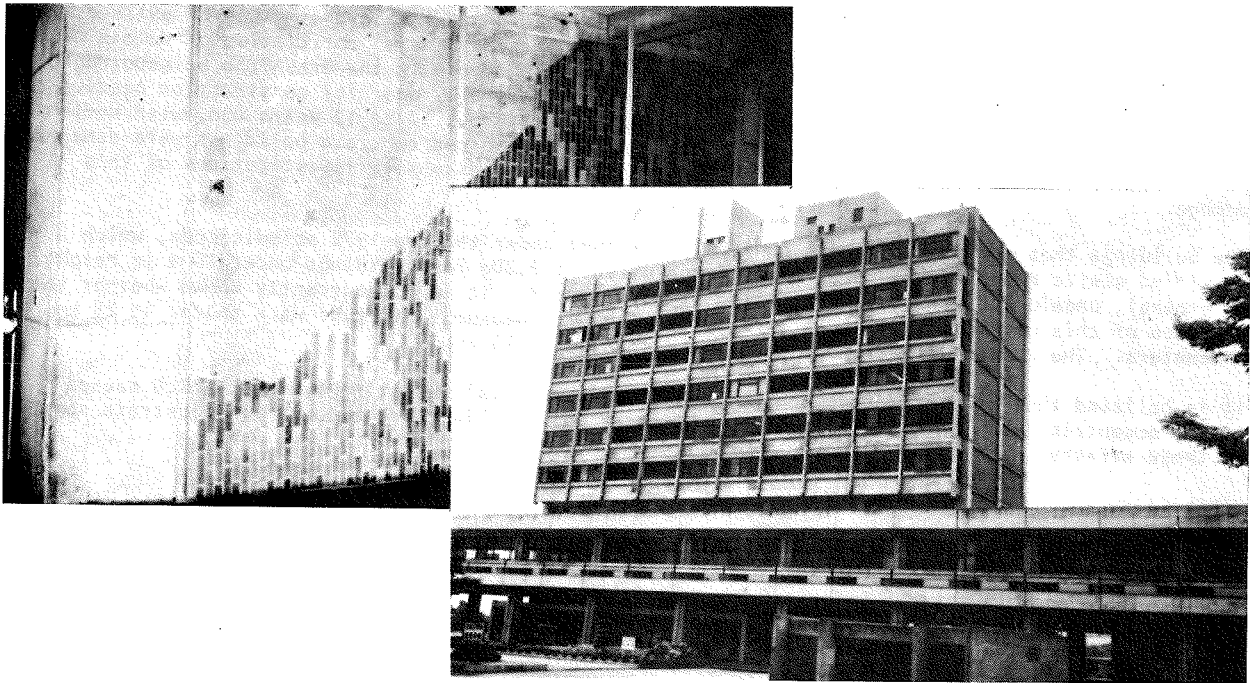


Figure 5 Faculty of Engineering building, Tohoku University: a general view (right) of the 9-story reinforced concrete frame building and a damaged transverse shear wall at the ground floor (left). Some of the glazed tile veneer has spalled along and above a diagonal crack.

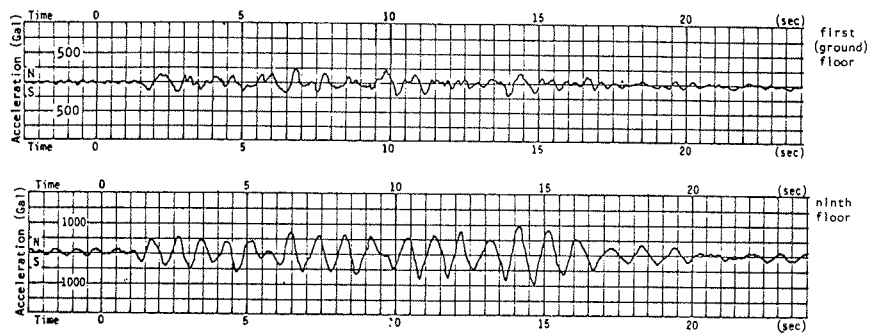


Figure 6 The ground-floor and ninth-floor acceleration time histories in the north-south direction; Faculty of Engineering building, Tohoku University (Courtesy Building Research Institute, Japan)

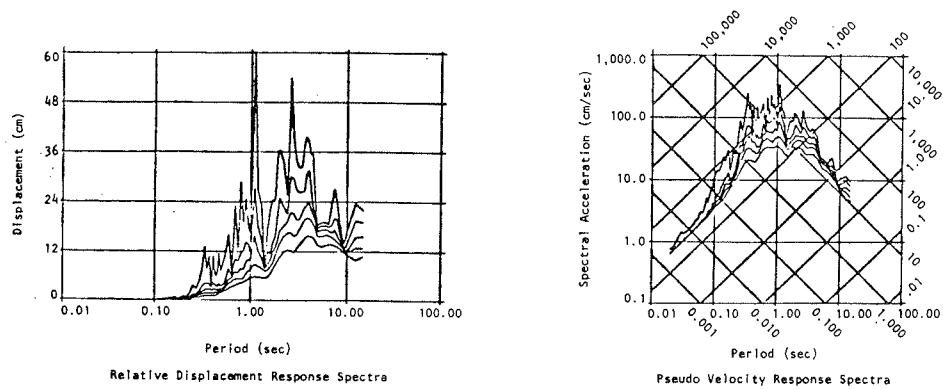


Figure 7 Spectral analyses of first floor, east-west component, Faculty of Engineering building, Tohoku University. The damping values are 0%, 2%, 5%, 10%, and 20% of critical. (Courtesy Building Research Institute, Japan)

REPRESENTATIVE LOW-RISE BUILDINGS

Many hundreds of low-rise reinforced concrete buildings in Sendai were subjected to the earthquake. Most of these buildings were undamaged or only slightly damaged. The several cases of extreme damage were scattered throughout Sendai. There appears to be a general correlation of damage with local soil conditions. There was a concentration of severe damage in the Oroshicho neighborhood, on the eastern edge of Sendai, where soil conditions are generally poor for construction needs. The area was once devoted to rice paddies but was developed about 10 to 12 years ago, with medium-density residential and commercial zoning. At least 10 reinforced concrete buildings were damaged seriously; four of them suffered collapse. BRI has conducted extensive investigations of this damage.

The buildings that were damaged were generally designed under the pre-1972 seismic code, which specified static design for a total shear force of about 0.20g for buildings under 16 m in height. In general, undeformed vertical reinforcing steel was used. It is not currently known whether the presence of this undeformed steel is correlated with high damage. Stirrups were spaced at 25 cm on centers. The current (1972) code requires a spacing of 10 cm.

It is believed that much of the damage was due to unsymmetrical resisting systems, which caused highly eccentric loads on critical columns and shear walls. Figures 8 through 11 illustrate some of these effects.

CONCLUSIONS

The total damage from the June 12, 1978, earthquake constituted only a small percentage of the total capital investment in buildings and structures, despite the recorded high ground accelerations, which generally ranged between 0.20g and 0.40g. Modern, properly designed structures, particularly high-rise buildings, performed well. The majority of the structural failures of reinforced concrete buildings occurred in low-rise structures that had strongly eccentric masses and unsymmetrical lateral resisting systems.

ACKNOWLEDGMENTS

Grateful acknowledgment is made of the many people who made the investigation possible. Dr. Tadayoshi Okubo, Chief of the Department of Planning and Research Administration, Public Works Research Institute, Ministry of Construction, Tokyo, and Mr. Toshio Iwasaki, Dr. Shinsuke Nakata, and Dr. Makoto Watabe of the Ministry of Construction provided most of the information and the strong-motion data on which the present text is based. Dr. Okubo made the basic arrangements for the investigation in cooperation with the United States - Japan Panel on Natural Resources, the U.S. National Bureau of Standards (NBS), and the Earthquake Engineering Research Institute, Berkeley. Dr. Edward O. Pfrang and Dr. H. S. Liu of NBS made the arrangements in the United States. Mr. James D. Cooper of the U.S. Federal Highway Administration and Mr. Bruce Ellingwood of NBS also participated in the investigation.

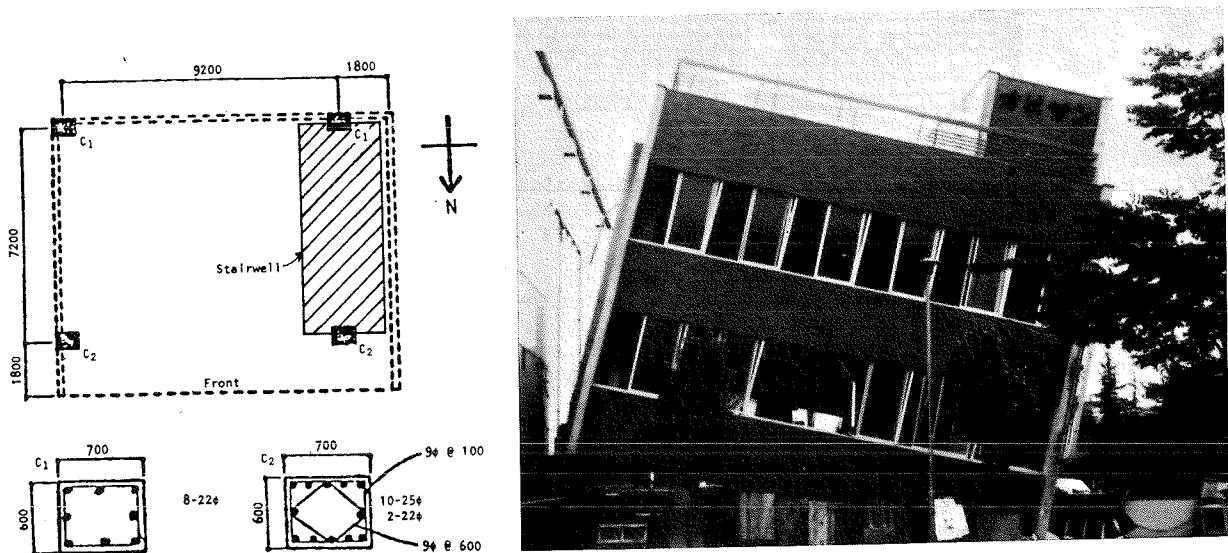


Figure 8 Obisan office building, Oroshicho area, Sendai: view from the north. The building was completed in 1969. It is a 3-story reinforced concrete frame building with a soft first story, one span in each direction, supported on four columns. The building has 1.8-m overhangs on the north and west sides of the upper floors. The stairwell is also placed eccentrically on the west (right) end of the building. The four corner columns of the ground floor were inadequate to resist the torsional force caused by the heavy eccentric masses.

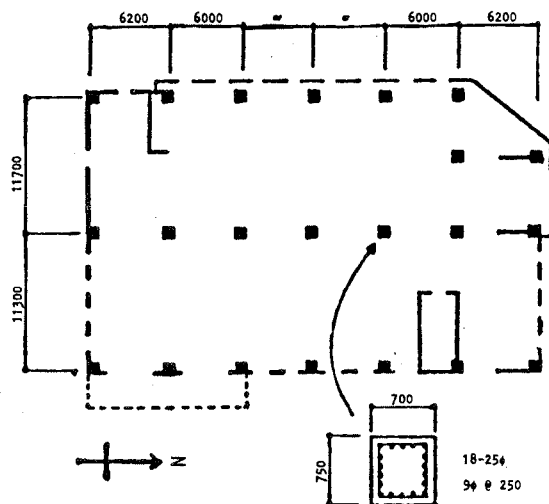
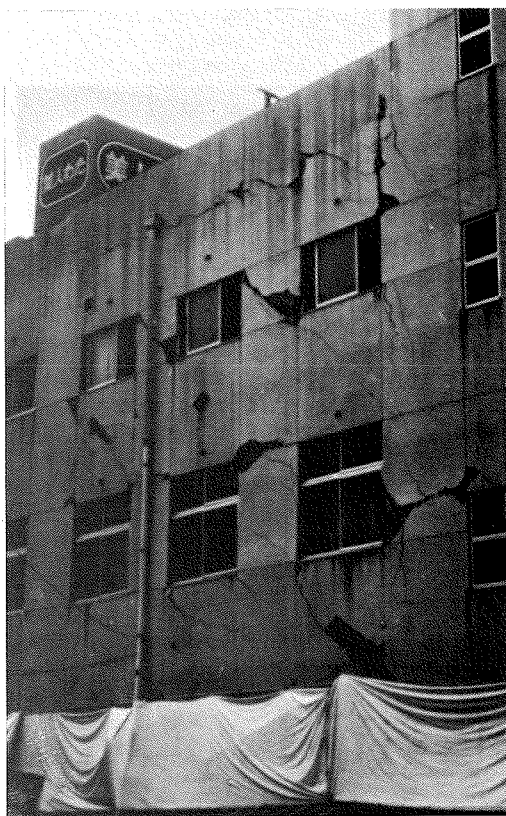


Figure 9 Kinoshita building, Oroshicho area, Sendai: view from the east (rear). This 3-story reinforced concrete building is two spans by six and was completed in 1969. The two spans in the east-west direction are long: approximately 11.5 m each. The structure is essentially a frame building. The first-floor columns along the centerline of the building in the north-south direction failed. In addition, the transverse foundation of the structure settled 10 to 15 cm along a middle column line, contributing to the extensive diagonal cracking. (Photograph courtesy J. D. Cooper)

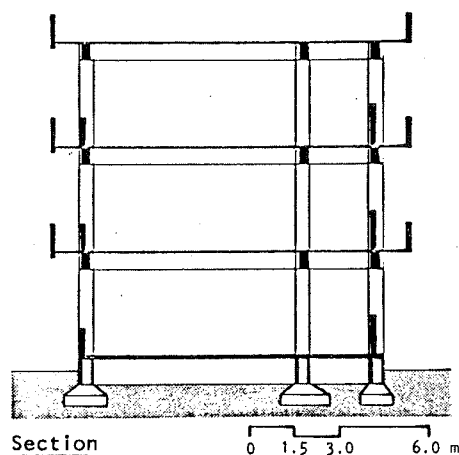
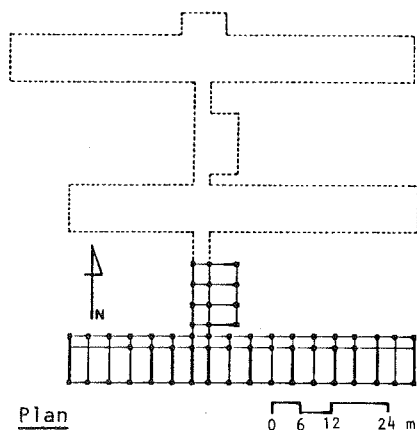


Figure 10 Plan and section of Izumi High School. The school's three adjacent reinforced concrete frame shear-wall structures, constructed after 1971, were damaged, but the school remained functional. Note in the plan the absence of shear walls in the east-west direction and the termination of the north-south shear walls at the corridor. Where shear failure in columns occurred, the architectural configuration had created short columns by the use of deep-poured concrete infill spandrels on one facade of the building but not on the other. The section shows how these spandrels, on the right, created short columns. (The opposite facade had longer, free-standing columns.) Furthermore, the use of shear walls in the north-south direction of these heavy, frame buildings was limited or omitted entirely because of the architectural need for full daylighting to classrooms. (Illustration courtesy C. Arnold)

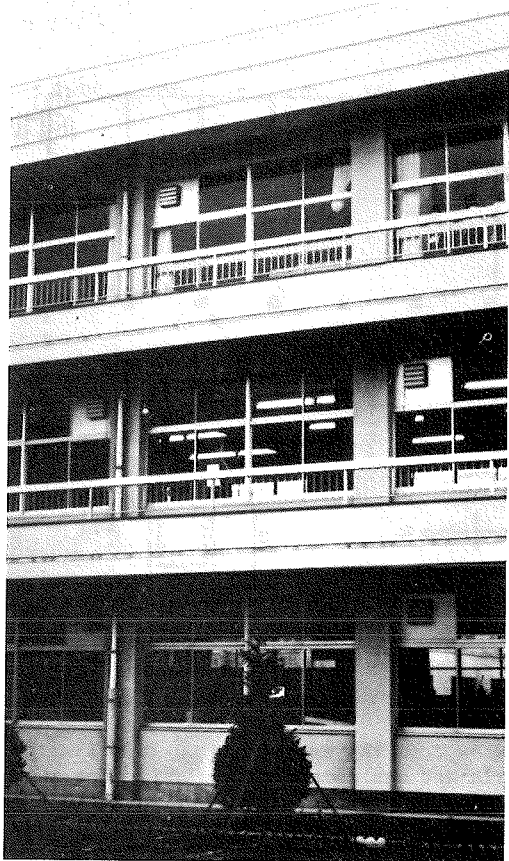


Figure 11 Izumi High School. The two illustrations show, respectively, two sides of a typical building. The rear of the building (left) is relatively open and suffered little apparent damage; damage was heavier on the side with partial-infill wall panels (right). The interior transverse shear walls frame into the columns on the rear but do not frame into the columns on the front because of a longitudinal corridor. All three buildings performed in the same manner.

REFERENCES

Peter I. Yanev (ed), Reconnaissance Report: *Miyagi-Ken-Oki, Japan, Earthquake, June 12, 1978* (contributing authors: C. Arnold, J. A. Blume, A. G. Brady, J. D. Cooper, B. R. Ellingwood, H. H. Fowler, E. L. Harp, D. K. Keefer, C. M. Wentworth, and P. I. Yanev), Earthquake Engineering Research Institute, Berkeley, California, December 1978.

A SURVEY ON THE COLLAPSE OF A THREE-STOREY REINFORCED CONCRETE FRAMED STRUCTURE DURING THE TANGSHAN EARTHQUAKES

| | |
|--------------------------------|--------------------------------|
| WEI LIAN | DAI GUO-YONG |
| Academy of Building Research | Academy of Building Research |
| Peking | Peking |
| The People's Republic of China | The People's Republic of China |

SYNOPSIS

A three-storeyed reinforced concrete framed structure of a factory building was severely damaged during the Tangshan Earthquake of July 28, 1976. It was later strengthened, but under the attack of a strong aftershock of November 15, 1976, the whole structure collapsed. Some experimental work of a full size model column subjected to cyclic loading and computer analysis for the nonlinear earthquake response of the structure were done. Other factors were also taken into account in analysing the causes leading to the entire collapse of the structure. Suggestions for future considerations in the design and strengthening of similar structures are recommended.

1. BRIEFING

Dimensions in plan and section of a three storeyed reinforced concrete framed structure factory building located in the Tientsin area are shown in Figure 1. It was a framed structure composed of weak columns and strong beams (strength of concrete: 150 kg/cm^2 ; reinforcing steel: NO.3 steel). Main reinforcement in the column sections: top storey $4\phi 16$; second floor outer columns: $6\phi 16$, inner columns $4\phi 19 + 4\phi 16$; ground floor outer columns $8\phi 19$, inner columns $10\phi 25$; with stirrups $\phi 6$ spaced at 3000 mm. The underlying soil of the factory building is sandy clay, but there is a layer of saturated plastic grocery fill about 3.5 metres thick in certain parts of the area.

During the Tangshan Earthquake of July 28, 1976 (the intensity in this area is 8), this factory building was severely damaged. The main visual damage due to this predominant earthquake occurred at the top and bottom parts of the columns where concrete was crushed and spalled off, the hooks of the stirrups being pulled straight, and the main reinforcements exposed and buckled (see photos 1-4). Residual storey displacements were observed. The earthquake damages occurred mainly in the second floor columns, but minor damages to the columns of the top and ground floors were also observed. The beams remained basically intact but some bending cracks were found at their ends. Partial strengthening had been done to the building after the earthquake of July 28. Strengthening was mainly applied to the damaged columns of the second floor. There were 16 columns of the second floor comprising 70% of the strengthened columns, and 3 columns of the top floor (13%), and 4 columns of the ground floor (17) strengthened as shown in Figure 2. All the strengthened columns were wrapped with reinforced concrete having a thickness of 6 cm. During a strong

aftershock in November 15, 1976 (the Tientsin area again suffered another shock of intensity 8), the whole building collapsed (see photos 5-6). The earth movements were recorded this time by a strong motion accelerograph set up near the factory some time earlier, with a predominate period of vibration of about 0.92 second and a peak acceleration value of 133 gal.

2. EVALUATION OF ASEISMIC CAPACITY OF THE FRAMED STRUCTURE

According to China's Aseismic Design Code for Industrial and Civil Buildings (TJ 11-74), and the Design Code for Reinforced Concrete Structure (TJ 10-74), calculation as to the aseismic capacity of the framed structure building was made for an earthquake intensity of 8. According to China's Code, the soil condition at the site was in the third category. The result of the calculation is given in Table 1.

Table 1 - Calculated Results of the Period of Natural Vibration and Aseismic Capacity of the Framed Structure.

| Item | Natural Vibration T sec. | Base shear at intensity 8 Q(T) | Ground floor storey shear T | | Second floor storey shear T | | Top floor storey shear T | |
|--------------------|--------------------------|--------------------------------|-----------------------------|--------------|-----------------------------|----------------|--------------------------|----------------|
| | | | Calculated value | Yielding lue | Calculated value | Yielding value | Calculated value | Yielding value |
| Calculated results | 1.07 | 22.60 | 22.60 | 29.40 | 17.20 | 17.20 | 9.30 | 9.50 |

The results of calculation show that the story shear of the columns in the second floor, according to the Code, has exceeded its yielding value, and the columns on the top floor were close to yielding. This explains why the structural damage was rather severe there. It shows that the original aseismic capacity of the factory structure was inadequate.

3. MODEL TEST OF COLUMNS

With regards to the inner columns of the second floor of the framed structure, a full size model column test by cyclic loading was carried out, the test being arranged as shown in Figure 3. The two ends of the column were subjected to axial compressive forces of $30T$ to simulate its actual loading condition. The load-deflection curve measured was shown in Figure 4. The result of the experiment showed that due to the sparse allocation of stirrups and the insufficient anchorage of the main reinforcement at the column ends (both being in nonconformity with the Code requirements), the columns did not have enough ductility, the average ultimate displacement at failure being only about 4.4 cm. This is one of the main reasons leading to severe damages at column ends and structural collapse.

4. ANALYSIS OF STRUCTURAL NONLINEAR EARTHQUAKE RESPONSE

Using a degenerated tri-linear mode restoring force characteristics curve as shown in Figure 5, and inputting the actual recorded earthquake ground motion, the nonlinear earthquake response of the frame was analysed with the use of an electronic computer (the mathematical model being of the storey shear system and of the linear bar system respectively). Comparison of the results of analysis was made between the unstrengthened frame and the strengthened one. It was found that the calculated results of the storey displacement for the

storey shear system and those for the linear bar system are rather close to each other, however, the partial strengthening has important effect on the computation results. The relative storey displacements are given in Figure 6 which shows the following points:

- (1). Under strong earthquake motion, the frame had reached the elasto-plastic deformation stage.
- (2). The maximum relative storey displacement of unstrengthened frame occurred at the second floor, but when strengthened, the maximum relative storey displacement of the frame transferred to the ground floor.
- (3). The maximum relative storey displacement of the frame exceeded its allowable ultimate deformation value, so that it is quite possible that the structure collapsed.

5. THE EFFECT OF THE RESIDUAL DEFORMATION OF THE FRAME

There were several centimeters of residual relative storey displacement for the columns of the second floor after the major shock. With consideration to the actual earthquake damage data, residual relative storey displacements $\Delta R_1 = -0.5$ cm, $\Delta R_2 = -2.0$ cm, $\Delta R_3 = 1.0$ cm were taken as the initial values of deformation of the structure and earthquake ground motion record was later fed into the computer in order to investigate the effect of residual deformation in the non-linear earthquake response. The result indicates that the existence of initial residual displacements will increase the final displacements of the frame, and has a harmful effect as to the stability of the frame.

CONCLUSION

The main factors causing the complete collapse of the reinforced concrete frame are:

The insufficiency of the aseismic capacity of the factory frame in the original design; the lack of sufficient ductility of the column, resulting in the small allowance for the ultimate relative storey displacement of the frame; the harmful effect of the residual deformation after the first strong shock on the earthquake resistance of the frame during the aftershocks; the inappropriate strengthening of the frame after the first strong shock. The following suggestions are recommended:

- (1). Aseismic inspection and strengthening should be made in advance to reinforced concrete structures in seismic regions.
- (2). Computational checking should be made as to the aseismic capacity of the structure after strengthening, so as to avoid the harmful effects of inappropriate partial strengthening of the structure.
- (3). Improve the arrangement of the reinforcing bars of the columns in order to increase their ductility and allowance of ultimate deformation. This is an effective measure for increasing the aseismic capacity of reinforced concrete framed structures.
- (4). Further research should be made in methods of analysis for structures which will undergo strong earthquake shocks.

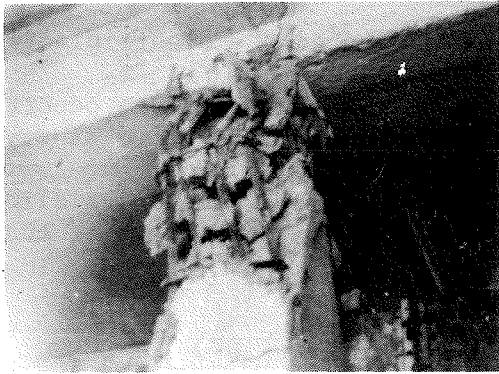


Photo 1 Damage at the top part of a column in the 2nd floor.

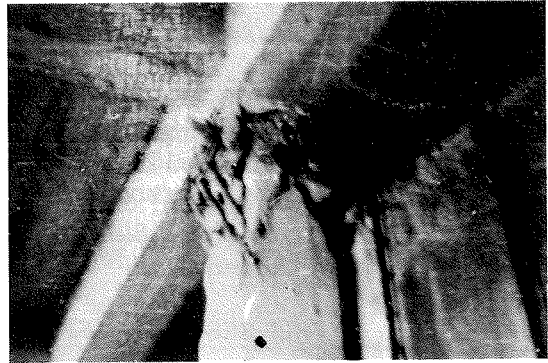


Photo 2 Damage at the top part of another column in the 2nd floor.

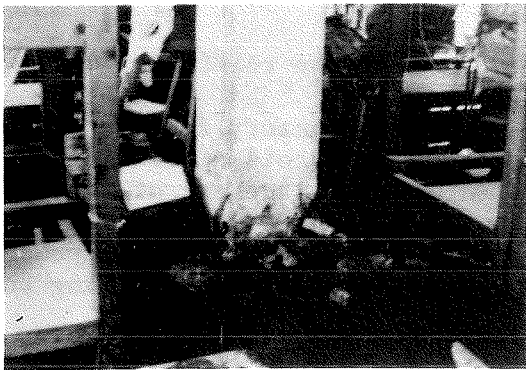


Photo 3 Damage at the bottom part of a column in the 2nd floor.



Photo 4 Damage at the bottom part of a column in the top floor.

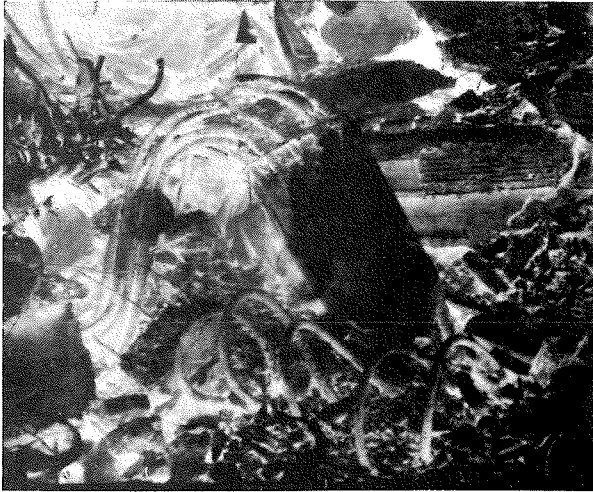


Photo 5 Collapse of the framed structure (view 1).

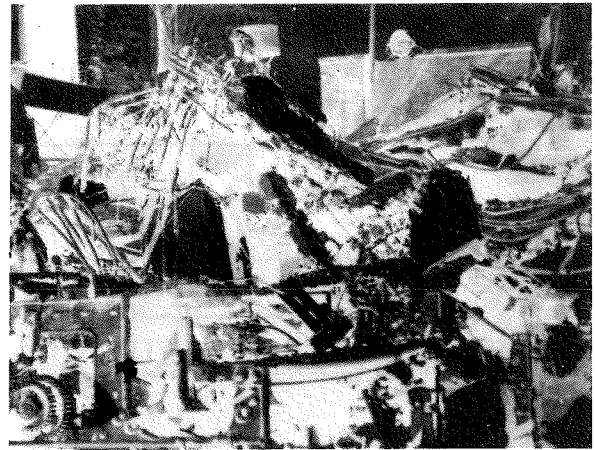


Photo 6 Collapse of the framed structure (view 2).

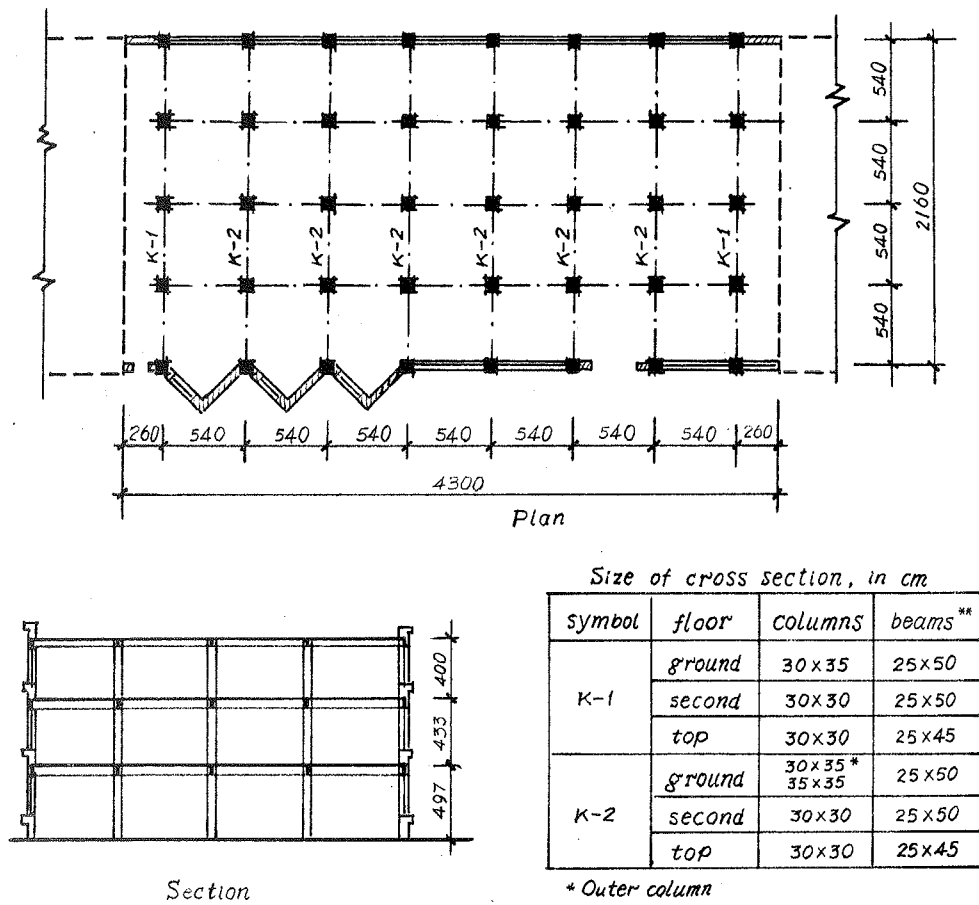


Fig.1 Plan and section of the factory structure.

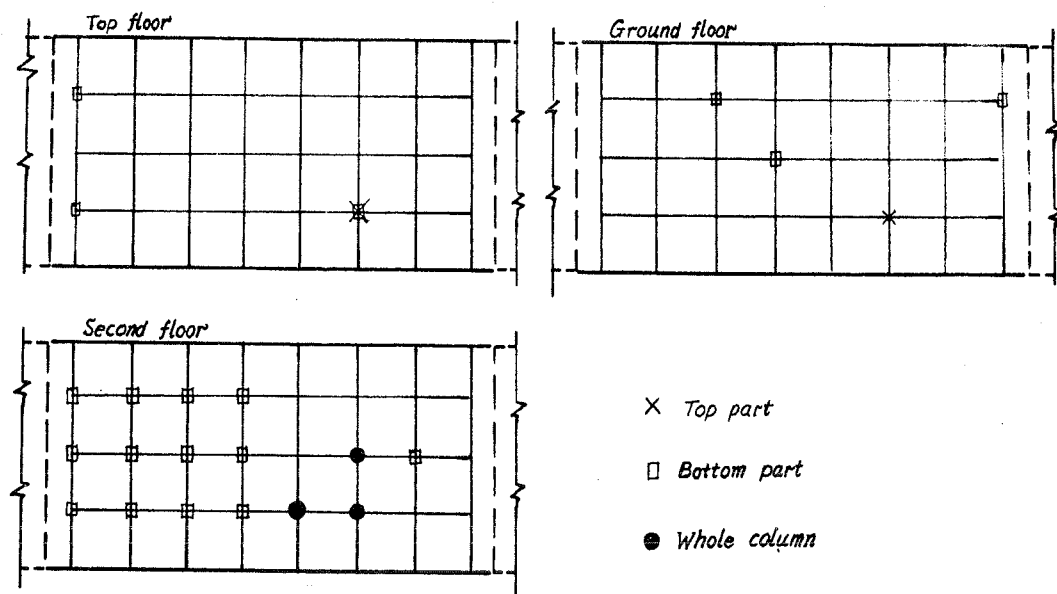


Fig.2 Strengthening of the damaged columns after the major shock.

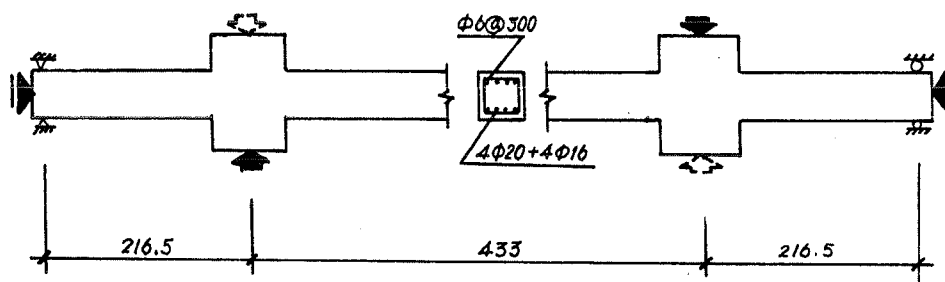


Fig.3 Arrangement of the full size model column.

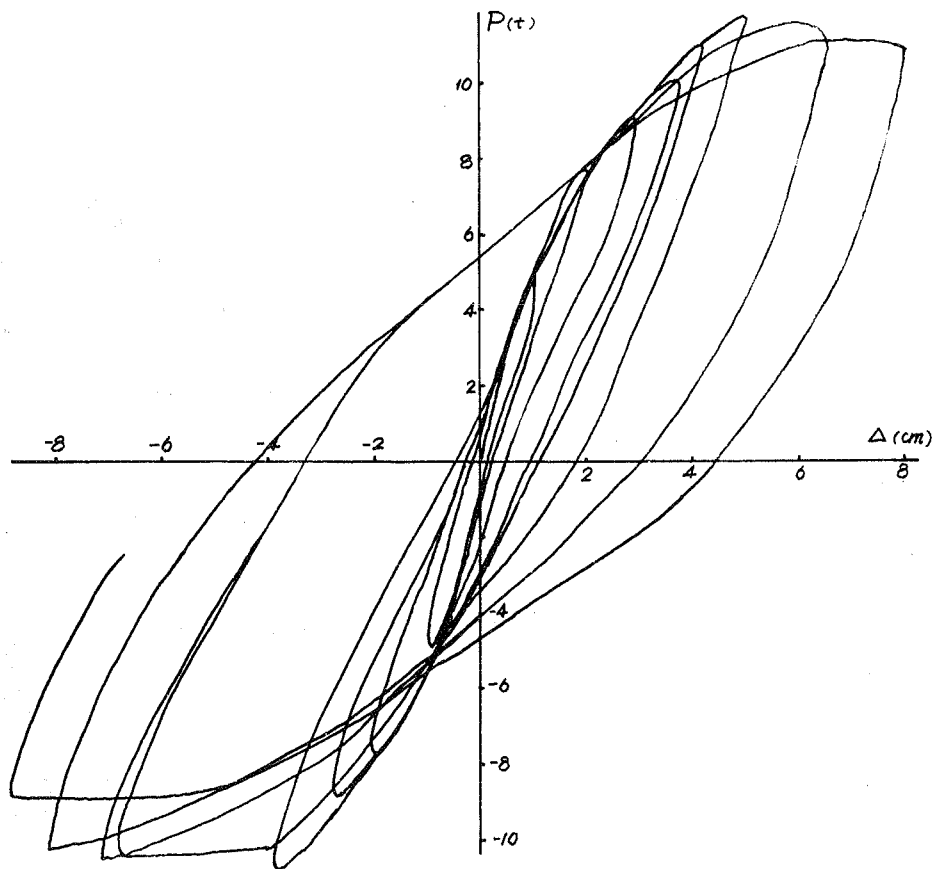


Fig.4 Load-deflection curve under cyclic loading.

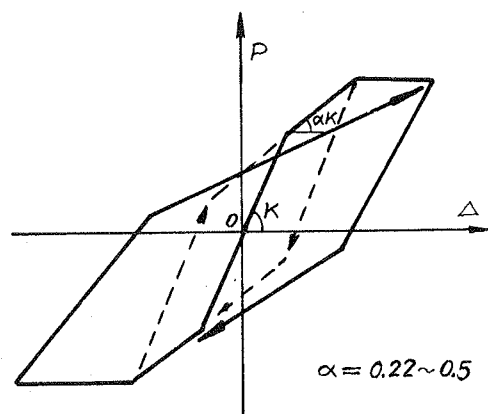


Fig.5 D-TRI Mode of restoring force characteristics curve ($\alpha = 0.22-0.5$).

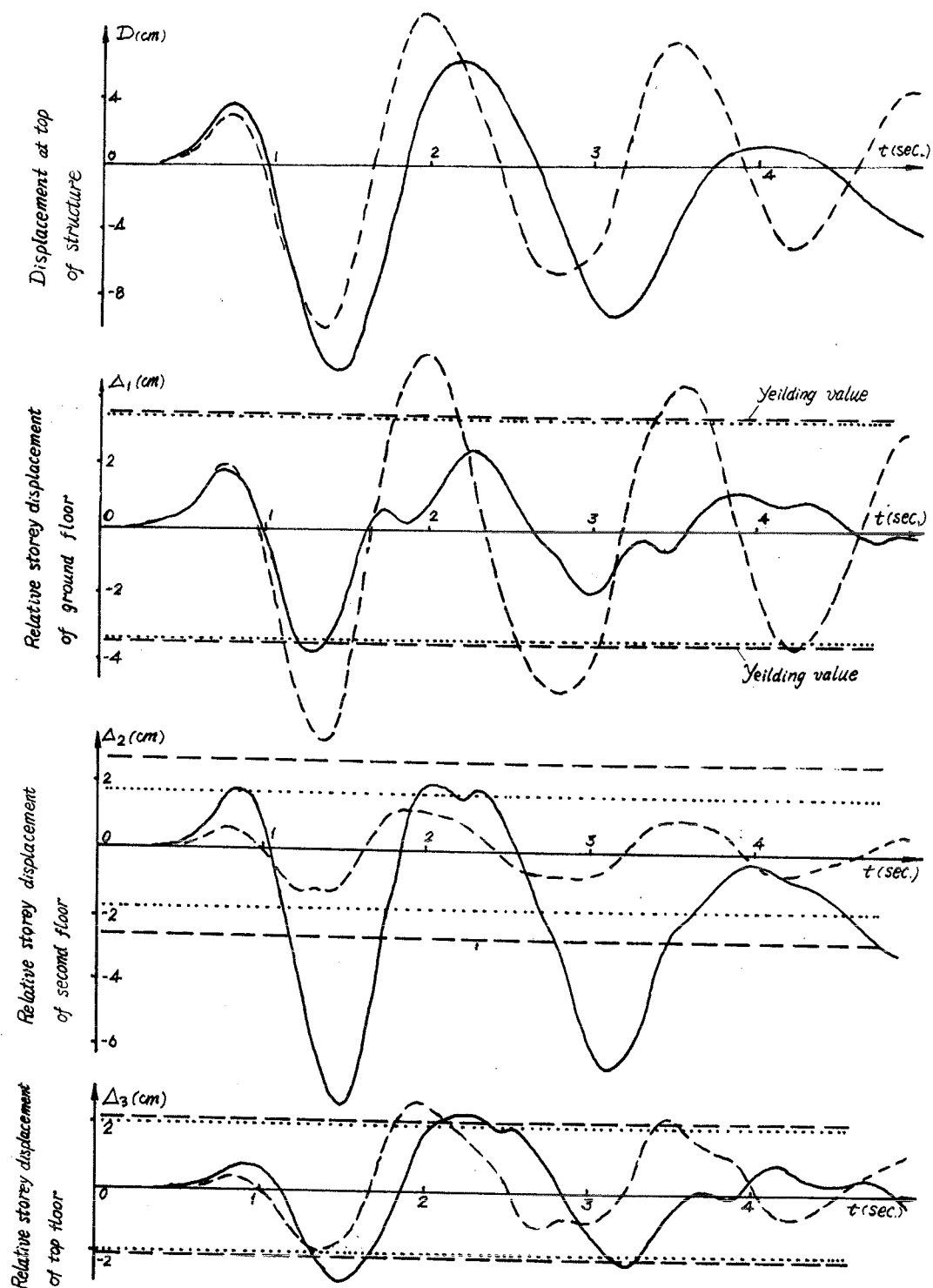


Fig.6 Comparison of the storey displacements response between the unstrengthened structure and the strengthened one (by storey shear model).

AN ECONOMIC ANALYSIS FOR RETROFITTING A REINFORCED CONCRETE BUILDING

Arthur MONSEY
HORNER & SHIFRIN, INC.
St. Louis, MO., U.S.A.

Summary

Seismic safety costs money. As the level of safety is increased, the magnitudes of losses in property and lives will generally decrease. With losses in property and lives normalized to monetary terms, it seems possible to determine a theoretical economic level of safety or design strategy. This study attacks this problem.

The methodology of analysis uses an existing eleven story reinforced concrete apartment house as a model for developing the procedure for economic optimization. Included in the analysis are provisions of recognized existing building codes. Data from the known seismic activity that is indigenous to the specific geographical area is incorporated in the decision making process. In addition to the static equivalent method of analysis for a seismic design, a dynamic analysis was also included as another design strategy. The dynamic analysis required the use of a spectrum developed specifically for the area. An adjunct to the dynamic analysis was a full scale dynamic test of the apartment house. The data obtained from the dynamic test was used to check the theoretical dynamic analysis and to estimate the energy absorbing capability of the existing structure. This data was in turn related to the probable tectonic activity.

The results of the research indicated that the methodology developed herein for a rational decision for seismic safety can be applied for practical purposes within the present state of the art of a seismic design.

INTRODUCTION:

It costs money to obtain safety against seismic forces. The more safety desired, the higher the cost. It is also generally recognized that if structures are "unsafe," then losses in property and lives will occur. Furthermore, damage to property and lives will be higher in and around structures that are not capable of resisting the tremors as compared with structures that can. Thus, the obvious dilemma - damage (costs) to property and lives will decrease if seismic resistance is increased and so will the respective costs. Wherein lies the optimum, or at least the most reasonable degree of protection for the project or perhaps society?

The recognized problem of "trade offs", particularly when dealing with the lives and property of millions of people is one that must be dealt with now since certain limitations are now obvious. First, there are limited resources of capital and material in the world and their judicious use is paramount. Secondly, the technology of seismicity and structural engineering is obtaining insight into the mechanisms and probabilities of success and failure. This sort of information is just beginning to suggest courses of action that engineers can take to partially control these hazards of seismic action. Thus, the new knowledge places responsibilities for decision making within the capabilities of the technologists. But society, with the aid of technology, should and must make the ultimate decisions.

This research deals with a possible approach of attempting to rationally determine the level of safety for seismic response and thus hopefully deal with this form of "macrochistic triage."

METHOD OF SOLUTION:

The procedure is based on the recognition of increasing costs (construction and engineering) and decreasing cost (lives and property) as seismic response capability is increased. Thus, if the level of is defined as design strategy, then the rising cost "curve" of protection and the decreasing damage cost "curve" combined should at some point show an optimum when argued against the design strategy.

The demonstration and use of this idea utilized a modern eleven story reinforced concrete abutment building located in St. Louis, Missouri. See Figure 1. As a part of a research program conducted by Washington University (St. Louis, Missouri) and funded by the National

Science Foundation, this tower-like structure was dynamically tested with low amplitude and high amplitude dynamic forces. In addition to other goals, this program provided an opportunity to check some methods of seismic design normally used by structural engineers as well as providing a prototype building that, indeed, might have been retrofitted (not only structurally) for rehabilitation.

The design strategies utilized were based on the zonation of the BOCA Code (3). The design method therein recommended is the "static equivalent" seismic loading. Thus, the number of strategies available were four (zone 0 thru 3, inclusive). Another strategy was a dynamic analysis (4)(5) utilizing a spectra that is indigenous to the St. Louis area (8)(9). Also, the unique characteristics such as "felt area," frequency, and length of activity, were included in the dynamic analysis.

The construction and engineering costs for each strategy were computed by developing a design that was compatible with the specific design strategy. Though several designs for stiffening the existing slab, beam, column system would have worked, the final design was a "shear wall" system for both directions. See Figure 2. The construction and engineering costs were based on the writer's experience and other pertinent data (7).

The estimates for property damage costs were based on work done by researchers at the Massachusetts Institute for Technology (1)(10). The results of this data, combined with updated construction costs, are shown in Figure 3.

The estimates for mortality rates were determined from studies in the Memphis, Tennessee area* and other literature and research (6). The value of a life was made by methods of compound interest and actuarial data (2). A summary of this data is given in Figure 3.

All expected value damage estimates (life and property) were based on the probabilities of tremors of various magnitudes or intensities and provided by Professor Otto M. Nuttley of St. Louis University (9). These probabilities were incorporated into the computation of Table 3-(9).

The results of combining the design strategies with the retrofitting costs and damages costs are shown in Figure 4.

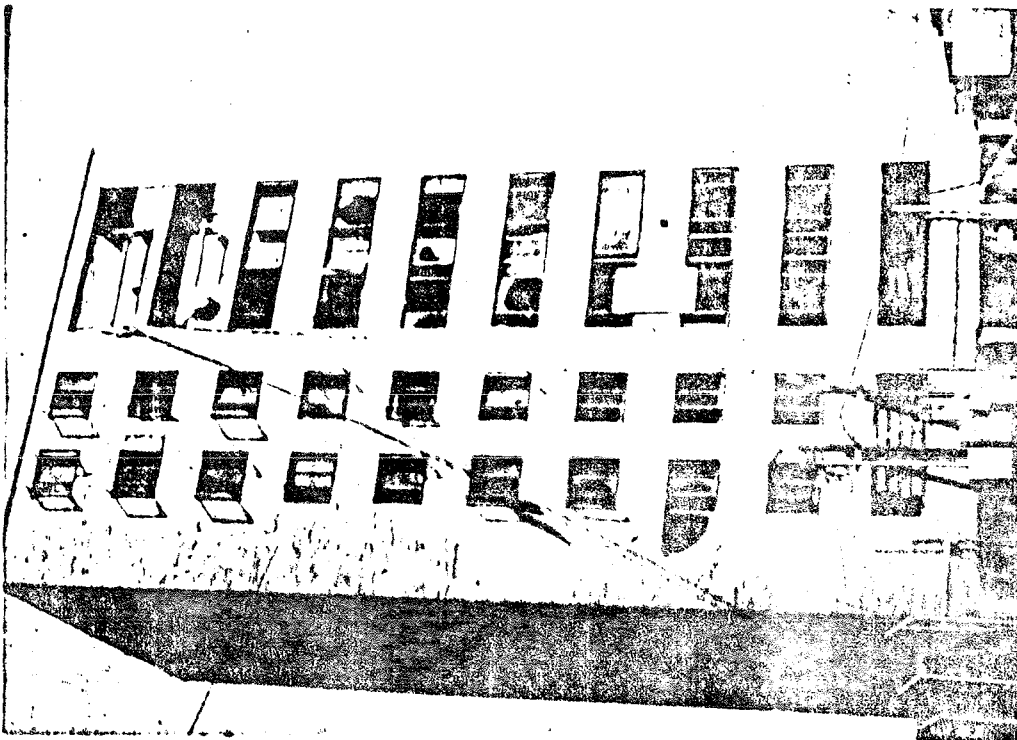
* The New Madrid fault zone is generally believed to be the most probable source area for severe tremors to Memphis and St. Louis.

CONCLUSIONS:

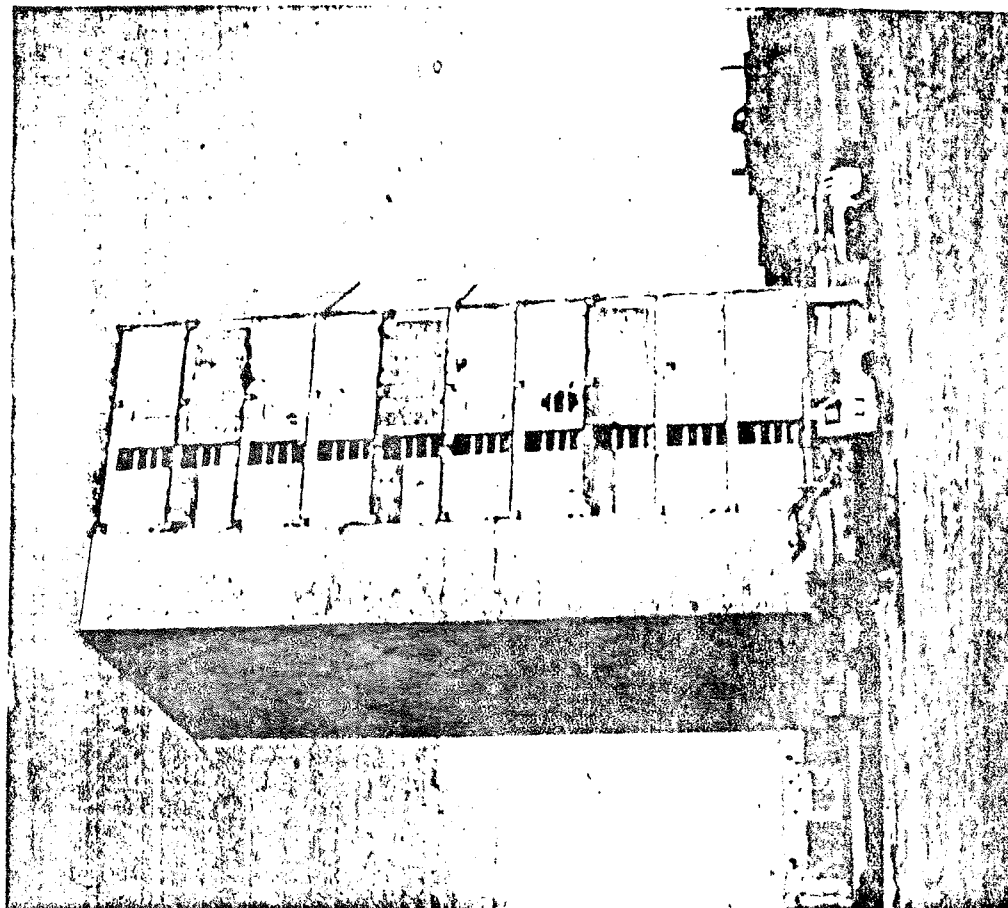
The following was concluded from this study:

- A. The St. Louis, Missouri area is in a seismic zone wherein earthquakes of considerable magnitude can occur, though very infrequently. The type of ground motions, frequencies, and attenuation characteristics are unique and do not compare with those of other areas and have the potential of inflicting great damage.
- B. The "tower like" structure that was constructed in 1955 was found to be in structural compliance with the ACI-318-71 for earthquake forces developed for zone 0 and 1 as defined by the BOCA 1975 Building Code.
- C. The forces developed in zones 2 and 3 developed structural conditions that were not acceptable by the criteria set forth in this study. This was particularly noticeable in the phenomenon of reverse bending of certain beams.
- D. Analysis using a dynamic method and reserve energy procedures for St. Louis suggested that the structure would suffer high damage, but the system could survive. The accelerations dictated by the spectra were about 0.4 g.
- E. Analysis of the cost relationships between design strategies and economic losses due to damage of property and/or life indicates that the criteria or design strategy of zone 1 was optimum.
- F. Unless the risk-taking policies of the owner of the project were reduced to virtually zero, the purchase of insurance for this project over the economic life appears unjustified. The project could, in effect, become self insured. It would appear that only in the case of extremely high damage or collapse was insurance justified. As a "middle of the road" alternative, a very high deductible amount could have been purchased at a lower cost than that used in this study.
- G. The cost to benefit ratio-studies also indicated that there is no economic justification for any retrofitting program. Only when the loss of life is included as an economic indicator is retrofitting suggested. The cost to benefit ratios then suggested that the strengthening program comply with at least the requirements of zone 3.

The conclusions reached from this analysis indicated that a rational approach to seismic retrofitting is possible. The amalgamation of data from structural analysis, geophysics, construction, economics, and architecture provides procedures that permit the engineer to conceptualize an optimum course of action. It may very well be that the course of action dictated by the methodology developed herein would not be used exclusively since other factors such as sociological or historical values might influence an ultimate decision. Perhaps even these factors might be quantified and lend themselves to a type of quantification. However, it is encouraging to observe that the technology available to date (with all its shortcomings) in the field of seismic design provides a mechanism that is as rational as possible. The future holds great promise that man's intellect will permit proper use and control of his environment, as nature undoubtedly intended.



South Elevation



East Elevation

FIGURE 1

PRUITT IGOE APT. PROJECT (1976)

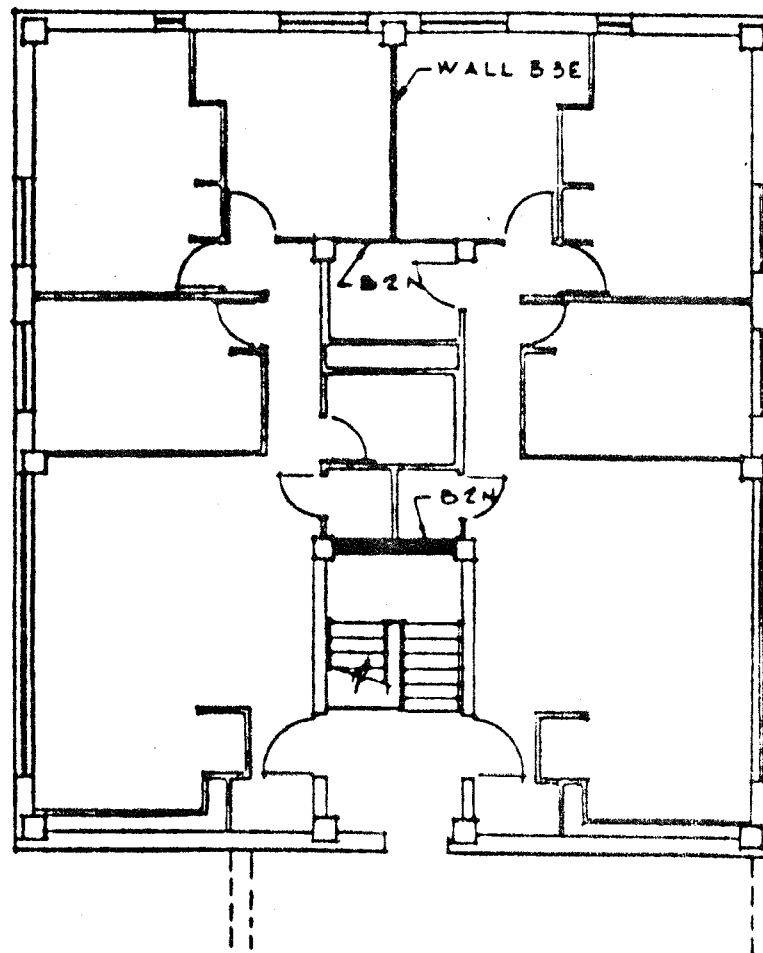


FIGURE 2
Shear Wall Plan

Physical Damage Estimates

Estimate of Damage

| Design Strategy | <u>VI</u> | <u>VII</u> | <u>VIII</u> | <u>IX</u> | <u>X</u> |
|-----------------|-----------|------------|-------------|-----------|-----------|
| 0.1 | \$1,988 | \$ 26,500 | \$265,000 | \$530,000 | \$530,000 |
| 2 | 1,325 | 13,250 | 90,100 | 530,000 | 530,000 |
| 3 | 795 | 10,600 | 53,000 | 238,500 | 530,000 |

Expectation Values

| | | | | | |
|-----|-------|--------|--------|-----|-----|
| 0.1 | 1,710 | 14,575 | 31,800 | 424 | 212 |
| 2 | 1,140 | 7,288 | 10,812 | 424 | 212 |
| 3 | 684 | 5,830 | 6,360 | 191 | 212 |

Normalized Expected Values

| | | | | | |
|-----|-----|-------|--------|-----|--------------------|
| 0.1 | 676 | 5,830 | 13,250 | 159 | 106 Σ 20021 |
| 2 | 431 | 2,915 | 3,505 | 159 | 106 7136 |
| 3 | 270 | 2,332 | 2,650 | 72 | 106 5430 |

Mean Loss of Life Ratio For 88
People Reference (53)

Design Strategy*

| | <u>VII</u> | <u>VIII</u> | <u>IX</u> | <u>X</u> |
|-----|-------------------------------|------------------------------|----------------|-----------------|
| 0-1 | 8.8×10^{-3} (\$1210) | 1.3 (\$39000) | 5.1 (\$102000) | 13.5 (\$135000) |
| 2 | 2.2×10^{-3} (\$303) | 0.3 (\$9000) | 4.2 (\$84000) | 7.6 (\$76000) |
| 3 | 0 (0) | 5.28×10^{-2} (1584) | 1.2 (\$24000) | 4.2 (\$42000) |

b

Relative Expected Values (\$250000/Life)

| | | | | |
|---|-------|---------|-------|----------------------|
| 0 | \$484 | \$16250 | \$383 | \$675 Σ 17792 |
| 1 | 484 | 16250 | 383 | 675 17792 |
| 2 | 121 | 3750 | 315 | 230 4186 |
| 3 | 0 | 660 | 90 | 210 960 |

X.X = number of fatalities

() = value of loss of life based on \$250000/ life
and probability of occurrence

FIGURE 3

Expectation Values of
Property Damage and Mortality

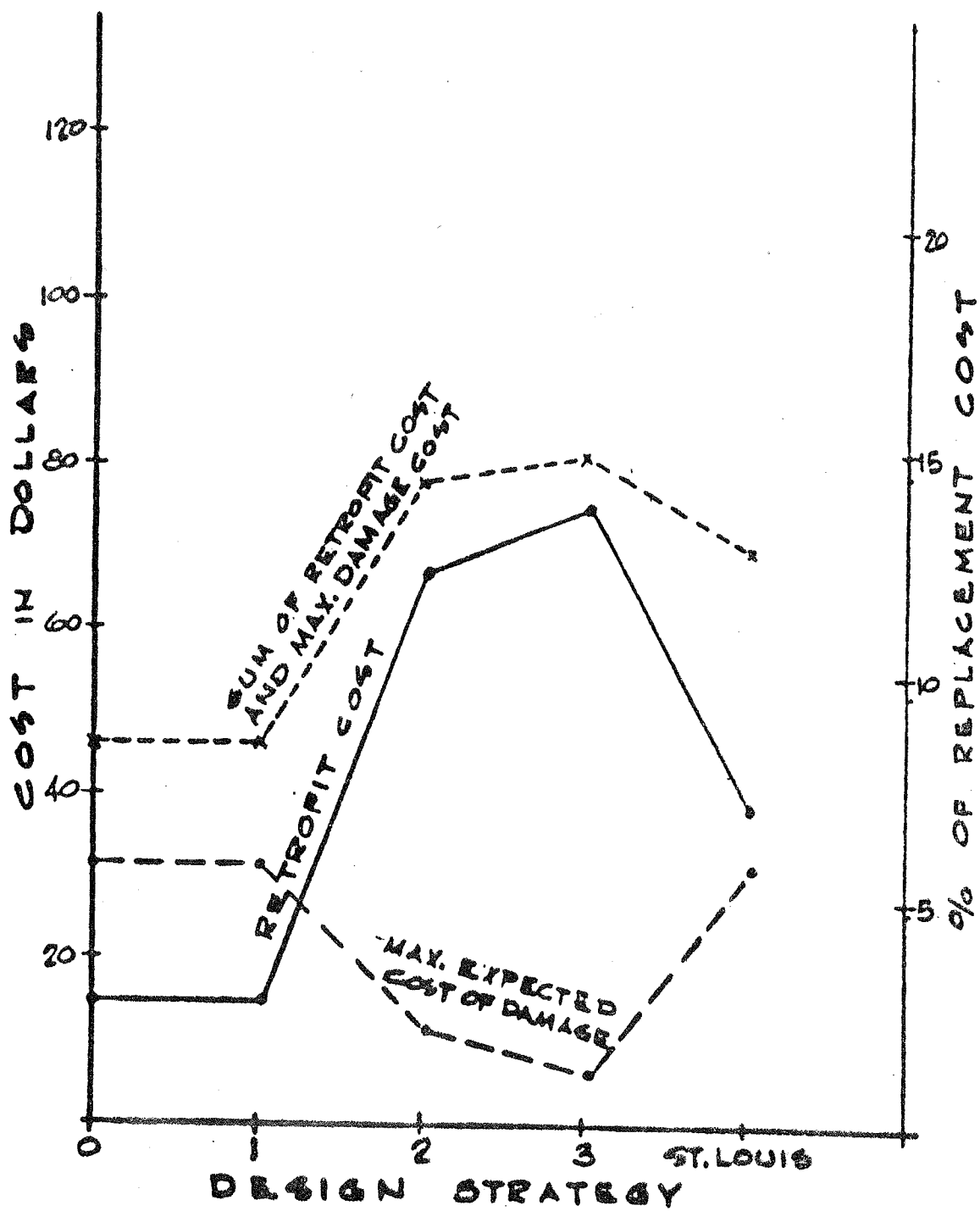


FIGURE 4

Design Strategy vs Damage Costs

Bibliography

1. Biggs, J. M.; Brennan, J. E.; Cornell, C. A.; deNoufville, R. L.; Whitman, R. V.; Vanmark, E. H.; "Seismic Design Decision Analysis," Journal of the Structural Division, ASCE, Vol. 101, No. ST5, pp 1067-1084, [May 1975]
2. Bower, J. W.; "Investment Analysis and Management," Richard D. Irwin, Inc., 4th Ed.; Homewood, Ill.; pp 16-17, [1977]
3. Building Officials Conference of America - Building Code [1975]
4. Clough, R. W.; Penzion, D.; "Dynamics of Structures," McGraw-Hill, Inc., pp 544-610, [1975]
5. Gould, P. L. - Class Notes - [1976]
6. M & H. Engineering and Memphis State University, "Regional Earthquake Risk Study, Technical Report," U. S. Department of Housing and Urban Development, [Sept. 30, 1974]
7. Means, R. S.; "Building Construction Cost Data;" Means Company, Inc., Duxbury, Mass. [1976]
8. Nacioglu, A.; Nuttli, O. W.; "Some Ground Motion and Intensity Relations for the Central United States;" Earthquake Engineering and Structural Dynamics, Vol. 3, pp 111-119, [1974]
9. Nuttli, Otto W., Conversations with Prof. Nuttli of St. Louis University [1977]
10. Whitman, R. V.; "Damage Probability Matrices for Prototype Buildings," Report #8, Nation Science Foundation Grant GK-27955 and GI-29936, Mass. Inst. of Technology, [Oct. 1973]